

Contents

1 Multidimensional Signal Processing	6
1.1 1D, 2D, and 3D Signals	6
1.2 Separable Signals	6
1.3 Delta Functions	6
1.3.1 Properties of the Delta Function	7
1.4 Transformations of Signals	7
1.5 Shift-Invariant Systems	8
1.6 LSI Systems and Complex Exponentials	9
1.7 Comments on the Fourier Transform	10
1.8 Properties of the Fourier Transform	10
1.9 Rect and Sinc	12
1.10 Hankel Transform	13
2 Image Quality	14
2.1 Contrast and Modulation	14
2.2 Resolution	16
2.3 Noise	17
2.4 Sampling	22
2.5 Sampling Theorem	25
2.6 Aliasing	26
2.7 Area Detector Analysis	27
2.8 Artifacts	28
2.9 Accuracy	28
3 Physics of Radiography	30
3.1 X-Ray Modalities	30
3.2 Atomic Structure	30
3.3 Ionizing Radiation	31
3.4 Electromagnetic EM Radiation	32
3.5 Energetic Electron Interactions	33
3.6 EM Interactions	34
3.7 Beam Strength: Photon Counts	36
3.8 EM Attenuation Geometries	37
3.9 EM Dose	39
4 Projection Radiography	40
4.1 Radiographic System	41
4.2 X-ray Tube	41

4.3	Filtration and Restriction	44
4.4	Scatter Control	46
4.5	Film, Screen, and Cassette	48
4.5.1	Intensifying Screen	49
4.5.2	Radiographic Cassette	50
4.5.3	Film	50
4.5.4	Digital Radiography: CR	52
4.5.5	Digital Radiography: DR	52
4.6	Basic Imaging Equation	54
4.7	Geometric Effects	54
4.7.1	Inverse Square Law	55
4.7.2	Obliquity	56
4.7.3	Beam Divergence and Flat Detector	56
4.7.4	Anode Heel Effect	57
4.7.5	Path Length of Slab	57
4.7.6	Object Magnification	58
4.7.7	Thin Slab Imaging Equation	58
4.7.8	Sources of Blurring	59
4.8	Noise	60
4.9	Signal-to-noise	61
4.10	Compton Scatter	63
5	Computed Tomography	63
5.1	Generations of CT Scanners	63
5.1.1	X-ray Tubes in CT	67
5.2	CT Detectors	67
5.3	CT Measurement Model	68
5.3.1	Line Integral	69
5.4	CT Numbers	70
5.4.1	Describing Lines	70
5.4.2	Line Parameters and Picture of a line	71
5.4.3	Line Integral: parametric form	71
5.4.4	Line Integral: set form	72
5.4.5	Physical meanings of $f(x, y)$ and $g(x, y)$	72
5.4.6	What is $g(l, \theta)$?	73
5.4.7	Sinogram	74
5.4.8	Backprojection(smearing back)	74
5.4.9	Backprojection summation	75
5.4.10	Properties of Laminogram	75
5.5	Projection-Slice Theorem	76

5.5.1	Illustration of Projection-Slice Theorem	77
5.6	Exact Reconstruction Formulas	77
5.6.1	Convolution, Backprojection, and Summation	79
5.7	Factors Affecting CT Resolution	80
5.7.1	Blurry Reconstruction	81
5.7.2	CT Impulse Response Function	82
5.7.3	PSF given by Hankel Transform	83
5.8	Noise in CT Measurements	84
5.8.1	Functions of Random Variables in CT	84
5.8.2	CBP Approximation	85
5.9	Conclusions	85
5.10	Signal-to-noise Ratio	86
5.11	SNR in a Good Design	87
5.12	SNR in Fan-Beam Case	87
5.13	Rule of Thumb	87
5.14	Fan Beam Geometry	88
6	Physics of Nuclear Medicine	89
6.1	Nomenclature	89
6.2	Mass Defect and Binding Energy	89
6.3	Radiotracers	90
7	Planar Scintigraphy	91
7.1	Gallium-67 scan	91
7.2	Gamma/Anger Camera Components	92
7.2.1	Collimators	93
7.2.2	Detector	93
7.2.3	Photomultiplier Tube Array	94
7.2.4	Photomultiplier Tube	94
7.2.5	Pulse Height	95
7.3	Pulse Height Analysis	96
7.3.1	Gamma Camera Photon Detection	96
7.3.2	Gamma Camera Event Positioning	97
7.3.3	Event Positioning Logic	97
7.4	Acquisition Modes	97
7.5	Imaging Geometry and Assumption	99
7.5.1	Photon Fluence in Collimator Hole	100
7.6	Planar Sources	101
7.7	Collimator Resolution	102
7.8	Intrinsic Resolution	102

7.9	Collimator Sensitivity	103
7.10	Resolution vs. Sensitivity	103
7.11	Detector Efficiency	103
7.12	Geometry and Nonuniformity	104
7.13	Image SNR	105
7.14	Energy Resolution	105
7.15	Pulse Pileup	106
8	Emission Tomography	106
8.1	SPECT	106
8.1.1	SPECT Hardware	106
8.1.2	SPECT Coordinate System	107
8.1.3	Multiple Head Tradeoffs	108
8.2	Basic Imaging Equation	108
8.3	Tomographic Imaging Equation	109
8.4	Approximate SPECT Imaging Equation	109
8.5	SPECT Reconstruction	109
8.6	Approximate SPECT Attenuation Correction	110
8.7	Myocardial Perfusion SPECT Dose	110
8.8	PET Principles	110
8.8.1	Annihilation Conincidence Detection (ACD)	111
8.8.2	PET Detector Block	112
8.8.3	Typical PET Detector Arrangement	112
8.8.4	2-D or 3-D PET Geometry	113
8.9	PET Imaging Equation	115
8.10	PET Reconstruction	116
8.11	Iterative Reconstruction Concept	117
8.11.1	Digital Representation of Cross Section	117
8.11.2	Computed Measurements in SPECT and PET	118
8.12	Algebraic Reconstruction Technique(ART)	119
8.13	Maximum Likelihood Expectation Maximization(ML-EM)	119
8.14	Resolution in Emission Tomography	119
8.14.1	Conincidence Timing	120
9	Ultrasound Physics	120
9.1	3-D Wave Equation	120
9.2	Plane Waves	121
9.2.1	Harmonic Waves	121
9.2.2	Spherical Waves	122
9.2.3	Characteristic Impedance	122

9.2.4	Acoustic Energy	122
9.2.5	Acoustic Power	123
9.2.6	Reflection and Refraction	123
9.2.7	Reflected and Refracted Waves	124
9.2.8	Attenuation and Absorption	124
9.2.9	Scattering	125
9.2.10	Field Patterns	125
9.2.11	Far Field=Fraunhofer Pattern	126
9.2.12	Focusing	126
10	Ultrasound Imaging	127
10.1	Ultrasound System Components	127
10.2	Transducers	128
10.2.1	Piezoelectric Effect	129
10.2.2	Resonance	129
10.2.3	Electronic Scanner	130
10.3	Shock Excitation	130
10.3.1	A-mode Display	131
10.3.2	Depth of Penetration	131
10.3.3	Pulse Repetition Time	132
10.4	Phased Arrays: Transmit Steering	132
10.5	Phased Arrays: Transmit Focussing	134
10.5.1	Dynamic Focusing	134
10.6	Imaging Equation	134

List of Figures

List of Tables

1 Multidimensional Signal Processing

1.1 1D, 2D, and 3D Signals

A 1D signal is:

- $f(t)$, a function of one variable, or
- a waveform, or
- a graph (a collection of points in a 2D space)

A 2D signal is:

- $f(x, y)$, a function of two variables, or
- an image, or
- a graph (a collection of points in a 3D space)

A 3D signal is:

- $f(x, y, z)$, a function of three variables, or
- a volumetric image, or
- a graph (a collection of points in a 4D space)

1.2 Separable Signals

- $f(x, y) = f_1(x)f_2(y)$
- $f(x, y, z) = f_1(x)f_2(y)f_3(z)$

1.3 Delta Functions

The 1D delta or impulse function is defined by two properties:

$$\delta(x) = 0, x \neq 0$$

$$\int_{-\infty}^{\infty} f(x)\delta(x) \, dx = f(0)$$

1.3.1 Properties of the Delta Function

$$\delta(-x) = \delta(x) \text{ Even}$$

$$\delta(x, y) = \delta(x)\delta(y) \text{ Separable}$$

$$\int_{-\infty}^{\infty} f(\xi)\delta(\xi - x) d\xi = f(x) \text{ Sifting}$$

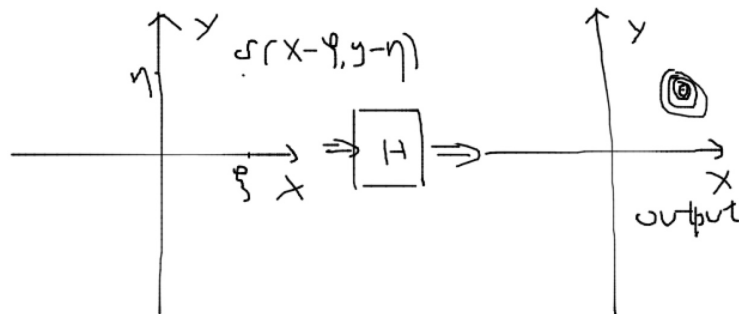
$$\int_{-\infty}^{\infty} \int_{-\infty}^{\infty} f(\xi, \eta)\delta(\xi - x, \eta - y) d\xi d\eta = f(x, y) \text{ 2D Sifting}$$

$$\int_{-\infty}^{\infty} \delta(x) dx = 1 \text{ The area under delta is unity}$$

1.4 Transformations of Signals

The impulse response or point spread function due to an impulse at (ξ, η) is
 $h(x, y; \xi, \eta) = H[\delta(x - \xi, y - \eta)]$

[docs/Medical Imaging Systems/images/fig1.jpg](#)



A linear System satisfies:

$$H[w_1f_1 + w_2f_2] = w_1H[f_1] + w_2H[f_2]$$

for all signals f_1 and f_2 and weights w_1 and w_2 A linear system satisfies the **superposition integral**:

$$g(x, y) = \int_{-\infty}^{\infty} \int_{-\infty}^{\infty} h(x, y; \xi, \eta) f(\xi, \eta) d\xi d\eta$$

1.5 Shift-Invariant Systems

A system that is **shift-invariant** is

$$g(x - x_0, y - y_0) = H[f(x - x_0, y - y_0)]$$

for every (x_0, y_0) and $f(., .)$

Therefore, a linear shift-invariant(LSI) system yields

$$h(x, y; \xi, \eta) \rightarrow h(x - \xi, y - \eta)$$

An LSI system satisfies the **convolution integral**:

$$g(x, y) = \int_{-\infty}^{\infty} \int_{-\infty}^{\infty} h(x - \xi, y - \eta) f(\xi, \eta) d\xi d\eta$$

which is abbreviated as

$$g(x, y) = h(x, y) * f(x, y)$$

If we let $\xi_0 = x - \xi$ and $\eta_0 = y - \eta$, we have the following:

$$\begin{aligned} g(x, y) &= \int_{-\infty}^{\infty} \int_{-\infty}^{\infty} h(\xi_0, \eta_0) f(x - \xi_0, y - \eta_0) d\xi_0 d\eta_0 \\ &= \int_{-\infty}^{\infty} \int_{-\infty}^{\infty} h(\xi, \eta) f(x - \xi, y - \eta) d\xi d\eta \end{aligned} \tag{1}$$

Community proved

1.6 LSI Systems and Complex Exponentials

A 1D complex exponential signal is

$$e^{j2\pi ux} = \cos(2\pi ux) + j\sin(2\pi ux)$$

A 2D complex exponential signal is

$$e^{j2\pi(ux+vy)} = e^{j2\pi ux} e^{j2\pi vy}$$

The response of an LSI system to

$$f(x, y) = e^{j2\pi(ux+vy)}$$

is

$$g(x, y) = H(u, v) e^{j2\pi(ux+vy)}$$

Use convolution integral

$$\begin{aligned} g(x, y) &= \int_{-\infty}^{\infty} \int_{-\infty}^{\infty} h(\xi, \eta) f(x - \xi, y - \eta) d\xi d\eta \\ &= \int_{-\infty}^{\infty} \int_{-\infty}^{\infty} h(\xi, \eta) e^{j2\pi(u(x-\xi)+v(y-\eta))} d\xi d\eta \\ &= \int_{-\infty}^{\infty} \int_{-\infty}^{\infty} h(\xi, \eta) e^{j2\pi ux} e^{-j2\pi u\xi} e^{j2\pi vy} e^{-j2\pi v\eta} d\xi d\eta \\ &= \int_{-\infty}^{\infty} \int_{-\infty}^{\infty} h(\xi, \eta) e^{-j2\pi(u\xi+v\eta)} d\xi d\eta f(x, y) \end{aligned} \tag{2}$$

ξ and η are just dummy variables, change them to x and y , we get the function

$$H(u, v) = \int_{-\infty}^{\infty} \int_{-\infty}^{\infty} h(x, y) e^{-j2\pi(ux+vy)} dx dy$$

which is called the **Fourier transform** of $h(x, y)$

The **inverse Fourier transform** of $H(u, v)$ is

$$h(x, y) = \int_{-\infty}^{\infty} \int_{-\infty}^{\infty} H(u, v) e^{+j2\pi(ux+vy)} du dv$$

1.7 Comments on the Fourier Transform

- $e^{-j2\pi(ux+vy)}$ is a complex sinusoid "oriented" in the (u,v) direction
- $2\pi ux$ has units of radians
- ux is unitless
- x has units of length
- u has units of inverse length
- u is referred to as cyclic/spatial frequency
- The 1D Fourier transform pair is given by

$$F(u) = \int_{-\infty}^{\infty} f(x)e^{-j2\pi ux}dx$$

$$f(x) = \int_{-\infty}^{\infty} F(u)e^{+j2\pi ux}du$$

1.8 Properties of the Fourier Transform

- Linearity:

$$\mathcal{F}[w_1f_1 + w_2f_2] = w_1F_1 + w_2F_2$$

- Scaling(proof):

$$\mathcal{F}\{f(\alpha x, \beta y)\} = \int_{-\infty}^{\infty} \int_{-\infty}^{\infty} f(\alpha x, \beta y)e^{-j2\pi(ux+vy)}dxdy$$

Let $x' = \alpha x$, $y' = \beta y$, we have $dx' = \alpha dx$ and $dy' = \beta dy$
For $\alpha, \beta > 0$

$$\mathcal{F}\{f(\alpha x, \beta y)\} = \int_{-\infty}^{\infty} \int_{-\infty}^{\infty} f(x', y')e^{-j2\pi(u\frac{x'}{\alpha} + v\frac{y'}{\beta})} d\frac{x'}{\alpha} d\frac{y'}{\beta}$$

If $\alpha < 0$, $x' = -|\alpha|x$

$$\mathcal{F}\{f(\alpha x, \beta y)\} = \int_{-\infty}^{\infty} \int_{-\infty}^{\infty} f(x', y')e^{-j2\pi(u\frac{x'}{|\alpha|} + v\frac{y'}{\beta})} d\frac{x'}{|\alpha|} d\frac{y'}{\beta}$$

$$\begin{aligned}
&= \int_{-\infty}^{\infty} \int_{-\infty}^{\infty} f(x', y') e^{-j2\pi(u\frac{x'}{\alpha} + v\frac{y'}{\beta})} d\frac{x'}{|\alpha|} d\frac{y'}{\beta} \\
&= \int_{-\infty}^{\infty} \int_{-\infty}^{\infty} f(x', y') e^{-j2\pi(x'\frac{u}{\alpha} + y'\frac{v}{\beta})} d\frac{x'}{|\alpha|} d\frac{y'}{\beta} \\
&= \boxed{\frac{1}{|\alpha\beta|} F\left(\frac{u}{\alpha}, \frac{v}{\beta}\right)}
\end{aligned}$$

- Shifting(proof):

$$\mathcal{F}\{f(x - \alpha, y - \beta)\} = F(u, v)e^{-j2\pi(u\alpha + v\beta)}$$

$$\begin{aligned}
\mathcal{F}\{f(x, y)e^{+j2\pi(\mu_0x + \nu_0y)}\} &= \int_{-\infty}^{\infty} \int_{-\infty}^{\infty} f(x, y) e^{+j2\pi(\mu_0x + \nu_0y)} e^{-j2\pi(ux + vy)} dx dy \\
&= \int_{-\infty}^{\infty} \int_{-\infty}^{\infty} f(x, y) e^{-j2\pi((u - \mu_0)x + (v - \nu_0)y)} dx dy \\
&= F(u - \mu, v - \nu)
\end{aligned} \tag{3}$$

- Convolution Theorem:

$$\mathcal{F}[f_1 * f_2] = F_1 F_2$$

- Correlation:

$$\begin{aligned}
\mathcal{F}\left[\int_{-\infty}^{\infty} \int_{-\infty}^{\infty} f_1(\xi, \eta) f_2^*(x + \xi, y + \eta) d\xi d\eta\right] \\
&= F_1(u, v) F_2^*(u, v)
\end{aligned}$$

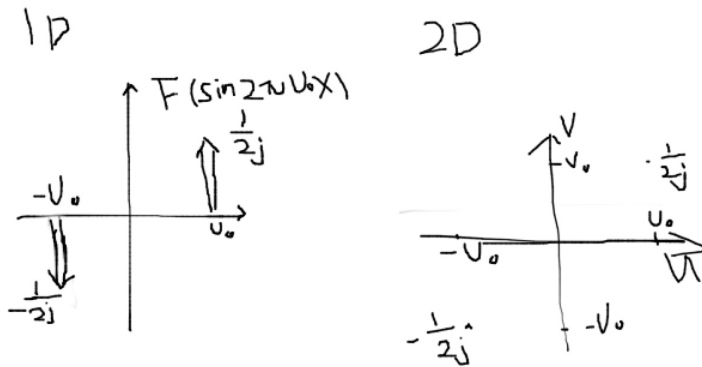
- Parseval's theorem:

$$\begin{aligned}
&\int_{-\infty}^{\infty} \int_{-\infty}^{\infty} |f(x, y)|^2 dx dy \\
&= \int_{-\infty}^{\infty} \int_{-\infty}^{\infty} |F(u, v)|^2 du dv
\end{aligned}$$

- Sinusoid (1D) (Proof):

we know that $\sin\theta = \frac{e^{j\theta} - e^{-j\theta}}{2j}$

$$\begin{aligned}
 \mathcal{F}\{\sin 2\pi u_0 x\} &= \int_{-\infty}^{\infty} \sin 2\pi u_0 x e^{-j 2\pi u x} dx \\
 &= \int_{-\infty}^{\infty} \frac{e^{j 2\pi u_0 x} - e^{-j 2\pi u_0 x}}{2j} e^{-j 2\pi u x} dx \\
 &= \frac{1}{2j} \left[\int_{-\infty}^{\infty} e^{-j 2\pi(u-u_0)x} dx - \int_{-\infty}^{\infty} e^{-j 2\pi(u+u_0)x} dx \right] \\
 &= \frac{1}{2j} [\delta(u - u_0) - \delta(u + u_0)]
 \end{aligned} \tag{4}$$



Similarly for cosine, we have

$$\mathcal{F}\{\cos 2\pi u_0 x\} = \frac{1}{2} [\delta(u - u_0) + \delta(u + u_0)] \tag{5}$$

1.9 Rect and Sinc

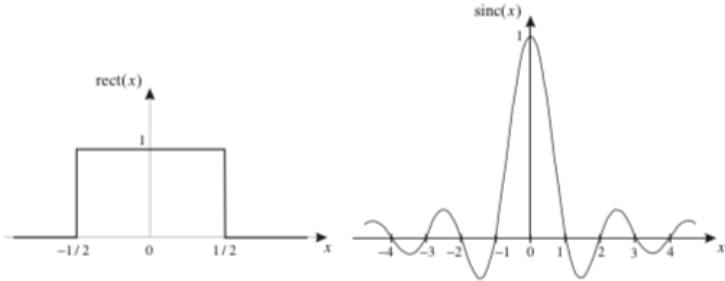
Rect function: ("gate" or "pedestal")

$$\text{rect}(x) = \begin{cases} 1 & \text{if } |x| \leq 1/2 \\ 0 & \text{otherwise} \end{cases}$$

Sinc function:

$$\text{sinc}(x) = \frac{\sin \pi x}{\pi x}$$

$$\begin{aligned}
 \mathcal{F}\{rect(x)\} &= \int_{-1/2}^{1/2} 1 \times e^{-j2\pi ux} dx \\
 &= \frac{-1}{j2\pi u} e^{-j2\pi u} \Big|_{-1/2}^{1/2} \\
 &= -\frac{1}{j2\pi u} [e^{-j\pi u} - e^{j\pi u}] \\
 &= \frac{\sin \pi u}{\pi u}
 \end{aligned} \tag{6}$$



e.g., a square detector having width D and PSF h can be described by the following equation

$$f(x, y) \rightarrow [h] \rightarrow g(x, y)$$

where, $h(x, y) = rect(\frac{x}{D})rect(\frac{y}{D})$ and $H(u, v) = D^2 \text{sinc}(Dx)\text{sinc}(Dy)$

1.10 Hankel Transform

Rotation(Rotate same angle in Fourier domain)

$$x' = x\cos\theta - y\sin\theta$$

$$y' = x\sin\theta + y\cos\theta$$

Circular Symmetry

- 2D signal is circularly symmetric if $f_\theta(x, y) = f(x, y)$ for every θ

- $\mathcal{F}_{2D}(f_\theta)(u, v)$ is also circularly symmetric
- $f(x, y)$ and $F(u, v)$ are functions of radii only

$$f(x, y) = f(r)$$

and

$$F(u, v) = F(q)$$

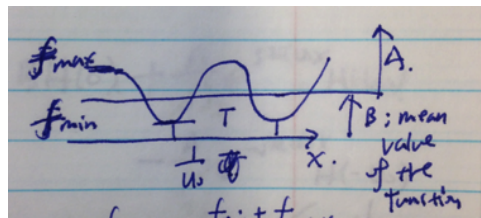
Hankel Transform

$$\mathcal{H}\{\exp(-\pi r^2)\} = \exp\{-\pi q^2\}$$

A Fourier transform of a Gaussian is a Gaussian.

2 Image Quality

2.1 Contrast and Modulation



Sinusoidal image brightness function:

$$f(x) = A \sin(2\pi u_0 x)$$

and

$$f_{mean} = \frac{f_{min} + f_{max}}{2} = B, \text{Amplitude} = \frac{f_{max} - f_{min}}{2} = A$$

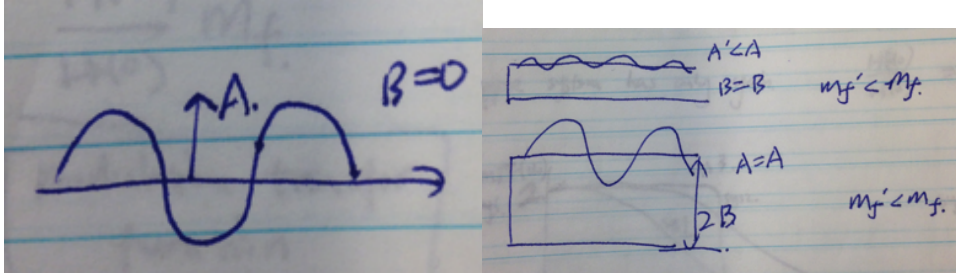
Thus, the image brightness function is

$$f(x) = B + A \sin(2\pi u_0 x)$$

And the contrast is

$$m_f = contrast = \frac{amplitude}{average} = \frac{A}{B} = \frac{\frac{f_{max}-f_{min}}{2}}{\frac{f_{min}+f_{max}}{2}} = \frac{f_{max}-f_{min}}{f_{min}+f_{max}}$$

e.g., a signal centered at 0 would have its contrast undefined?



Now let's consider expressing $g(x)$ in time domain. For that, we need to rewrite the signal $\sin(2\pi u_0 x) = \frac{1}{2j}(e^{-j2\pi u_0 x} - e^{j2\pi u_0 x})$.

$$\begin{aligned}
 f(x) \rightarrow [H(u)] \rightarrow g(x) &= BH(0) + \frac{A}{2j}e^{-j2\pi u_0 x}H(u_0) - \frac{A}{2j}e^{+j2\pi u_0 x}H(-u_0) \\
 &= BH(0) + \frac{A}{2j}|H(u_0)|[e^{-j(2\pi u_0 x - \angle H(u_0))} - e^{j(2\pi u_0 x + \angle H(-u_0))}] \\
 &= BH(0) + A|H(u_0)|\sin(2\pi u_0 x + \angle H(u_0))
 \end{aligned} \tag{7}$$

and,

$$H(u_0) = |H(u_0)|e^{j\angle H(u_0)}$$

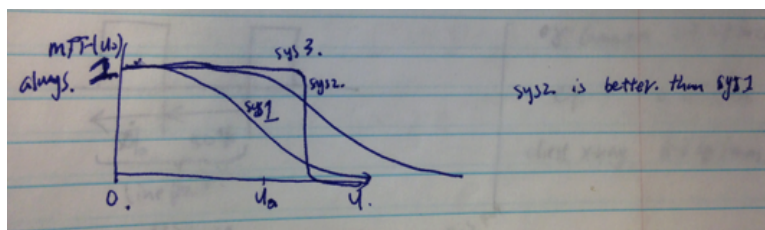
Contrast: modulation of the output

$$m_g = \frac{A|H(u_0)|}{BH(0)} = \frac{|H(u_0)|}{H(0)}m_f$$

Modulation Transfer Function

$$MTF = \frac{m_g}{m_f} = \frac{|H(u, 0)|}{H(0, 0)}$$

If a system has only gain, its MTF is 1.



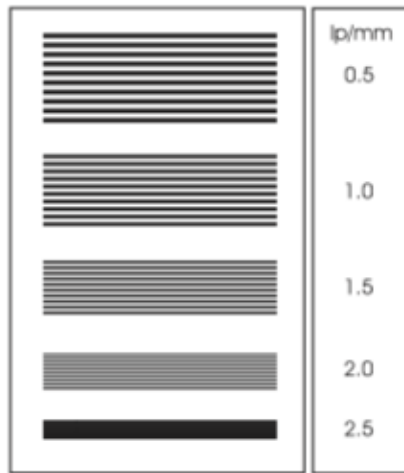
Local Contrast

$$C = \frac{f_t - f_b}{f_b}$$

where f_t is the target intensity and f_b is the background intensity.

2.2 Resolution

Resolution is defined as the highest line density such that lines can be distinguished.



Units:

- gamma camera: 2-3 lp/**cm**
- CT: 2 lp/mm
- chest x-ray: 6-8 lp/mm

Line function, $f(x, y)$

$$f(x, y) = \delta_l(x, y) = \delta(x) \int_{-\infty}^{\infty} \delta(y) dy = \int_{-\infty}^{\infty} \delta(x) \delta(y) dy = \int_{-\infty}^{\infty} \delta(x, y) dy$$

$$\begin{aligned}
g(x, y) &= \int_{-\infty}^{\infty} \int_{-\infty}^{\infty} [h(\xi, \eta) \delta_l(x - \xi, y - \eta)] d\xi d\eta \\
&= \int_{-\infty}^{\infty} \int_{-\infty}^{\infty} [h(\xi, \eta) \delta(x - \xi)] d\xi d\eta \\
l(x) &= \int_{-\infty}^{\infty} h(x, \eta) d\eta
\end{aligned} \tag{8}$$

where, $l(x)$ is the **Line Spread Function(LSF)**.

Note that $l(x) = l(-x)$ and $\int_{-\infty}^{\infty} l(x) dx = 1$

$$\begin{aligned}
\mathcal{F}\{l(x)\} &= \int_{-\infty}^{\infty} \left[\int_{-\infty}^{\infty} h(x, y) dy \right] e^{-j2\pi ux} dx \\
&= \int_{-\infty}^{\infty} \int_{-\infty}^{\infty} h(x, y) e^{-j2\pi ux} e^{-j2\pi 0y} dx dy \\
L(u) &= H(u, 0)
\end{aligned} \tag{9}$$

Therefore, MTF can also be expressed using $L(u)$ as follows:

$$MTF(u) = \frac{|L(u)|}{L(0)} = \frac{|H(u, 0)|}{H(0, 0)}$$

e.g., $h(x) = e^{-\frac{x^2}{2\sigma^2}}$

To find its FWHM, first calculate $x_{1/2}$

$$\frac{1}{2} = e^{-\frac{x_{1/2}^2}{2\sigma^2}} \Rightarrow x_{1/2} = \sqrt{2\sigma^2 \ln 2} = 1.1776 \Rightarrow FWHM = 2 \times 1.1776$$

2.3 Noise

- Typical imaging model:

$$g(x, y) = f(x, y) * h(x, y) + N(x, y)$$

- $N(x, y)$ is noise
- $N(x, y)$ is a random variable at each (x, y)

- $N(x,y)$ could be continuous or discrete
- Probability Distribution Function (PDF)

$$P_N(\eta) = Pr[N \leq \eta]$$

Continuous Random Variables

- Probability density function(pdf):

$$p_N(\eta) = \frac{dP_N(\eta)}{d\eta}$$

- Mean:

$$\mu_N = \int_{-\infty}^{\infty} \eta p_N(\eta) d\eta$$

- Variance:

$$\sigma_N^2 = \int_{-\infty}^{\infty} (\eta - \mu_N)^2 p_N(\eta) d\eta$$

- Standard deviation:

$$\sigma_N = \sqrt{\sigma_N^2}$$

Gaussian Random Variable

- pdf

$$p_N(\eta) = \frac{1}{\sqrt{2\pi\sigma^2}} e^{-\frac{(\eta-\mu)^2}{2\sigma^2}}$$

- mean:

$$\mu_N = \mu$$

- variance:

$$\sigma_N^2 = \sigma^2$$

- standard deviation:

$$\sigma_N = \sigma$$

Discrete Random Variables

- Probability mass function(PMF):

$$p_N(\eta_i) = Pr[N = \eta_i]$$

- Mean:

$$\mu_N = \sum_{all\eta_i} \eta_i p_N(\eta_i)$$

- Variance:

$$\sigma_N^2 = \sum_{all\eta_i} (\eta_i - \mu_N)^2 p_N(\eta_i)$$

- Standard deviation:

$$\sigma_N = \sqrt{\sigma_N^2}$$

Poisson Random Variable

- Probability mass function(PMF):

$$p_N(k) = \frac{a^k e^{-a}}{k!}, \text{ for } k = 0, 1, \dots$$

- Mean:

$$u_N = a$$

- Variance:

$$\sigma_N^2 = a$$

- Standard deviation

$$\sigma_N = \sqrt{a}$$

Expectation

$$E[f(N)] = \int_{-\infty}^{\infty} f(\eta) p_N(\eta) d\eta$$

$$\mu_N = E[N]$$

$$\sigma_N^2 = E[(N - \mu_N)^2]$$

$$\sigma_N^2 = E[N^2] - \mu_N^2$$

Sum of Independent Random Variables

- Let N and M be joint random variables

- Let $Q = N + M$

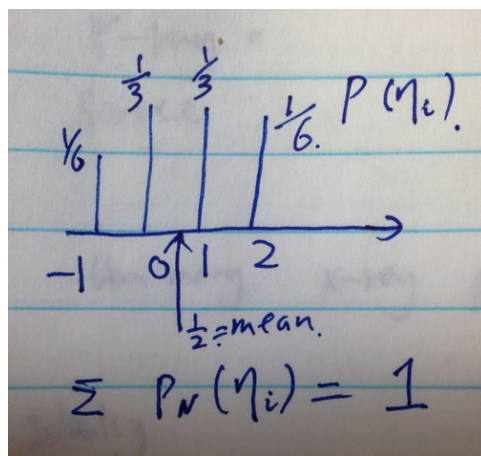
- Then

$$\mu_Q = \mu_N + \mu_M$$

- If N and M are independent then

$$\sigma_Q^2 = \sigma_N^2 + \sigma_M^2$$

e.g., Given the following probability mass function, calculate the mean and variance.



Mean:

$$\mu_N = \sum_{all \eta_i} \eta_i p_N(\eta_i) = (-1)(1/6) + (0)(1/3) + (1)(1/3) + (2)(1/6) = \frac{1}{2}$$

Variance:

$$\sigma_N^2 = \sum_{all \eta_i} (\eta_i - \mu_N)^2 p_N(\eta_i) = E[N^2] - \mu_N^2 = (-1)^2(1/6) + (0)^2(1/3) + (1)^2(1/3) + (2)^2(1/6) - (1/2)^2 = \frac{11}{12}$$

Signal In Noise

- Signal is f
- Noise if N

- Signal-to-noise ratio

$$SNR_a = \frac{amplitude(f)}{amplitude(N)}$$

$$SNR_p = \frac{power(f)}{power(N)}$$

- SNR in decibels

$$SNR(dB) = 20\log_{10}SNR_a$$

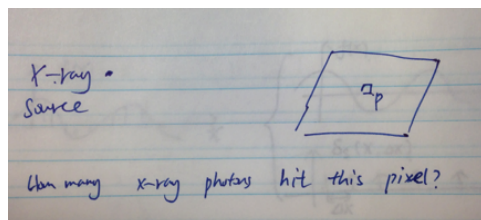
$$SNR(dB) = 10\log_{10}SNR_p$$

- Common example of SNR

- signal height is A
- noise standard deviation is σ_N
- SNR is then

$$SNR_a = \frac{A}{\sigma_N}$$

e.g., given a point x-ray source, how many x-ray photons hit this pixel?

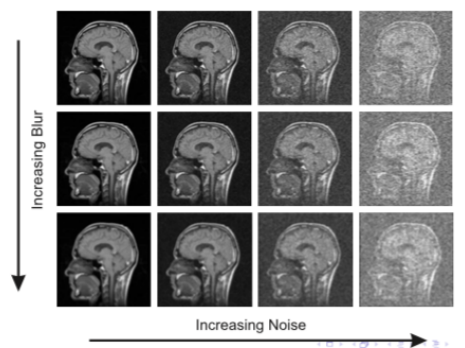


Soln:

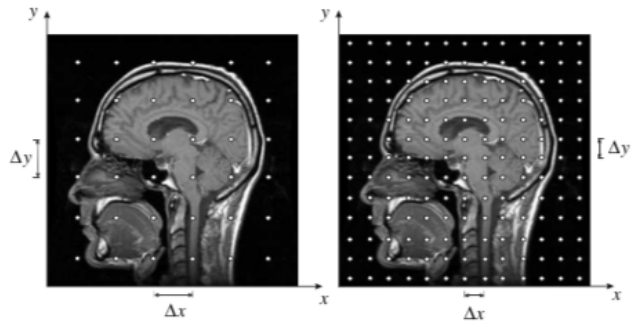
Ideally, whatever number of photons you can get.

Actually, the number of photons you get is a Random variable (R.V.).

Noise and Blurring Degrade Quality

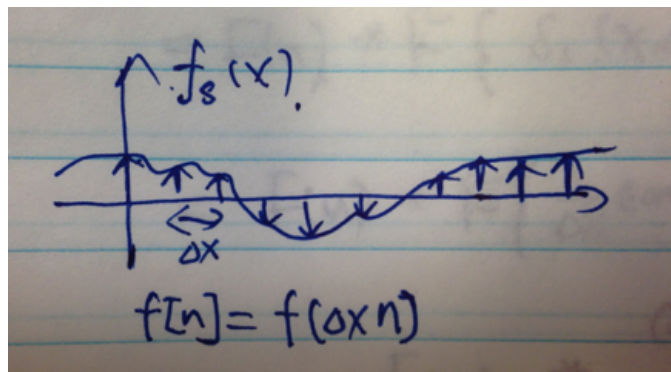


2.4 Sampling



- Point Sampling

$$f[m, n] = f(m\Delta x, n\Delta y)$$



Impulse Trains

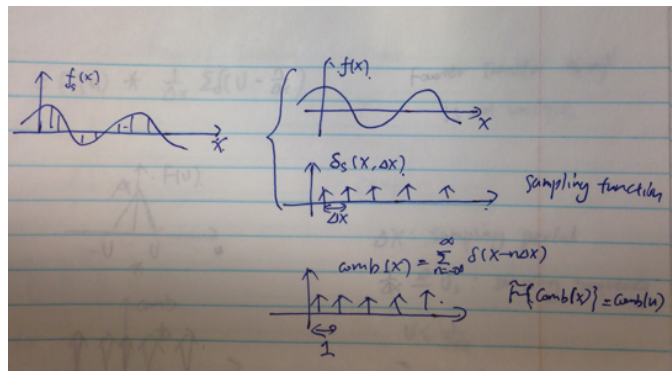
- Impulse train or comb or shah function:

$$\text{comb}(x) = \sum_{n=-\infty}^{\infty} \delta(x - n)$$

- Fourier transform of comb

$$\mathcal{F}\{\text{comb}(x)\} = \text{comb}(u)$$

- Impulse scaling property:



we know that

$$\mathcal{F}\{\delta(x)\} = 1$$

$$\mathcal{F}\{f(ax)\} = \frac{1}{|a|} F\left(\frac{u}{a}\right) \text{ and } \mathcal{F}\{\delta(ax)\} = \frac{1}{|a|} \text{ and } \mathcal{F}\left\{\frac{1}{|a|}\delta(x)\right\} = \frac{1}{|a|}$$

So we can infer the following expression:

$$\boxed{\delta(ax) = \frac{1}{a}\delta(x)}$$

which shows the **Impulse Scaling Property**

- Relation(sampling function) to shah/comb function:

$$\sum_{n=-\infty}^{\infty} \delta(x - n\Delta x) = \sum_{n=-\infty}^{\infty} \delta\left(\Delta x\left(\frac{x}{\Delta x} - n\right)\right) \quad (10)$$

$$= \sum_{n=-\infty}^{\infty} \frac{1}{\Delta x} \delta\left(\frac{x}{\Delta x} - n\right) \quad (11)$$

$$\delta_s(x, \Delta x) = \frac{1}{\Delta x} \text{comb}\left(\frac{x}{\Delta x}\right) \quad (12)$$

- Sampled signal

$$f_s(x) = f(x)\delta_s(x; \Delta x)$$

- $f_s(x)$ contains the same information as

$$f[k] = f(k\Delta x)$$

- Fourier transform of sampling function, $f_s(x)$

$$F_s(u) = F(u) * \mathcal{F}\{\delta_s(x; \Delta x)\} \quad (13)$$

$$= F(u) * \mathcal{F}\left\{\frac{1}{\Delta x} \text{comb}\left(\frac{x}{\Delta x}\right)\right\} \quad (14)$$

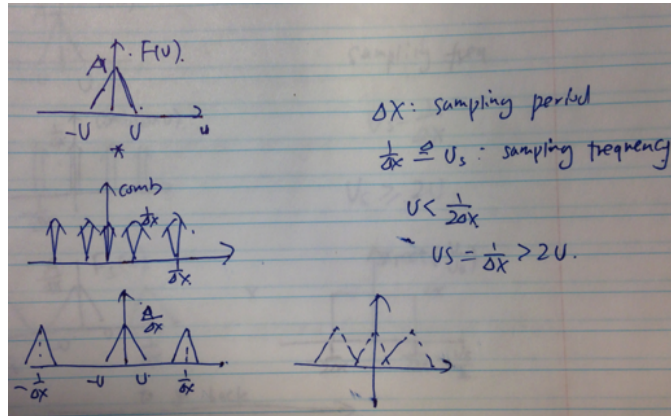
$$= F(u) * \text{comb}(\Delta xu) \quad (15)$$

$$= F(u) * \sum_{n=-\infty}^{\infty} \delta(\Delta xu - n) \quad (16)$$

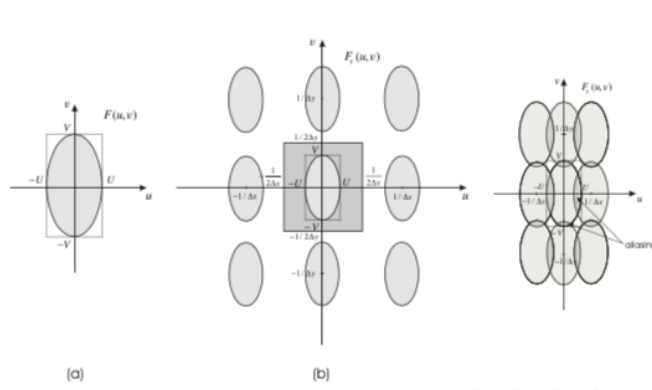
$$= F(u) * \frac{1}{\Delta x} \sum_{n=-\infty}^{\infty} \delta(u - \frac{n}{\Delta x}) \quad (17)$$

- Sampled spectrum is therefore:

$$F_s(u) = \frac{1}{\Delta x} \sum_{n=-\infty}^{\infty} F(u) * \delta(u - \frac{n}{\Delta x})$$



- Sampled spectrum in 2D



2.5 Sampling Theorem

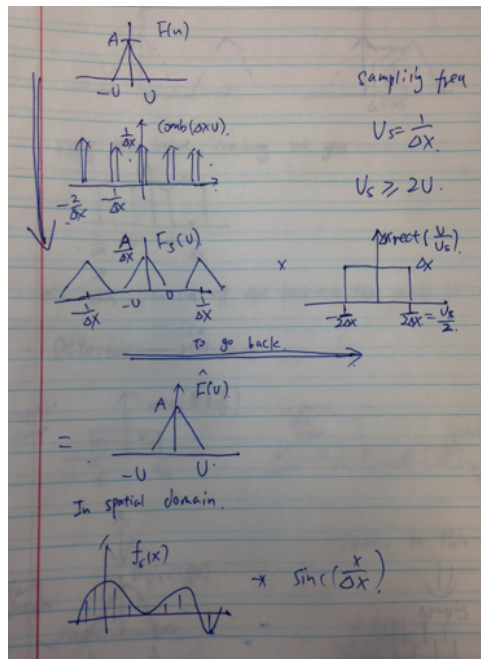
- The spatial sampling frequency is:

$$u_s = \frac{1}{\Delta x}$$

- Let U be the highest frequency in $F(u)$.
- Then Sampled spectra do not overlap if

$$u_s > 2U$$

- $2U$ is called the Nyquist rate

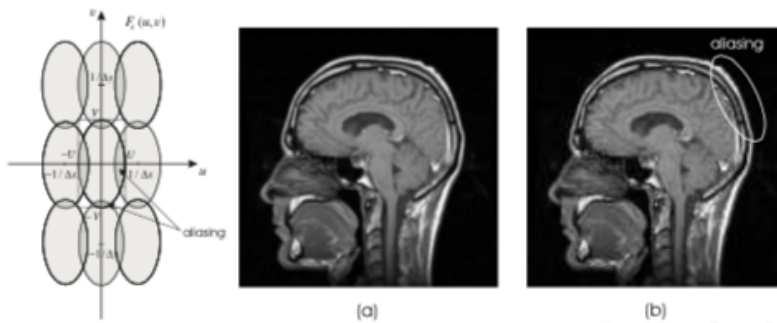


2.6 Aliasing

Aliasing occurs if

$$u_s < 2U$$

- Overlapping sampled spectra.
- Corruption of high frequencies
- Artifacts are high frequency patterns



Anti-aliasing Filters

- $u_s = \frac{1}{\Delta x}$
- Highest frequency in $f(x)$ is U .
- Need to filter the signal $f(x)$ before sampling.
- Use low pass filter with cutoff frequency $u_s/2$

2.7 Area Detector Analysis

- Shape of detector: $p(x)$ [maybe $\text{rect}(x/D)$]
- Area detector sampling model:

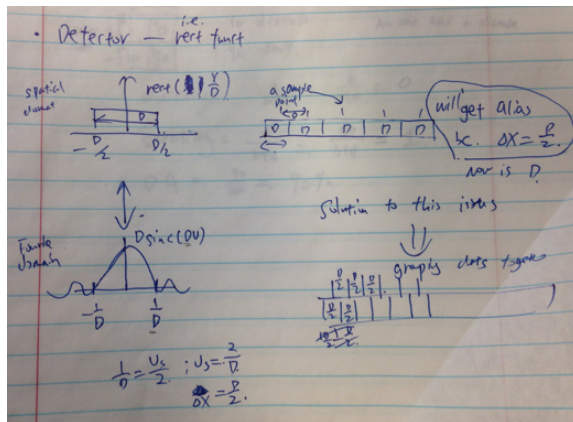
$$f_s(x) = [p(x) * f(x)]\delta_s(x; \Delta x)$$

- Fourier domain:

$$F_s = [P(u)F(u)] * \text{comb}(\Delta xu) \quad (18)$$

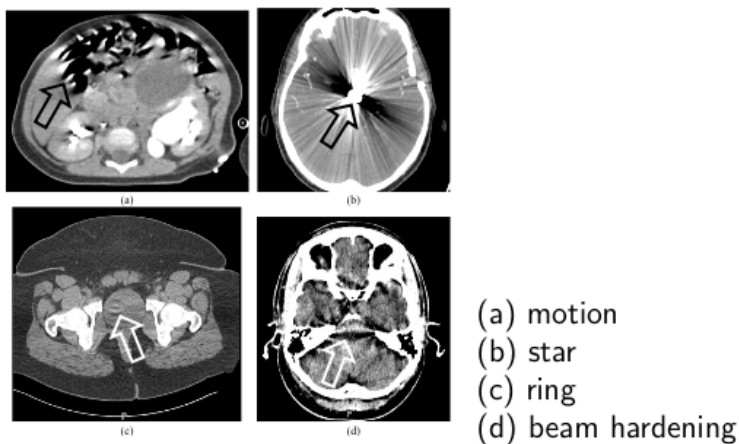
$$= [P(u)F(u)] * \frac{1}{\Delta x} \sum_{n=-\infty}^{\infty} \delta(u - \frac{n}{\Delta x}) \quad (19)$$

e.g. A detector represented by a rect function having aliasing can be anti-aliased by grouping them together.



2.8 Artifacts

- Artifacts: image features that do not correspond to a real object, and are not due to noise
 - star artifact, beam hardening artifact, ring artifact, ghosts
- Distortion: geometric or intensity changes not corresponding to the real object
 - magnification, barrel or pincushion distortion, quantization, saturation



2.9 Accuracy

- Accuracy: 1. Conformity to truth(quantitative accuracy) 2. clinical utility(diagnostic accuracy)
- Quantitative accuracy: 1. Numerical accuracy(bias, precision) 2. Geometric accuracy(dimensions)
- Diagnostic accuracy(accurate diagnosis of disease)

Diagnostic Quality

- Contingency table:

		Disease	
		+	-
Test	+	a	b
	-	c	d

- Variables:

$$\begin{aligned}
 a &= \# \text{ w/ disease \& test says disease} \\
 b &= \# \text{ w/o disease \& test says disease} \\
 c &= \# \text{ w/ disease \& test says normal} \\
 d &= \# \text{ w/o disease \& test says normal}
 \end{aligned}$$

Diagnostic Accuracy

- sensitivity = $\frac{a}{a+c}$
- specificity = $\frac{d}{b+d}$
- diagnostic accuracy = $\frac{a+d}{a+b+c+d}$

Disease Prevalence

- positive predictive value = $\frac{a}{a+b}$
- negative predictive value = $\frac{d}{c+d}$
- prevalence = $\frac{a+c}{a+b+c+d}$

e.g.

e.g. 100 patients + disease	10/0	Assume our test tells us No one has a disease
Test	+ 0 0	
	0 0 0 0	
	- 10 90	
		90 don't.
		sensitivity = $\frac{a}{a+c} = \frac{0}{0+10} = 0$
		specificity = $\frac{d}{b+d} = \frac{90}{90+0} = 1$.
		DA = $\frac{90}{100} = 90\%$

3 Physics of Radiography

3.1 X-Ray Modalities

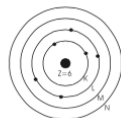
- Chest x-rays
- Mammography
- Dental x-rays
- Fluoroscopy
- Angiography
- Computed tomography
- These do not involve radioactivity

3.2 Atomic Structure

- nucleons = (protons, neutrons)
- mass number A is number of nucleons
- atomic number Z is number of protons
- nuclide is particular combination of nucleons

Electrons

Orbit in shells			
Shell Number n	Shell Label	# Electrons	$2n^2$
1	K	≤ 2	
2	L	≤ 8	
3	M	≤ 18	
4	N	≤ 32	



Electron Binding Energy

Definition: Nuclear binding energy is the energy required to split the nucleus of an atom into its component parts. The component parts are neutrons and protons, which are collectively called nucleons. The binding energy of nuclei is usually a positive number, since most nuclei require net energy to

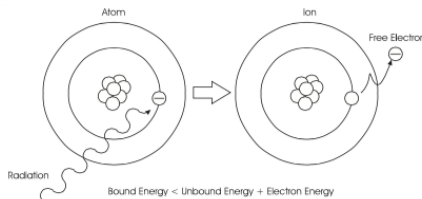
separate them into individual protons and neutrons. Thus, the mass of an atom's nucleus is usually less than the sum of the individual masses of the constituent protons and neutrons when separated. This notable difference is a measure of the nuclear binding energy, which is a result of forces that hold the nucleus together. During the splitting of the nucleus, some of the mass of the nucleus (i.e. some nucleons) gets converted into huge amounts of energy (according to Einstein's equation $E=mc^2$) and thus this mass is removed from the total mass of the original particles, and the mass is missing in the resulting nucleus. This missing mass is known as the mass defect, and represents the energy released when the nucleus is formed.

Facts

- Binding energy of hydrogen electron: 13.6 eV
- 1 eV is the kinetic energy gained by an electron that is accelerated across a one (1) volt potential

Ionization and Excitation

- Ionization is knocking an electron out of atom, which creates one electron and one ion
- Excitation is knocking an electron to a higher orbit



Characteristic Radiation

Definition: Ionized or excited atom returns to ground state by rearranging of electrons, which causes atom to give off energy. This energy is given off as characteristic radiation(infrared, light, and x-rays).

3.3 Ionizing Radiation

- Radiation with energy > 13.6 ev is ionizing
- Energy required to ionize:

- air =34 ev
- lead = 1 kev
- tungsten =4 kev

- Radiation energies in medical imaging 30 KeV-511KeV, which can ionize 10-40,000 atoms

Particulate Radiation

Definition: Particle radiation is the radiation of energy by means of fast-moving subatomic particles. Particle radiation is referred to as a particle beam if the particles are all moving in the same direction, similar to a light beam. Due to the wave-particle duality, all moving particles also have wave character. Higher energy particles more easily exhibit particle characteristics, while lower energy particles more easily exhibit wave characteristics. In the course, we are primarily concerned with electron(x-ray tube) and position in later chapters.

Note: an electron accelerated across 100 kV potential difference yields a 100 keV electron.

3.4 Electromagnetic EM Radiation

Definition: Electromagnetic radiation (EM radiation, EMR, or light) is a form of energy released by electromagnetic processes. In physics, all EMR is referred to as light, but colloquially light often refers exclusively to visible light, or collectively to visible, infrared and ultraviolet light. Classically, EMR consists of electromagnetic waves, which are synchronized oscillations of electric and magnetic fields that propagate at the speed of light. The oscillations of the two fields are perpendicular to each other and perpendicular to the direction of energy and wave propagation, forming a transverse wave. Electromagnetic waves can be characterized by either the frequency or wavelength of their oscillations to form the electromagnetic spectrum, which includes, in order of increasing frequency and decreasing wavelength: radio waves, microwaves, infrared radiation, visible light, ultraviolet radiation, X-rays and gamma rays. **Electromagnetic waves are produced whenever charged particles are accelerated**, and they can subsequently interact with any charged particles. EM waves carry energy, momentum and angular momentum away from their source particle and can impart those quantities to matter with which they interact. EM waves are massless, but they are still affected by gravity.

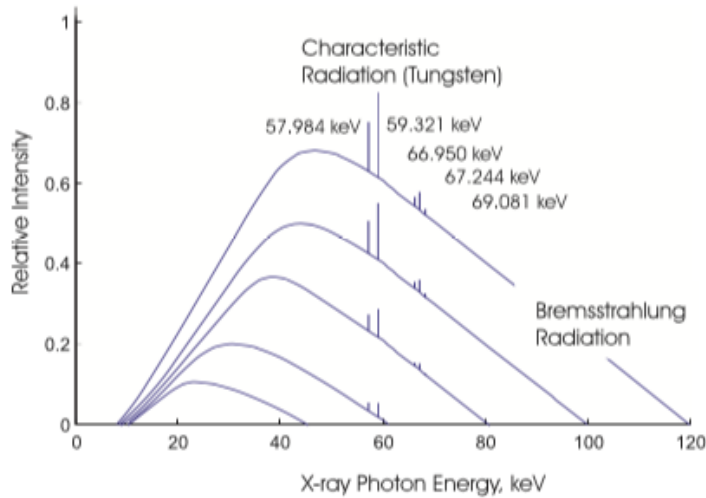
- Electric and magnetic wave at right angles

- waves with frequency ν , or
- "particles(photon)" with energy E

$$E = h\nu$$

- Planck's constant $h = 4.14 \times 10^{-15} \text{ ev} - \text{sec}$

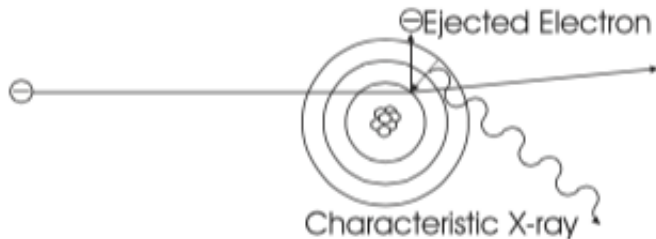
X-ray Spectrum



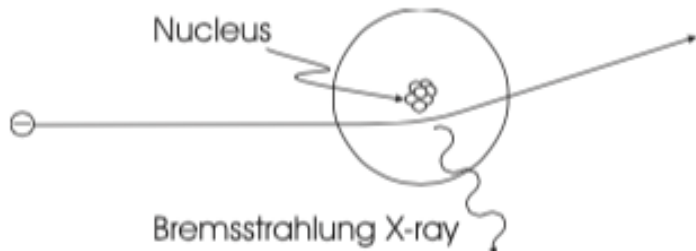
3.5 Energetic Electron Interactions

- Two primary interactions:
 - Collisional transfer
 - Radiative transfer
- Collisional transfer
 - Electron hits other electrons
 - Occasionally produces delta ray (secondary electrons with enough energy to escape a significant distance away from the primary radiation beam and produce further ionization)
- Two types of radiative transfer:

- characteristic x-rays (emitted from heavy elements when their electrons make transitions between the low energy atomic energy levels. Vacancies are produced and electrons drop down from above to fill the gap.)



- bremsstrahlung x-rays
 - * electron grazes nucleus, slows down
 - * energy loss generates x-ray



3.6 EM Interactions

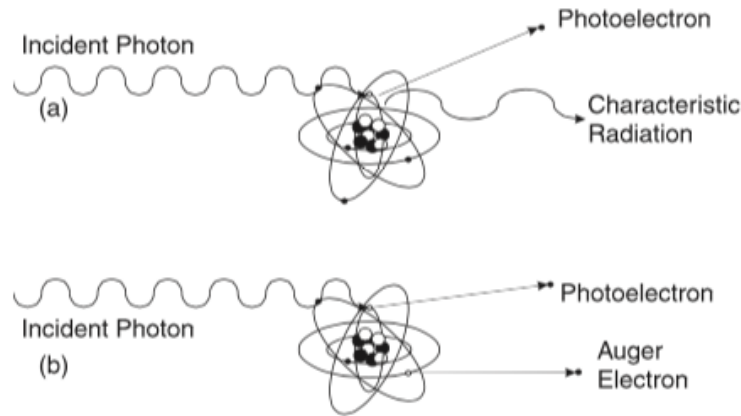
- Photoelectric effect
- Compton scattering

Photoelectric effect

- Atom completely absorbs incident photon
- All energy is transferred
- Atom produces
 - characteristic radiation, and/or

- energetic electron(s)
- Characteristic radiation might be
 - x-ray, or
 - light

Illustration of Photoelectric Effect



Auger Electron

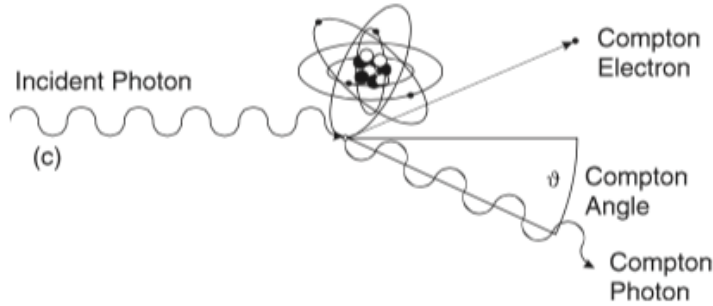
Definition: When a core electron is removed, leaving a vacancy, an electron from a higher energy level may fall into the vacancy, resulting in a release of energy. Although most of the time this energy is released in the form of an emitted photon, the energy can also be transferred to another electron, which is ejected from the atom. **Compton Scattering**

- Photon collides with outer-shell electron
- Photon is deflected, angle θ
- Deflected photon has lower energy:

$$E' = \frac{E}{1 + E \frac{1 - \cos\theta}{m_0 c^2}}$$

- m_0 is rest mass of electron
- $m_0 c^2 = 511 \text{ keV}$

Illustration of Compton Scattering



Probability of EM Interactions

- Photoelectric effect:

$$\text{Prob}[\text{photoelectric event}] \propto \frac{Z_{eff}^4}{(h\nu)^3}$$

- Photons are more penetrating at higher frequencies/energies
- Compton scattering:

$$\text{Prob}[\text{Compton event}] \propto ED$$

- ED is approximately constant over diagnostic range

3.7 Beam Strength: Photon Counts

- Photon fluence:

$$\Phi = \frac{N}{A}$$

- Photon fluence rate:

$$\phi = \frac{N}{A\Delta t}$$

Beam Strength: Energy Flow

- Energy fluence:

$$\Psi = \frac{N}{Ah\nu}$$

- Energy fluence rate:

$$\psi = \frac{Nh\nu}{A\Delta t}$$

- Intensity: ($= \psi$)

$$I(E) = \frac{NE}{A\Delta t}$$

Polyenergetic Beam Strength

- X-ray spectrum $S(E)$:

- $S(E)$ is the number of photons per unit area per unit energy per unit time

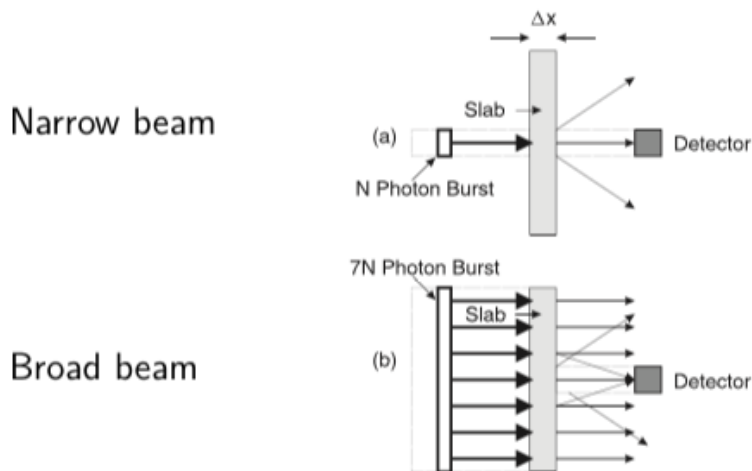
- Photon fluence rate from spectrum:

$$\phi = \int_0^{\infty} S(E')dE'$$

- Intensity from spectrum:

$$I = \int_0^{\infty} E' S(E')dE'$$

3.8 EM Attenuation Geometries



Monoenergetic

- Non-homogeneous slab:

$$\frac{dN}{N} = -\mu(x)dx$$

- Integration yields:

$$N(x) = N_0 \exp\left\{-\int_0^x \mu(x')dx'\right\}$$

- For intensity:

$$I(x) = I_0 \exp\left\{-\int_0^x \mu(x')dx'\right\}$$

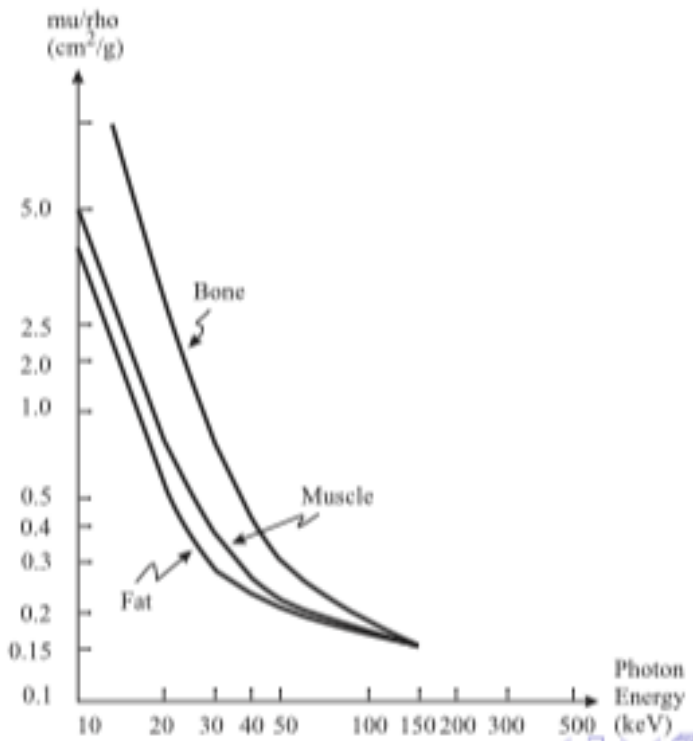
Polyenergetic

- Must deal with x-ray spectrum $S_0(E)$
- Abandon photon counting: use intensity
- For heterogeneous materials

$$I(x) = \int_0^\infty S_0(E')E' \exp\left\{-\int_0^x \mu(x'; E')dx'\right\} dE'$$

- Not very useful
- Better to define effective energy, use monoenergetic approximation

Mass Attenuation Coefficient, μ/ρ



3.9 EM Dose

Exposure: (the creation of ions)

- How many ions are created?
- Exposure X, the number of ion pairs produced in a specific volume of air by EM radiation
- SI Units: C/kg
- Common Units: roentgen, R

$$1C/kg = 3876R$$

Dose: (the deposition of energy)

- How much energy is deposited into material?
- Dose, D, the energy deposited per unit volume

- SI unit: Gray (Gy) $1 \text{ Gy} = 1 \text{ J/kg}$

- Common unit: rad

$$1\text{Gy} = 100\text{rads}$$

- When $X = 1 \text{ R}$ soft tissue incurs 1 rad absorbed dose.

Kerma

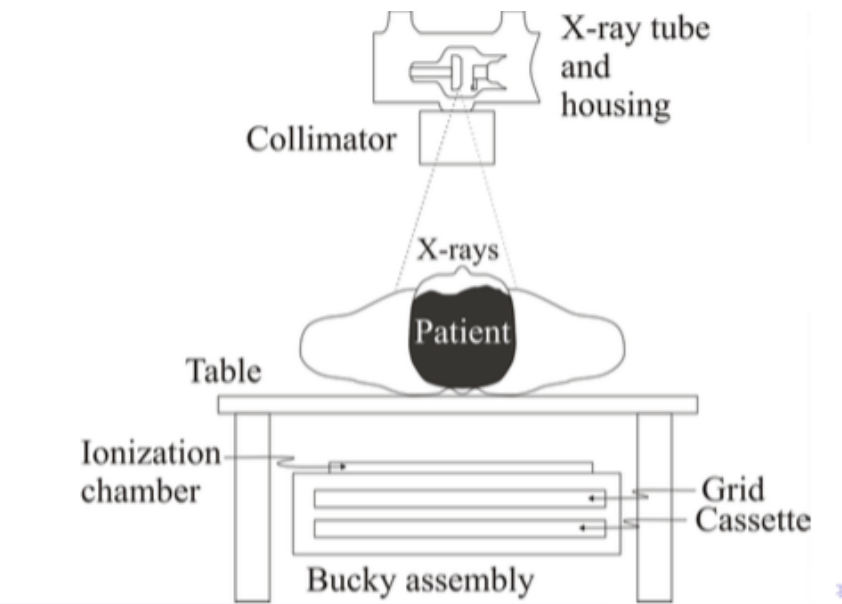
- Kerma, K, is the energy deposited into the electrons of a material
- At diagnostic energies in the body, $K(\text{kerma}) = D$ (dose)
- In general, $K \geq D$. Some electrons can cause bremsstrahlung and their energy irradiated away \Rightarrow no dose. Not likely in body.

4 Projection Radiography

Properties

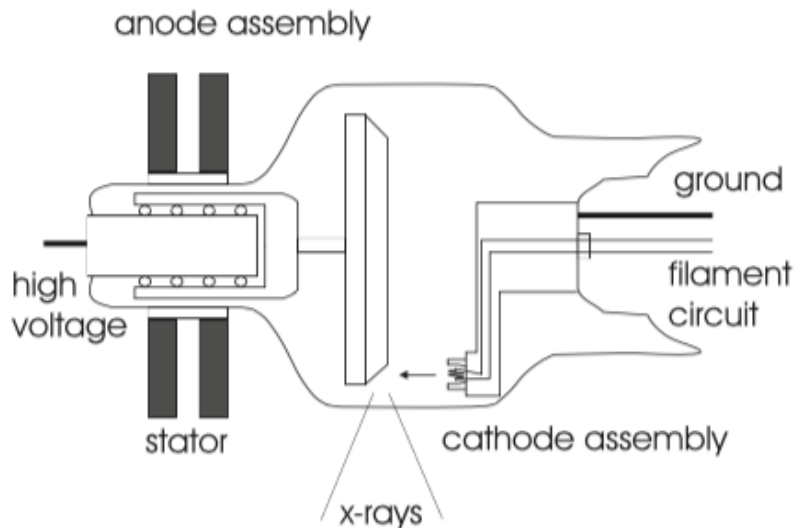
- High resolution
- Low dose
- Broad coverage
- Short exposure time

4.1 Radiographic System



4.2 X-ray Tube

A current, typically 3-5 amperes at 6-12 volts, is passed through a thin thoriated tungsten wire, called the *filament*, contained within the cathode assembly. Electrical resistance causes the filament to heat up and discharge electrons in a cloud around the filament through a process called *thermionic emission*. These electrons are now available to flow (i.e., be accelerated) toward the anode when the anode voltage is applied, producing the *tube current*, which is referred to as the *mA*. **The filament current directly controls the tube current because the filament current controls filament heat, which in turn determines the number of discharged electrons.** The x-ray control console is calibrated according to the tube current, which typically ranges between 50 and 1,200 mA.



Once the filament current is applied, the x-ray tube is primed to produce x-rays. This is accomplished by applying a high voltage, the *tube voltage* or *kVp*, between the anode and cathode for a brief period of time. The abbreviation kVp refers to the peak kilovoltage applied to the anode; the voltage ripple(temporal variation) below the peak value depends on the specific type of high-voltage generator in use. Typical values for the tube voltage lie in the range 30-150 kVp.

Focusing cup

Definition: A focusing cup is a small depression in the cathode containing the filament and is shaped to help focus the electron beam toward a particular spot on the anode. **X-ray Tube Components**

- Filament controls tube current(mA)
- Cathode and focusing cup
- Anode is applied a high voltage
 - 30-150 kVp
 - Made of tungsten
 - Bombarded by energetic electrons which transfer energy by both collisional and radiative transfer, resulting in both characteristic and bremsstrahlung x-rays.
 - Bremsstrahlung is 1 percent

- Head is 99 percent
- Spins at 3,200-3,600 rpm
- Glass housing; vacuum

Exposure control

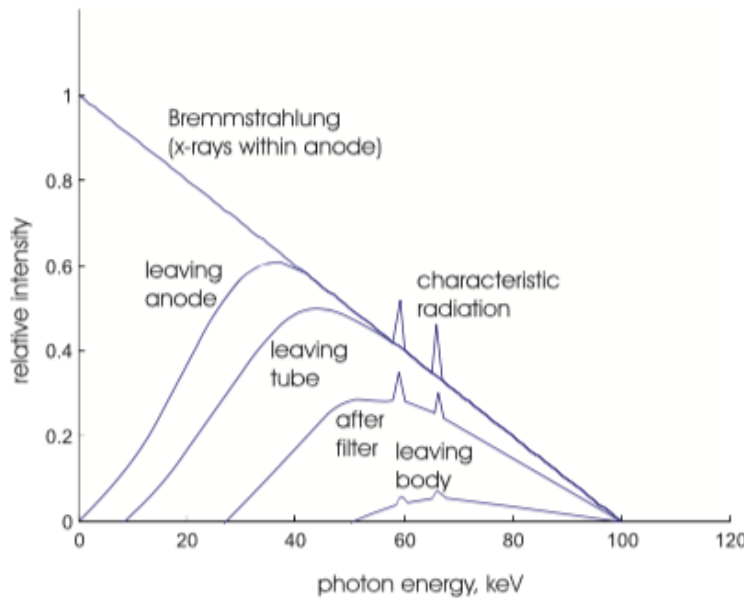
The overall exposure is determined by the duration of the applied kVp, which is controlled by either a fixed timer circuit or an automatic exposure control(AEC) timer. A fixed timer is generally a silicon-controlled rectifier(SCR) switch timed by a microprocessor. Timing accuracy for these circuits is approximately 0.001 seconds. AEC timers have 5-mm-thick parallel-plate ionization chambers placed between the patient table the film screen cassette. An ionization chamber is a radiation detector that generates a current when air molecules are ionized by x-rays passing through the chamber and the free electrons and ions are attached to anode and cathode plates, respectively, which are held at a constant voltage. The voltage achieved across the plates is used to trigger the SCR, which shuts off the tube voltage and terminates the exposure.

- Tube current mA controlled by filament current, and kVp
- mA times exposure time yields mAs

mAs measures x-ray exposure

- when a fixed timer is used, the radiologist controls both the mA and the exposure time directly and thereby determines the mAs for the exposure.
- In AEC timers, the mAs is set by the radiologist and the exposure time is determined automatically by the AEC circuitry. A maximum time is set to prevent accidental overdose in the event the AEC circuit malfunctions or the ionization chamber is missing or incorrectly positioned.

X-ray Spectra



The profile above shows a progressive shift in the position of the spectrum "to the right" (i.e., to higher average energies) as the beam passes through successive materials. This increase in the beam's "effective energy" is called **beam hardening**.

4.3 Filtration and Restriction

Definition: The bremsstrahlung x-rays that are generated within the anode do not all enter the patient, and not all that enter the patient end up leaving the patient. In this section, we discuss modifications to the x-ray beam that take place before the x-rays enter the body. **Filtration** is the process of absorbing low-energy x-ray photons before they enter the patient. **Restriction** is the process of absorbing the x-rays outside a certain field of view.

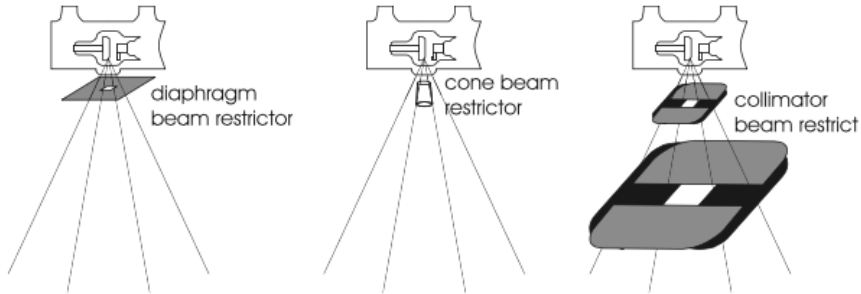
Filtration

The maximum energy of emitted x-ray photons is determined by the tube voltage. For example, if the tube voltage is 100 kVp, then the maximum photon energy is 100 keV (recall that an electron accelerated across 100 kV potential difference yields a 100 keV electron, and if this electron gets completely stopped by the nucleus, then its loss is equal to 100 keV, which is then dissipated as x-ray). Because the x-ray photons emitted from an x-ray tube have a distribution of energies, the x-ray sources used in medical imaging systems are **polyenergetic**.

- Inherent filtration
 - within anode
 - glass housing and dielectric oil that surrounds the x-ray tube(this effect might be accentuated over time since aging x-ray tube tend to accumulate a tungsten file on the inside of the housing due to vaporization of the filament during repeated heating)
- Added filtration
 - Aluminum(1-3mm thick)
 - For higher energy systems, copper might be used, but need to note that copper must be followed by aluminum in order to attenuate the 8 keV characteristic x-ray photons created within the copper.
 - Measured in mm Al/Eq

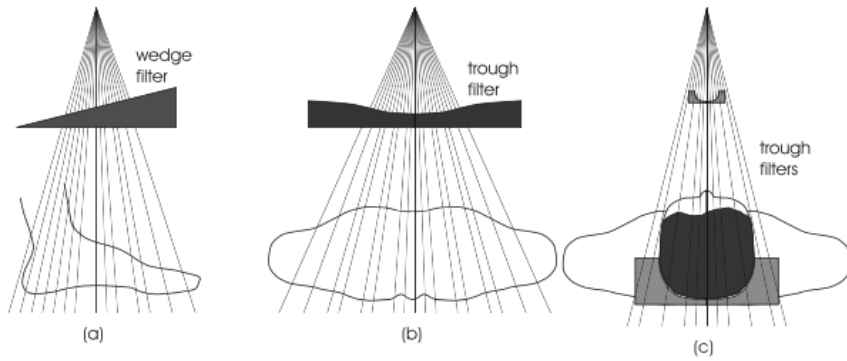
Restriction

- Goal: To direct beam toward desired anatomy.



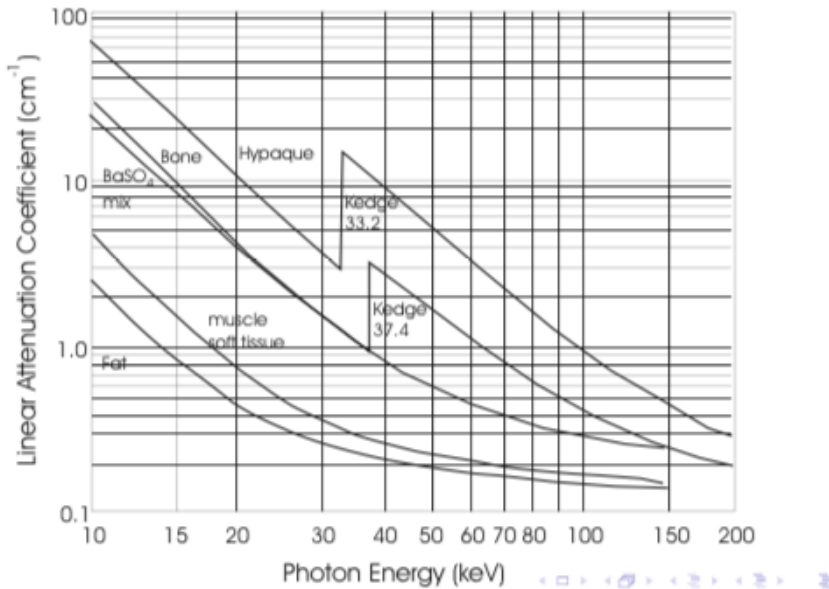
Compensation Filters

- To even out detector exposure



Contrast Agents

Definition: Different attenuation in the body gives rise to contrast in the x-ray image. Often, however, different soft tissue structures are difficult to visualize because of insufficient intrinsic contrast. This situation can be improved by using **contrast agents**-chemical compounds that are introduced into the body in order to increase x-ray absorption within the anatomical regions into which they are introduced, thereby enhancing x-ray contrast (compared with neighboring regions without such agents).



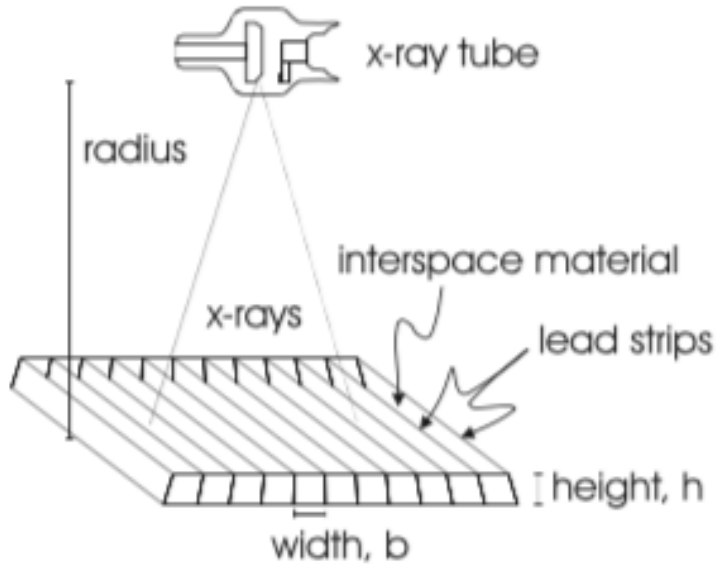
4.4 Scatter Control

- Ideal x-ray path: a line!!!

- Compton scattering causes blurring
- how to reduce scatter?
 - airgap
 - scanning slit
 - grid

Grid

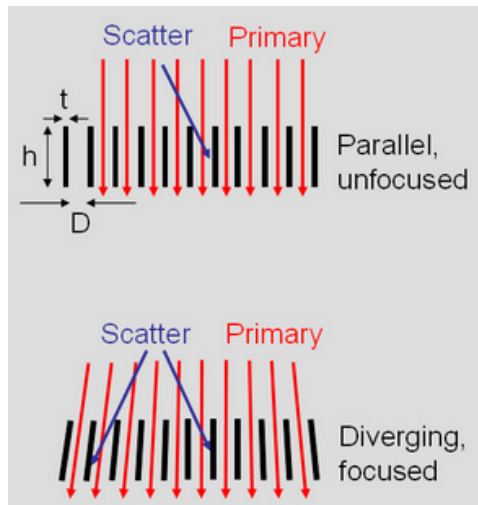
Definition: Scatter-reducing grids use thin strips of lead alternating with highly transmissive interspace material, typically aluminum and sometimes plastic. A typical x-ray grid is shown below.



- Effectiveness in scatter reduction?

$$\text{gridratio} = \frac{h}{b}$$

- 6:1 to 16:1 (radiography) or 2:1 (mammo)
- Grid spacing is generally reported using its reciprocal, which is known as grid frequency, which ranges from 60 cm^{-1} for conventional radiographic systems to as much as 80 cm^{-1} for mammography systems.



Problems with Grids

- Radiation is absorbed by grid as grid ration increases(the lead strips become more closely packed)
- the grid conversion factor(GCF) characterizes the amount of additional exposure required for a particular grid.

$$GCF = \frac{mAs \text{ with the grid}}{mAs \text{ without the grid}}$$

- Grid visible on x-ray detector
 - move grid during exposure
 - linear or circular motion

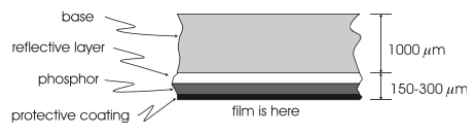
4.5 Film, Screen, and Cassette

Film-Screen Detectors In 1895, Roentgen discovered x-rays and made the first radiograph by allowing the x-rays to directly expose a photographic plate. X-rays can directly expose today's modern photographic film, but this is a very inefficient way to create a radiograph. In fact, only about 1-2 percent of the x-rays are stopped by the film, so creating radiographs by direct film exposure requires an unnecessarily large x-ray dose to the patient. To greatly improve their efficiency, film-based diagnostic x-ray units always have intensifying screens on both sides of the radiographic film. **The intensifying screen stops most of the x-rays and convert them to**

light, which then exposes the film. This is a very efficient process, and the screens cause only a small amount of additional image blurring.

4.5.1 Intensifying Screen

- Film stops only 1-2
- Film stops light really well



- Screens are used on both the front and back of the radiographic film, all parts of the screen except the phosphor must be uniformly radiolucent.
- Phosphor is the active part of an intensifying screen; its purpose is to transform x-ray photons into light photons.
- The light photons then travel into the film, causing it to be exposed and to form a latent image.
- The latent image is the virtual image resident in the file, but it is not yet viewable by human.

Phosphors

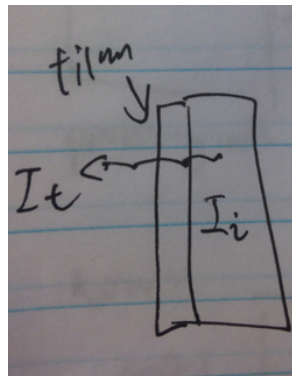
Definition: Phosphors are examples of materials that are luminescent; that is, they convert one form of energy, in this case x-rays, into light. Two types of luminescence are distinguished: fluorescence, in which the emission of light takes place entirely within $1 * 10^{-8}$ second of the excitation, and phosphorescence, in which light emission can be delayed and extended over a longer period of time. For screens, it is desirable to use a luminescent material that is much more fluorescent than phosphorescent. This way, there is little chance of an afterglow that might spoil the exposure by either motion after exposure or by light from a previous exposure.

The speed of a screen is really just a measure of its conversion efficiency. If the conversion efficiency is higher, then the screen is faster, because the larger numbers of light photons emitted by the phosphor will expose the film faster.

4.5.2 Radiographic Cassette

- Cassette holds two screens; makes "sandwich"
- one side is radiolucent, the other side includes a sheet of lead foil

4.5.3 Film



- Optical transmissivity

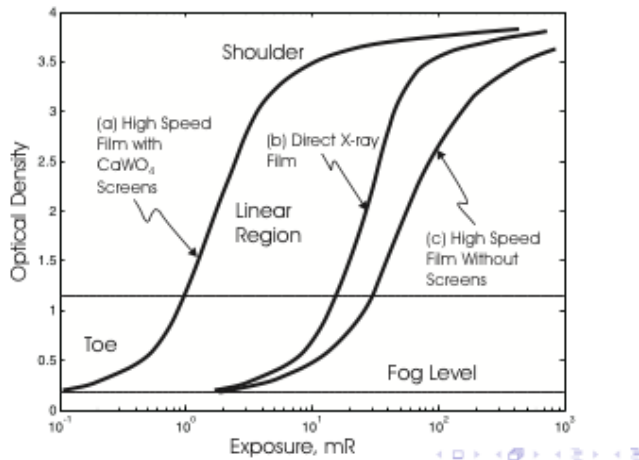
$$T = \frac{I_t}{I_i}$$

- Optical density

$$D = \log_{10} \frac{I_t}{I_i}$$

- $O = 1/T$ is optical opacity
- Usable density $0.25 \leq D \leq 2.25$
- Best densities $1 \leq D \leq 1.5$

H D Curve, optical density from x-ray exposure for film-screen combination

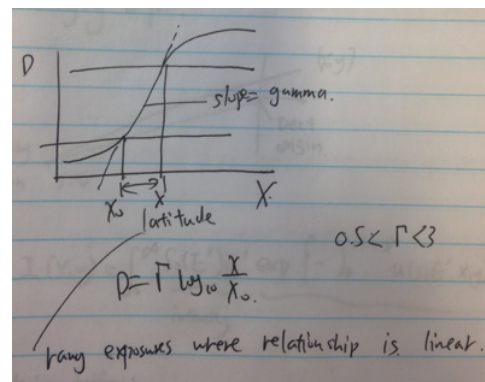


X-ray Exposure to Film Density

- X-ray exposure yields optical density

$$D = \Gamma \log_{10} \frac{X}{X_0}$$

- Γ is film gamma
- Typical ranges: $0.5 \leq \Gamma \leq 3.0$
- Latitude is range exposures where relationship is linear



- Speed is inverse of exposure at which

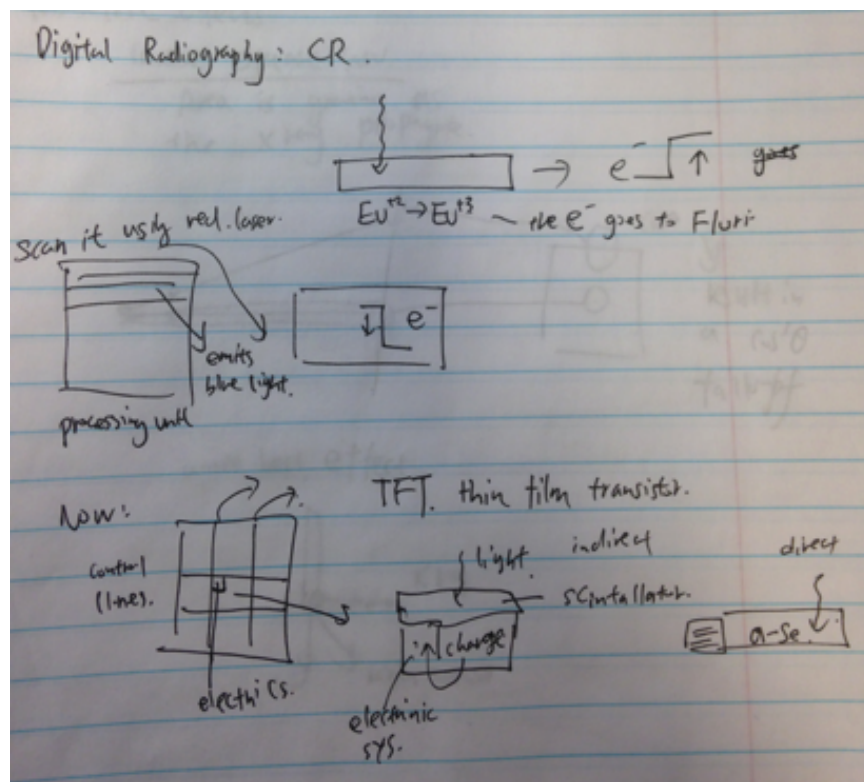
$$D = 1 + \text{fog level}$$

4.5.4 Digital Radiography: CR

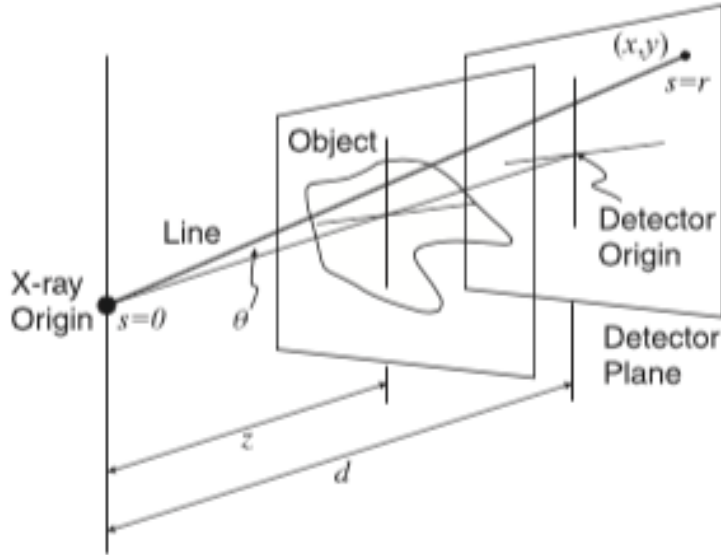
- Introduced in 1980's; replacing film
- Indirect systems: computed radiography (CR)
 - phosphor = barium fluorohalide bromide with europium activator
- Readout using read focused laser scanning device
 - Blue light is emitted in proportion to number of tapped electrons
- 10 pixels/mm, 16-bit word, 2K * 2K pixels

4.5.5 Digital Radiography: DR

- Direct systems: direct digital radiography(DR)
- Indirect:
 - x-rays to light using scintillator (e.g., CsI: TI)
 - light to charge using amorphous silicon (a-Si) photodetector
- Direct:
 - x-rays to charge using amorphous selenium(a-Se)
- Charge read out using thin film transistor(TFT)
- 8 pixels/mm, 16-bit word, 1K * 1K pixels



4.6 Basic Imaging Equation



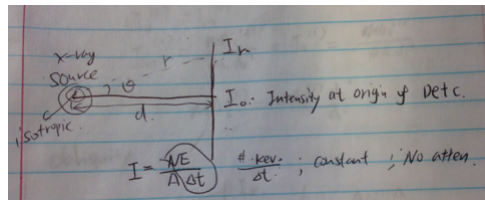
$$I(x, y) = \int_0^{\infty} S_0(E') E' \exp\left\{-\int_0^{r(x,y)} \mu(s; E', x, y) ds\right\} dE'$$

4.7 Geometric Effects

- X-rays are diverging from source
- Undesirable effects:
 - $\cos^3\theta$ falloff across detector
 - anode heel effect
 - pathlength irregularities
 - magnification
- I_0 is intensity at $(0, 0)$
- r is distance from (x, y) to x-ray origin
- θ is angle between $(0, 0)$ and (x, y)

4.7.1 Inverse Square Law

Consider isotropic burst of x-rays with intensity $I = NE/A\Delta t$ on a sphere.



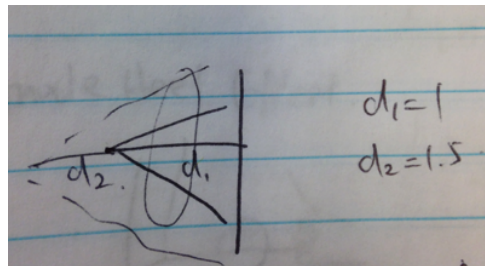
we know that IA is constant, so we have

$$I_0 4\pi d^2 = I_r 4\pi r^2$$

$$I_r = I_0 \frac{d^2}{r^2} = I_0 \cos^2 \theta$$

e.g., A density maintenance example

In the case of moving the source away to increase field of view.



Question: what mAs (proportional to the number of photons) do I need to keep the same intensity?

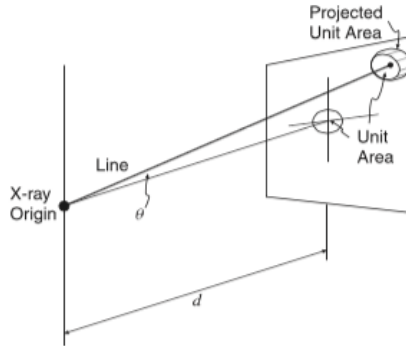
Soln: we want $I_0^{(2)} = I_0^{(1)}$, and we know that

$$I_0^{(2)} = \frac{mAs_s^{(2)}}{4\pi d_2^2} = I_0^{(1)} = \frac{mAs_s^{(1)}}{4\pi d_1^2}$$

therefore,

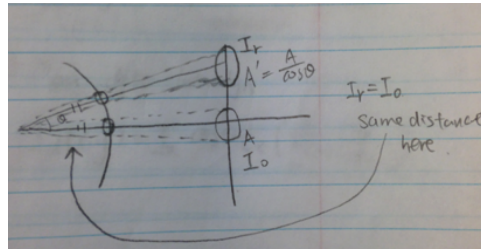
$$mAs_s^{(2)} = mAs_s^{(1)} \frac{d_2^2}{d_1^2}$$

4.7.2 Obliquity



$$I_d = I_0 \cos \theta$$

The following setup gives the proof of the above equation:



From the above setup, we know that

$$\frac{NE}{\Delta t} = I_0 A = I_r A'$$

$$I_r = I_0 \frac{A}{A'} = I_0 \frac{\frac{A}{\cos \theta}}{A} = I_0 \cos \theta$$

4.7.3 Beam Divergence and Flat Detector

- Inverse square law and obliquity combine

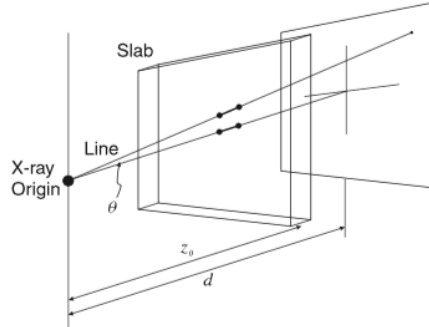
$$I_d(x_d, y_d) = I_0 \cos^3 \theta$$

- can usually be ignored. Why? Because detector is far away and field of view is often small

4.7.4 Anode Heel Effect

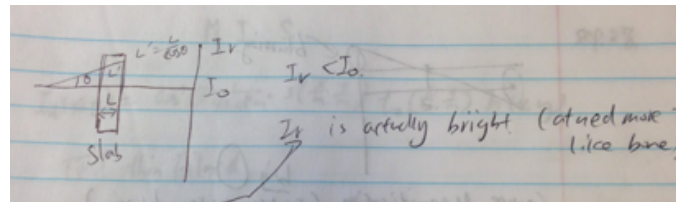
- Intensity within the x-ray cone
 - not uniform
 - stronger in the cathode direction
 - 45 percent variation is typical
 - compensate, use to advantage, or ignore
 - we will ignore in math

4.7.5 Path Length of Slab



Uniform slab yields different intensities

The following is the proof.



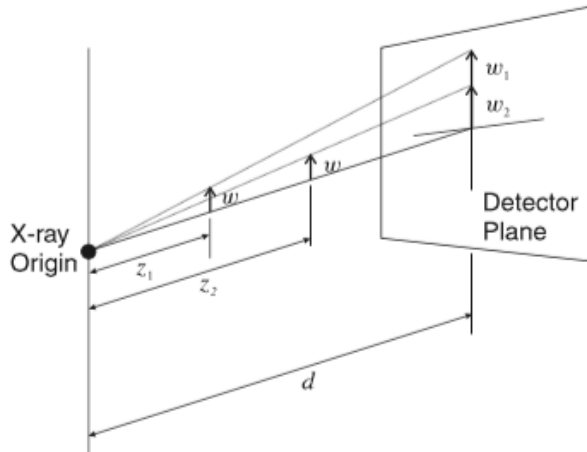
$$I_d(x_d, y_d) = I_0 \exp\left(-\frac{uL}{\cos\theta}\right)$$

Together with inverse law and obliquity, we have the following equation:

$$I_d(x_d, y_d) = I_0 \cos^3\theta \exp\left(-\frac{uL}{\cos\theta}\right)$$

4.7.6 Object Magnification

Size on detector depends on distance from source



$$\frac{w}{w_1} = \frac{z_1}{d}$$

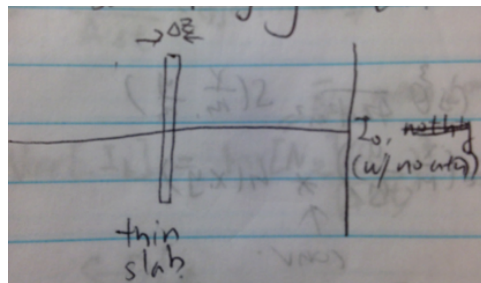
$$w_1 = w \frac{d}{z_1} = w M(z)$$

- Magnification is

$$M(z) = \frac{d}{z}$$

- Can lead to edge blurring and misleading sizes

4.7.7 Thin Slab Imaging Equation



Define **Transmittivity** to be

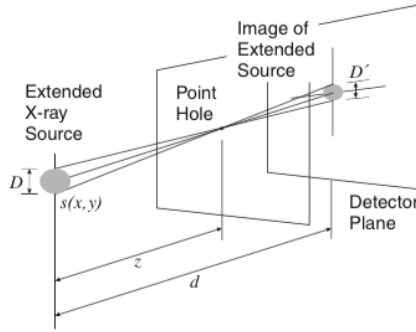
$$t_z(x, y) = \exp(-\mu(x, y)\Delta z)$$

So, on the detector, the intensity is

$$I_d(x_d, y_d) = I_0 \cos^3 \theta t_z \left(\frac{x}{M(z)}, \frac{y}{M(z)} \right) = I_0 \left(\frac{d}{\sqrt{d^2 + x^2 + y^2}} \right)^3 t_z \left(\frac{xz}{d}, \frac{yz}{d} \right)$$

4.7.8 Sources of Blurring

- Extended source



where $s(x, y)$ is the source spatial distribution

Source diameter on detector:

$$D' = -\frac{d-z}{z} D$$

Source magnification(negative sign means inverted):

$$m(z) = -\frac{d-z}{z} = 1 - M(z)$$

- Source Blurring

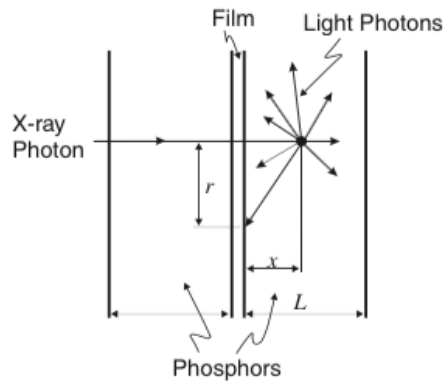
- Image of source through pinhole at z

$$I_d(x, y) = \frac{1}{4\pi d^2 m^2(z)} s\left(\frac{x}{m(z)}, \frac{y}{m(z)}\right)$$

- Intensity at detector:

$$I_d(x, y) = \frac{\cos^3 \theta}{4\pi d^2 m^2} t_z \left(\frac{x}{M}, \frac{y}{M} \right) * s\left(\frac{x}{m}, \frac{y}{m}\right)$$

- Film-Screen Blurring



Film-screen impulse response: $h(x, y)$

- Overall Imaging Equation

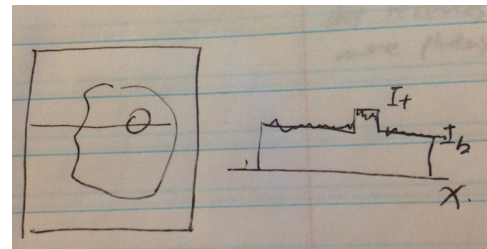
$$I_d(x, y) = \frac{\cos^3\theta}{4\pi d^2 m^2} t_z\left(\frac{x}{M}, \frac{y}{M}\right) * s\left(\frac{x}{m}, \frac{y}{m}\right) * h(x, y)$$

4.8 Noise

- Local Contrast,

$$C = \frac{I_t - I_b}{I_b}$$

- Signal is $I_t - I_b$



- Variance of noise in background: σ_b^2

- Signal to noise

$$SNR = \frac{I_t - I_b}{\sigma_b} = \frac{I_t - I_b}{I_b} \frac{I_b}{\sigma_b} = C \frac{I_b}{\sigma_b}$$

4.9 Signal-to-noise

- Model x-ray burst as monoenergetic
 - effective energy is $h\nu$
 - background intensity is therefore equal to

$$I_b = \frac{N_b h\nu}{A\Delta t}$$

N_b is Poisson random variable

- Expected value of I_b :

$$E[I_b] = \frac{\bar{N}_b E}{A\Delta t}$$

- Variance of I_b :

$$\text{Var}[I_b] = \text{Var}[N_b] \left(\frac{E}{A\Delta t} \right)^2 = \bar{N}_b \left(\frac{E}{A\Delta t} \right)^2$$

Note that $\text{Var}[N_b] = \bar{N}_b$ for Poisson

- Standard deviation of I_b

$$\text{std}[I_b] = \sqrt{\bar{N}_b} \frac{E}{A\Delta t}$$

- Signal-to-noise is

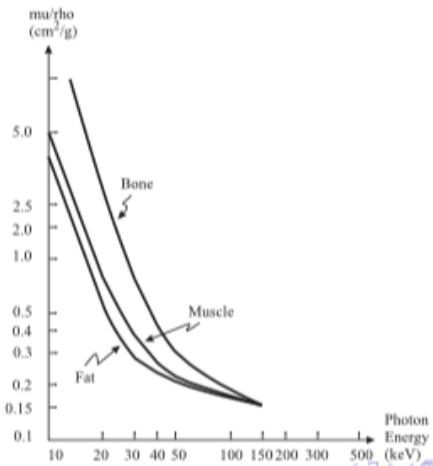
$$\text{SNR} = C \frac{\bar{I}_b}{\sigma_b} = \frac{C \frac{\bar{N}_b E}{A\Delta t}}{\sqrt{\bar{N}_b} \frac{E}{A\Delta t}} = C \sqrt{\bar{N}_b}$$

More Photons is better

Question: How to increase SNR? Two Options: either increase C or \bar{N}_b .

Option 1: To increase \bar{N}_b , one needs to increase tube current mAs , which results in higher average photon energy. As a result of that, the body becomes more transparent so detector receives more photons.

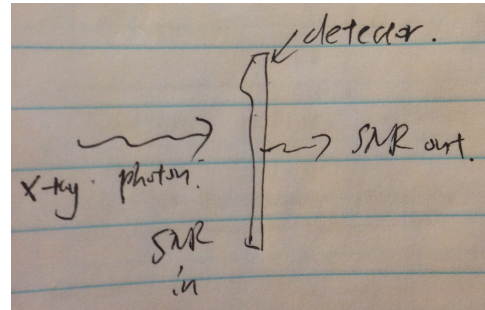
Option 2: Use contrast agent or decrease the average photon energy.



- Detective Quantum Efficiency

- How good is a detector?
- Quantum efficiency(QE):Probability of stopping a photon
- Detective quantum efficiency(DQE)

$$DQE = \left(\frac{SNR_{out}}{SNR_{in}} \right)^2$$



- * Degradation of SNR during detection
- * "fraction" of photons that are detected correctly

e.g., Given QE=0.5 and assume perfect detector response. Find the Detective Quantum Efficiency of the detector. Soln: $SNR_{in} = \sqrt{\bar{N}}$ and $SNR_{out} = \sqrt{0.5\bar{N}}$

$$DQE = \left(\frac{\sqrt{0.5\bar{N}}}{\sqrt{\bar{N}}} \right)^2 = 0.5$$

Note: This only happens with perfect detector response.
 e.g., given the following setup, find the Detective Quantum Efficiency of the detector.

$$DQE = \left(\frac{SNR_{out}}{SNR_{in}} \right)^2 = \left(\frac{\frac{8000}{\sqrt{40000}}}{\sqrt{10000}} \right)^2 = 0.16$$

What is QE? We don't know but we know for sure that

$$DQE \leq QE$$

4.10 Compton Scatter

- Compton scattering adds intensity fog; I_s

$$C' = \frac{I_t + I_s - (I_b + I_s)}{I_b + I_s} = \frac{I_t - I_b}{I_b + I_s} = \frac{I_t - I_b}{I_b} \frac{I_b}{I_b + I_s} = C \frac{I_b}{I_b + I_s} = \frac{C}{1 + \frac{I_s}{I_b}}$$

- Resulting SNR

$$SNR' = \frac{SNR}{\sqrt{1 + \frac{I_s}{I_b}}}$$

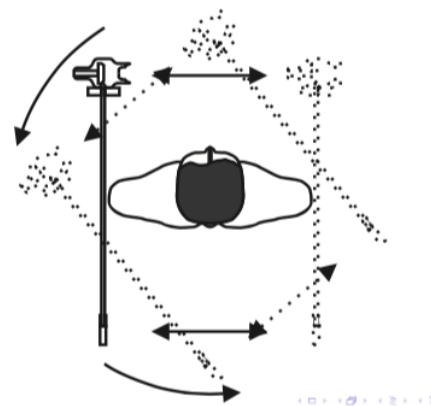
Scattering reduces contrast!!

5 Computed Tomography

5.1 Generations of CT Scanners

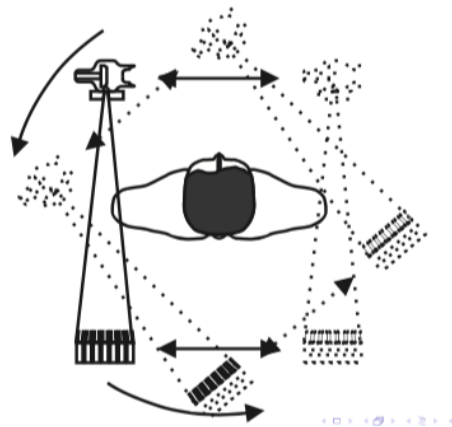
- 1G CT Scanner

Too slow, slide source and detector.



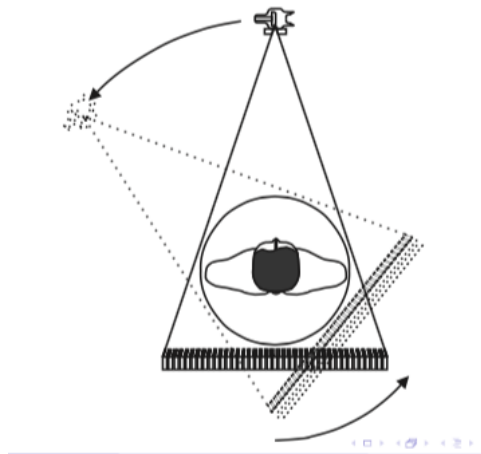
- 2G CT Scanner

More detectors, can move far in angular direction, some angles are captured already.



- 3G CT Scanner

700-1000 detectors, covers whole body

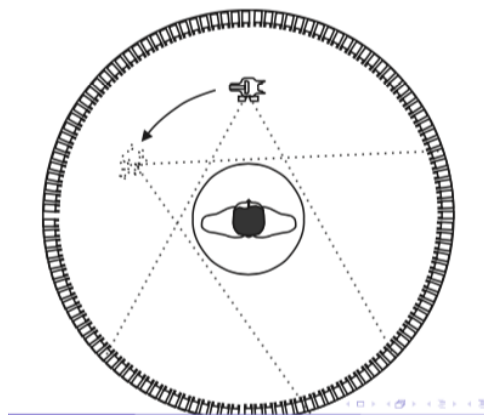


- 4G CT Scanner

No moving parts, but has scattering problem

This generation scanner has a single rotation source with a larger ring of stationary detectors. A variation on this theme has the source outside the detectors with slight gaps between the detectors through which the x-rays can be fired. **Collimation cannot be used in this**

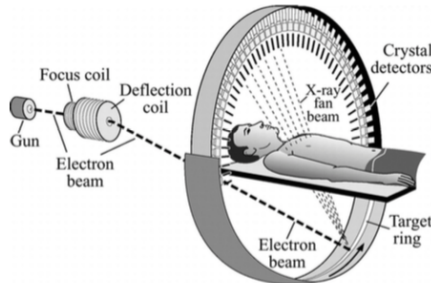
geometry since a detector must receive energy from a source that moves through many positions. Therefore, the detectors are highly susceptible to scattering. This factor is so significant that the image quality in 4G systems is only comparable to that of 3G systems, not better.



- 5G CT Scanner

Electron beam, tungsten in between detectors, expensive, hard to calibrate.

Electron beam computed tomography(EBCT) scanners use a flying electron beam, steered electronically, to hit one of four tungsten anode strips that encircle the patient. X-rays are generated when the electron beam strikes the tungsten anode; the resultant radiation is collimated into a fan-beam, which passes through the patient and is detected on the other side by a stationary ring of detectors, as in 4G CT systems. **Since the anodes and detectors are stationary, no moving parts are required, and this allows a full set of fan-beam projection data to be acquired in about 50 milliseconds.** EBCT is an expensive design, but because of the extremely small scan-time it is the only commercially available CT method that can capture stop-action images of a beating heart without electrocardiographic(ECG) gating.



- 6G CT Scanner

Helical path of the source

Helical CTs were developed in the late 1980s to address the need for rapid volumetric data acquisition. With helical CT, a full 60-cm torso scan can be obtained in about 30 seconds, a full 24-cm lung study in 12 seconds, and a detailed 15-cm angiography study in 30 seconds. A helical CT scanner consists of a conventional arrangement of the x-ray source and detectors(as in 3G and 4G systems) which can continuously rotate. While the tube is rotating and acquiring projection data, the patient table is set into motion, sliding the patient through the source-detector plane. The position of the source carves out a helix with respect to the patient. Continuous rotation of the large mass comprising the x-ray source and detectors requires what is called *slip ring* technology in order to communicate with the controlling stationary hardware. Power is provided using rings and brushes, while data are passed using optical links. Rotation periods are typically 0.3 to 0.5 seconds per revolution in modern scanners.

- 7G CT Scanner

A seventh-generation scanner has emerged with the advent of multiple-row detector CT(MDCT) scanners. In these scanners, a thick fan-beam is used, and multiple (axial) parallel rows of detectors are used to collect the x-rays within this thick fan. (some scanners have fan beams that are so thick they can be thought of as cone beams.)

- 16-320 parallel detector rows(each row contains 896 single solid state detectors 1.0mm by 1.25 mm in size)
- 20mm-400mm detector "height"
- 16-320 slices with each gantry revolution

- Dual-Energy CT

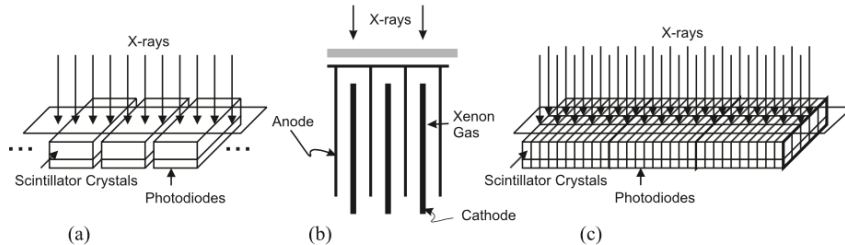
It's a way to gather more information about tissue characteristics since the linear attenuation of all tissues is a function of energy. The strategy is used in dual-energy x-ray absorptiometry projection scanning to determine bone mineral density in the diagnosis of osteoporosis.

5.1.1 X-ray Tubes in CT

- Use only one tube
 - exception: EBCT
 - exception: dual-source CT
- 80kVp-140kVp, continuous excitation
 - dual-energy is possible
- fan-beam(1-10mm thick), or
- thin-cone collimation 20-80 mm
- More filtering than projection radiography
 - copper followed by aluminum
 - better approximation to monoenergetic

5.2 CT Detectors

Most modern scanners use solid-state detectors. These detectors contain a scintillation crystal in the first stage, typically a cadmium tungstate, sodium iodide, bismuth germanate, yttrium-based, or cesium iodide crystal. X-ray interact with the crystal mainly by photoelectric effect, producing photo-electrons, similar to what happens to the phosphor in an intensifying screen. These electrons are excited and emit visible light when they spontaneously de-excite. This scintillation process results in a burst of light. The light is then converted to electric current using a solid-state photomultiplier tubes to convert light to electricity.



In 3G scanners, very small and highly directional detectors are required. Either solid-state detectors, or xenon gas detectors, as shown in fig(b). Xenon gas detectors use compressed xenon gas in long, thin tubes, which when ionized generate a current between an anode and cathode(maintained at a high potential difference).

- Single-slice scanners:
 - Area: 1.0 mm * 15.0 mm
 - Thick in 3G, thin in 4G and EBCT
- Multi-slice scanners:
 - Area: 1.0mm * 1.25 mm
 - Grouped in multiples of 1.25 mm
- Xenon gas detectors for less expensive scanners

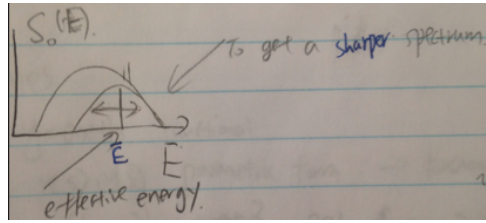
5.3 CT Measurement Model

- From Polyenergetic to Monoenergetic model

$$I_d = \int_0^{\infty} E S_0(E) \exp\left\{-\int_0^d \mu(s; E) ds\right\} dE = I_0 \exp\left\{-\int_0^d \mu(s; \bar{E}) ds\right\}$$

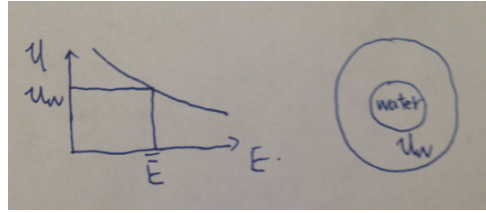
- \bar{E} is effective energy, which is that energy which in a given material will produce the same measured intensity from a monoenergetic source as from the actual polyenergetic source.

$$\bar{E} = \frac{\int_0^{\infty} E S_0(E) dE}{\int_0^{\infty} S_0(E) dE}$$



5.3.1 Line Integral

e.g., As shown below, one needs to calibrate the CT using a bucket of water, get μ_w and get \bar{E} .



we know that $S_0(E) = \frac{N_0\delta(E - \bar{E})}{A\Delta t}$ and

$$\begin{aligned}
 I_d &= \int_0^\infty E S_0(E) \exp\left\{-\int_0^d \mu(s; E) ds\right\} dE \\
 &= \int_0^\infty E \frac{N_0\delta(E - \bar{E})}{A\Delta t} \exp\left\{-\int_0^d \mu(s; E) ds\right\} dE \\
 &= \frac{N_0\bar{E}}{A\Delta t} \exp\left\{-\int_0^d \mu(s; E) ds\right\} \\
 &= I_0 \exp\left\{-\int_0^d \mu(s; E) ds\right\}
 \end{aligned}$$

Rearrange the above equation, we have

$$-\ln \frac{I_d}{I_0} = - \int_0^d \mu(s; E) ds = g_d$$

which is a **line integral** of the linear attenuation coefficient at the effective energy. This is the basic measurement of CT. This requires calibration measurement of I_0 .

5.4 CT Numbers

In order to compare data from different scanners, which may have different x-ray sources and hence different effective energies, CT numbers are computed from the measured linear attenuation coefficients at each pixel.

Theory: Different CT scanners have different x-ray tubes, which in turn have different effective energies. Thus, the exact same object will produce different numerical values of μ on different scanners. Worse, since the x-ray tube on a busy CT scanner will produce a different scan of the same object in successive years, which is not a desirable situation.

- Consistency across CT scanners desired
- CT number is defined as:

$$h = 1000 \times \frac{\mu - \mu_{water}}{\mu_{water}}$$

- h has Hounsfield units (HU)
- Usually rounded or truncated to nearest integer
- Range:-1000 to about 3000
 - -1000-air($\mu = 0$ in air)
 - 3000-bone
 - 4000-metal

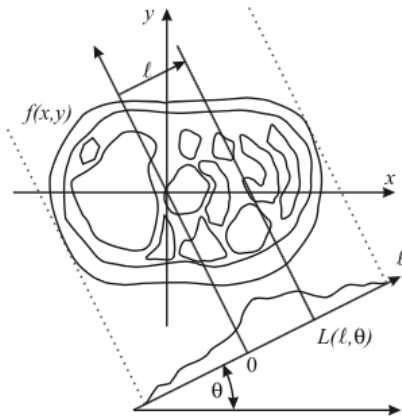
5.4.1 Describing Lines

- Possible descriptions of lines:
 - functional: $y = ax + b$
 - parametric form(forward problem): $x(s), y(s)$
 - set form(inverse problem): $L = \{(x, y) | a \text{ property}\}$
- Critique:
 - Functional: what about vertical lines??
 - Parametric: good for model of process
 - Set: good for theory of reconstruction

5.4.2 Line Parameters and Picture of a line

- Described by:
 - Orientation of angle, θ
 - Lateral translation or position, l
- Written as $L(l, \theta)$

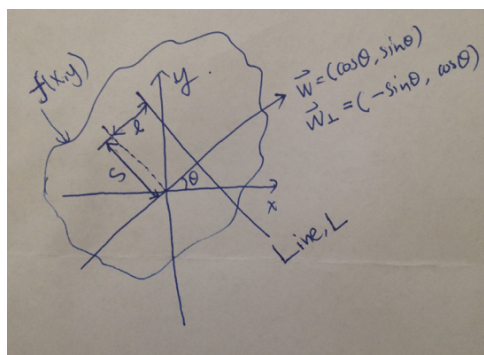
$$L(l, \theta) = \{(x, y) | (x, y) \text{ are on the line with position } l \text{ and angle } \theta\}$$



5.4.3 Line Integral: parametric form

Question: What is integral of $f(x, y)$ on $L(l, \theta)$?

Step 1: Parameterize $L(l, \theta)$



$$\begin{aligned}\vec{p}(s) &= l\vec{w} + s\vec{w}_{\perp} \\ &= \begin{bmatrix} x(s) \\ y(s) \end{bmatrix} = \begin{bmatrix} l\cos\theta - s\sin\theta \\ l\sin\theta + s\cos\theta \end{bmatrix}\end{aligned}$$

Step 2: Integrate $f(x, y)$ over parameter s

$$g(l, \theta) = \int_{-\infty}^{\infty} f(x(s), y(s)) ds$$

A line in the plane

$$L(l, \theta) = \{(x, y) | x\cos\theta + y\sin\theta = l\}$$

Also, $\delta(x\cos\theta + y\sin\theta - l)$ means that everything else is equal to 0, except on the line - "i'm on the line".

5.4.4 Line Integral: set form

- Integrate over whole plane; non-zero only on $L(l, \theta)$
- Key is sifting property

$$q(l) = \int_{-\infty}^{\infty} q(l') \delta(l' - l) dl'$$

- Use line impulse on $L(l, \theta)$

$$g(l, \theta) = \int_{-\infty}^{\infty} \int_{-\infty}^{\infty} f(x, y) \delta(x\cos\theta + y\sin\theta - l) dx dy$$

5.4.5 Physical meanings of $f(x, y)$ and $g(x, y)$

- Recall monoenergetic model:

$$I_d = I_0 \exp \left\{ - \int_0^d \mu(s; \bar{E}) ds \right\}$$

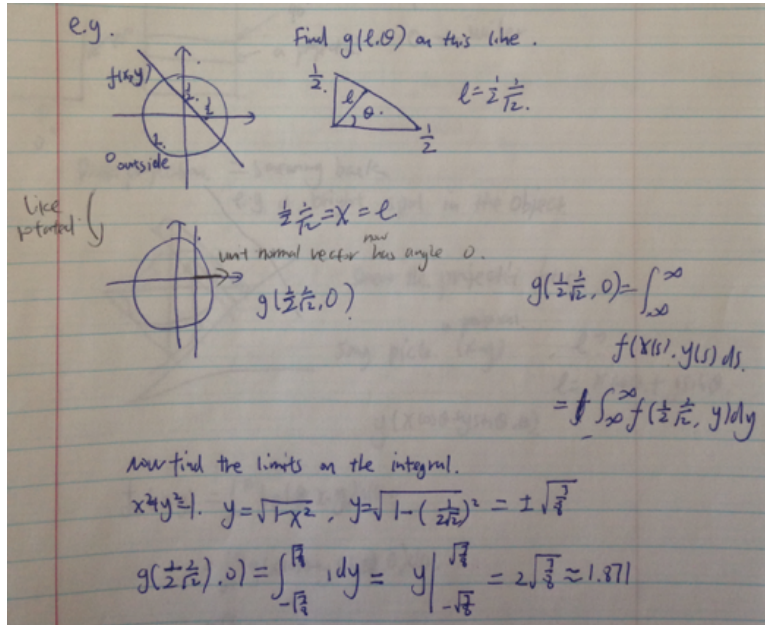
- Rearrange:

$$g(l, \theta) = -\ln \frac{I_d}{I_0} = \int_0^d \mu(x(s), y(s); \bar{E}) ds$$

- Relationship is:

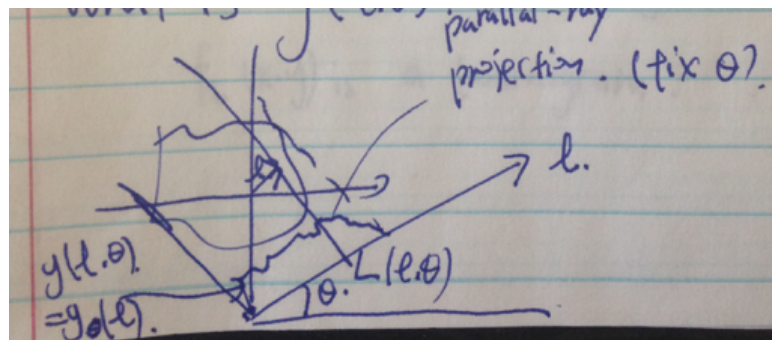
$$- f(x, y) = \mu(x, y; \bar{E})$$

$$- g(l, \theta) = -\ln \frac{I_d}{I_0}$$



5.4.6 What is $g(l, \theta)$?

- Fix l and θ : line integral of $f(x, y)$
- Fix θ only: projection of $f(x, y)$ at angle θ



- Function of θ and l : $g(l, \theta)$ is the **Radon transform** of $f(x, y)$

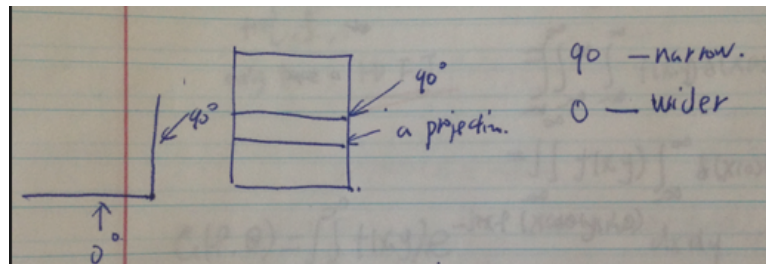
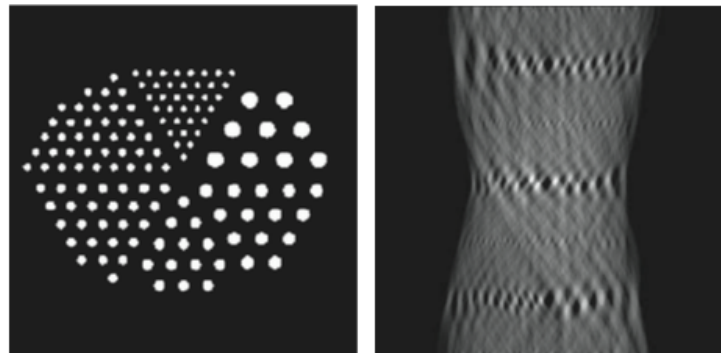
$$g(l, \theta) = \mathcal{R}\{f(x, y)\}$$

- An inverse transform

$$f(x, y) = \mathcal{R}^{-1}\{g(l, \theta)\}$$

5.4.7 Sinogram

- CT data acquired for collection of l and θ
- CT scanners acquires a sinogram

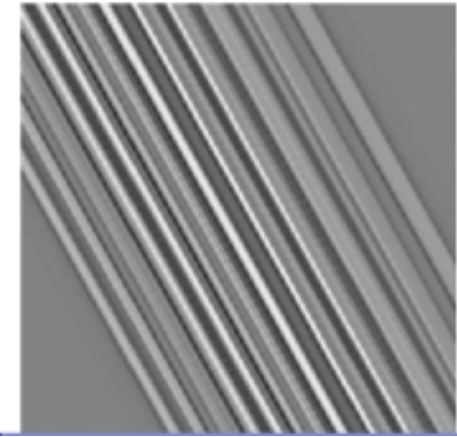


5.4.8 Backprojection (smearing back)

- Goal: find $f(x, y)$ from $g(l, \theta)$
- Strategy: "smear" $g(l, \theta)$ back into plane
- Formally:

$$b_\theta(x, y) = g(x \cos \theta + y \sin \theta, \theta)$$

- $b_\theta(x, y)$ is a laminar image



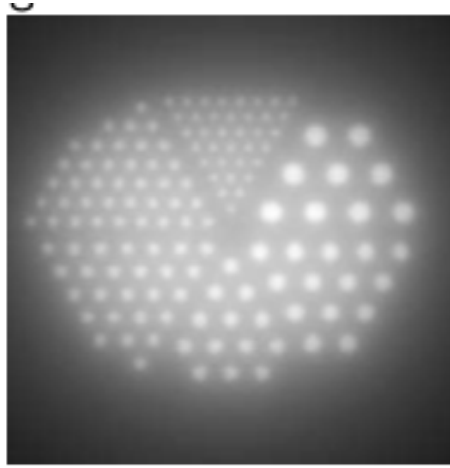
5.4.9 Backprojection summation

”add up” all the backprojection images:

$$\begin{aligned} f_b(x, y) &= \int_0^{\pi} b_{\theta}(x, y) d\theta \\ &= \int_0^{\pi} g(x \cos \theta + y \sin \theta, \theta) d\theta \\ &= \int_0^{\pi} [g(l, \theta)_{l=x \cos \theta + y \sin \theta}] d\theta \end{aligned}$$

5.4.10 Properties of Laminogram

- ”Bright spots” tend to reinforce
- Problem” $f_b(x, y) \neq f(x, y)$



5.5 Projection-Slice Theorem

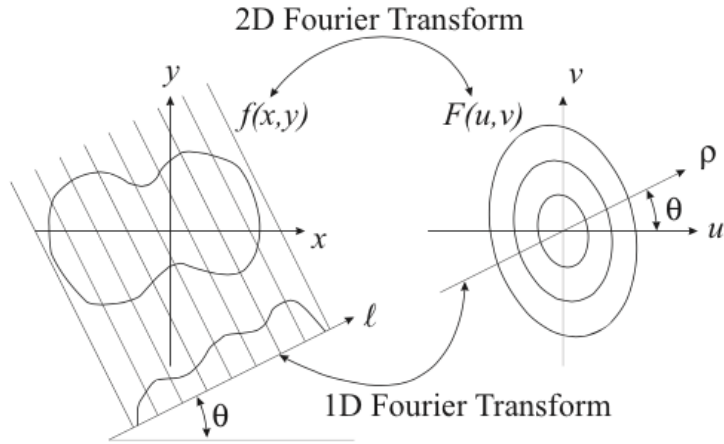
$g(l, \theta)$ is a projection. Taking the 1-D fourier transfer of it yields

$$\begin{aligned}
 G(\rho, \theta) &= \mathcal{F}_1\{g(l, \theta)\} = \int_{-\infty}^{\infty} g(l, \theta) e^{-j2\pi\rho l} dl \\
 &= \int_{-\infty}^{\infty} \int_{-\infty}^{\infty} \int_{-\infty}^{\infty} f(x, y) \delta(x\cos\theta + y\sin\theta - l) dx dy e^{-j2\pi\rho l} dl \\
 &= \int_{-\infty}^{\infty} \int_{-\infty}^{\infty} f(x, y) \int_{-\infty}^{\infty} \delta(x\cos\theta + y\sin\theta - l) e^{-j2\pi\rho l} dl dx dy \\
 &= \int_{-\infty}^{\infty} \int_{-\infty}^{\infty} f(x, y) e^{-j2\pi l(x\cos\theta + y\sin\theta)} dx dy \\
 &= \int_{-\infty}^{\infty} \int_{-\infty}^{\infty} f(x, y) e^{-j2\pi(x\rho\cos\theta + y\rho\sin\theta)} dx dy \\
 &= F(\rho\cos\theta, \rho\sin\theta)
 \end{aligned}$$

Note that $(\rho\cos\theta, \rho\sin\theta) = \rho\vec{w}$, and $\vec{w} = (\cos\theta, \sin\theta)$, which is the same in the frequency domain.

5.5.1 Illustration of Projection-Slice Theorem

A projection in spatial domain \Leftrightarrow a slice in fourier domain.



5.6 Exact Reconstruction Formulas

- Fourier reconstruction:

$$f(x, y) = \mathcal{F}_{2D}^{-1}\{G(\rho, \theta)\}$$

- Filtered backprojection:

$$f(x, y) = \int_0^{\pi} \left[\int_{-\infty}^{\infty} |\rho| G(\rho, \theta) e^{+j2\pi\rho l} d\rho \right]_{l=x\cos\theta+y\sin\theta} d\theta$$

- $|\rho|$ is actually a ramp filter
- ramp filter, $c(l) = \mathcal{F}^{-1}\{||\rho|\}$, but this is actually not the actual ramp filter, which to be discovered soon.

Proof: need to use projection slice theorem and to switch to polar

coordinates, where $u = \rho \cos\theta$ and $v = \rho \sin\theta$

$$\begin{aligned} f(x, y) &= \mathcal{F}^{-1}\{F(u, v)\} = \int_{-\infty}^{\infty} \int_{-\infty}^{\infty} F(u, v) e^{+j2\pi(xu+yv)} du dv \\ &= \int_0^{2\pi} \int_0^{\infty} F(\rho \cos\theta, \rho \sin\theta) e^{+j2\pi(x\rho \cos\theta + y\rho \sin\theta)} \rho d\rho d\theta \\ &= \int_0^{2\pi} \int_0^{\infty} G(\rho, \theta) e^{+j2\pi(x\rho \cos\theta + y\rho \sin\theta)} \rho d\rho d\theta \end{aligned}$$

Now need to adjust the limits to cover the $f(x, y)$ that we need to cover, which ρ is from $-\infty$ to ∞ and $\theta = [0, \pi]$. See problem 6.15 for the details.

- Convolution backprojection:

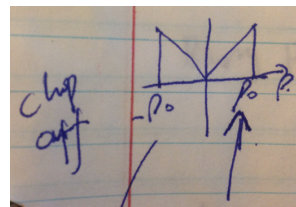
$$\begin{aligned} f(x, y) &= \int_0^{\pi} [c(l) * g(l, \theta)]_{l=x \cos\theta + y \sin\theta} d\theta \\ &= \int_0^{\pi} \int_{-\infty}^{\infty} g(l, \theta) c(x \cos\theta + y \sin\theta - l) dl d\theta \end{aligned}$$

where, $c(l) = \mathcal{F}^{-1}\{|\rho|\}$ Proof:

$$\begin{aligned} \hat{f}(x, y) &= \int_0^{\pi} \left[\int_{-\infty}^{\infty} |\rho| G(\rho, \theta) W(\rho) e^{+j2\pi\rho l} d\rho \right]_{l=x \cos\theta + y \sin\theta} d\theta \\ &= \int_0^{\pi} [c(l) * g(l, \theta)]_{l=x \cos\theta + y \sin\theta} d\theta \end{aligned}$$

where the **actual ramp filter** is $\tilde{c}(l) = \mathcal{F}^{-1}\{|\rho|W(\rho)\}$
e.g., the simplest window function is $W(\rho) = \text{rect}(\frac{\rho}{2\rho_0})$

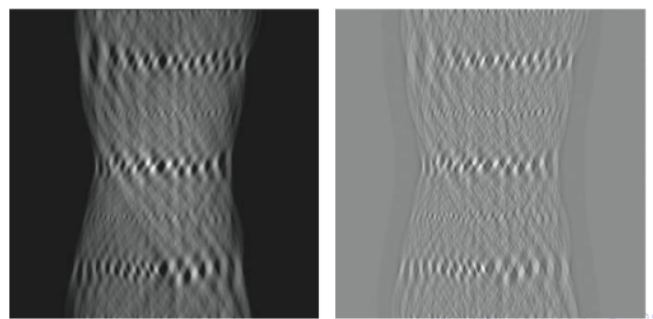
Below is a picture showing that "chop off" capability of $|\rho|W(\rho)$



5.6.1 Convolution, Backprojection, and Summation

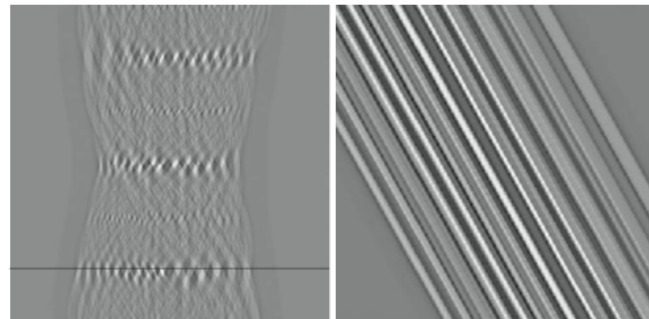
Step 1: Convolution

- Convolve every projection with $c(l)$
- the horizontal direction in a sinogram



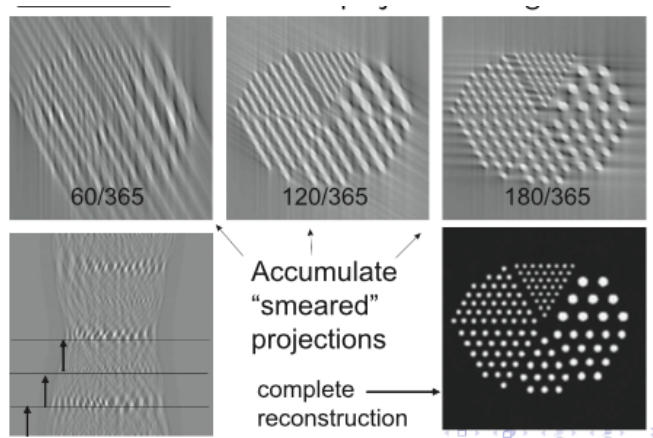
Step 2: Backprojection

- 1D projection \Rightarrow 2D laminar function



Step 3: Summation

- Accumulate sum of backprojection images



5.7 Factors Affecting CT Resolution

- Detector width \sim area detectors
- detector indicator function = $s(l)$
- approximate CBP:

$$f(x, y) = \int_0^{\pi} \left[\int_{-\infty}^{\infty} |\rho| G(\rho, \theta) S(\rho) e^{+j2\pi\rho l} d\rho \right]_{l=x\cos\theta+y\sin\theta} d\theta$$

where $S(\rho) = \mathcal{F}(s(l))$, and $S(\rho)$ is a sinc function

Factors Affecting CT Res.

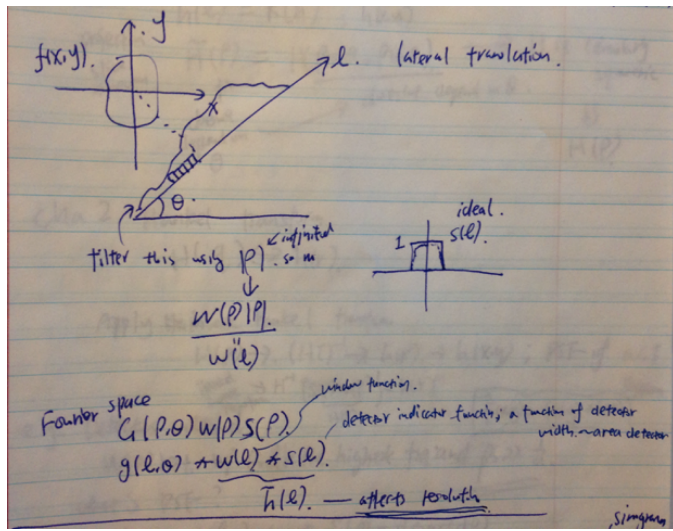
$$\hat{f}(x, y) = \int_0^{\pi} \left[\int_{-\infty}^{\infty} g(\rho, \theta) s(\rho) |P(\rho)| P(\rho) e^{+j2\pi\rho l} d\rho \right]_{l=x\cos\theta+y\sin\theta} d\theta$$

$\stackrel{\text{sinc}}{\approx}$

$g(\ell, \theta) * s(\ell)$

ℓ : Analytical
 $d\theta$: Det. indicator function

$s(\ell, \theta)$



5.7.1 Blurry Reconstruction

- Blurry projection:

$$\begin{aligned}\hat{g}(l, \theta) &= g(l, \theta) * s(l) * w(l) \\ &= g(l, \theta) * \tilde{h}(l)\end{aligned}$$

- What is reconstructed image?

$$\hat{f}(x, y) = \mathcal{R}^{-1}\{g(l, \theta) * \tilde{h}(l)\}$$

- Radon transform convolution theorem

$$\mathcal{R}\{f *_2 h\} = \mathcal{R}\{f\} *_1 \mathcal{R}\{h\}$$

OR

$$f *_2 h = \mathcal{R}^{-1}\{\mathcal{R}\{f\} *_1 \mathcal{R}\{h\}\}$$

Use the Radon transform property and let $g(l, \theta) = \mathcal{R}\{f\}$, $f(x, y)$ and $\tilde{h}(l) = \mathcal{R}\{h\}$, $h(x, y)$, we will derive the following results

From prob 6.9.

$$R\{f * h\} = R(f) * R(h)$$

$\square \times \square$ = $\begin{array}{c} \text{synopsis of } f \\ \hline \text{row 1} * \end{array} \quad \begin{array}{c} \text{synopsis of } h \\ \hline \text{row 2.} \end{array}$

$$f * h = R^{-1}\{R(f) * R(h)\}$$

↑
circular
symmetric.
because this
is not a func of θ

e) Prob 6.9

$$R\{f * h\} = R(f) * R(h)$$

$\square \times \square$ $f \quad h \quad \xrightarrow{\text{synopsis}} \quad R(f) R(h)$

$$f * h = R^{-1}\{R(f) * R(h)\}$$

Now, let $\begin{cases} g(\theta) = R(f), f(\theta) \\ \tilde{h}(\theta) = R(h), h(\theta) \end{cases} \Rightarrow$

$$\tilde{h}(\theta) = W(\theta) * S(\theta). \text{ not dependent on } \theta.$$

$$\tilde{h}(k, \theta) \text{ independent of } \theta.$$

5.7.2 CT Impulse Response Function

- Leads to

$$\hat{f}(x, y) = f(x, y) *_2 h(x, y)$$

where,

$$h(x, y) = \mathcal{R}^{-1}\{\tilde{h}(l)\}$$

- Fourier transform of $\tilde{h}(l)$

$$\tilde{H}(\rho) = \mathcal{F}_1\{\tilde{h}(l)\} = S(\rho)W(\rho)$$

which is independent of θ

- Therefore, $H(u, v)$ is circularly symmetric

5.7.3 PSF given by Hankel Transform

- PSF is circularly symmetric and given by

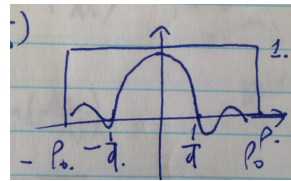
$$h(r) = \mathcal{H}^{-1}\{S(\rho)W(\rho)\}$$

- Reconstructed image given by

$$\hat{f}(x, y) = f(x, y) * h(r)$$

e.g. given detector width d, $W(\rho)$ rect with ρ_0 be the highest frequency and $\rho_0 >> \frac{1}{d}$, what is the PSF?

soln: $s(l) = \text{rect}(\frac{l}{d}) \leftrightarrow S(\rho) = dsinc(d\rho)$ and $W(\rho) = \text{rect}(\frac{\rho}{2\rho_0})$



So we can ignore $W(\rho)$ and now $\hat{h}(l) = s(l)$, therefore $H(q) = S(q) = dsinc(dq)$.

Now we need to find the inverse Hankel transform of $H(q)$.

We know that

$$\text{sinc}(r) \leftrightarrow \frac{2\text{rect}(q)}{\pi\sqrt{1-4q^2}}$$

Two problems: 1. q is in frequency domain. 2 It is scaled by d.

Recall the scaling property of Hankel transform

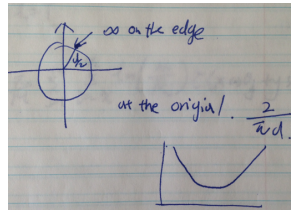
$$\mathcal{H}\{f(ax)\} = \frac{1}{a^2}F\left(\frac{q}{a}\right)$$

Use this property, we have

$$\frac{2d\text{rect}(\frac{r}{d})}{d^2\pi\sqrt{1-4(\frac{r}{d})^2}} \leftrightarrow dsinc(dq)$$

Therefore,

$$h(r) = \frac{2\text{rect}(\frac{r}{d})}{\pi\sqrt{d^2-4r^2}}$$



5.8 Noise in CT Measurements

- Basic measurement is the line integral:

$$g_{i,j} = -\ln\left(\frac{N_{ij}}{N_0}\right)$$

- N_{ij} is the mean counts for i th detector and j th angle
- line L_{ij}
- angel i
- position j
- Noise is in Poisson random variable N_{ij}
 - mean \bar{N}_{ij}
 - variance \bar{N}_{ij}

5.8.1 Functions of Random Variables in CT

- It follows that g_{ij} is a random variable

$$\bar{g}_{ij} \approx \ln\left(\frac{N_0}{\bar{N}_{ij}}\right)$$

$$Var(g_{ij}) \approx \frac{1}{\bar{N}_{ij}}$$

- $\hat{u}(x, y)$ is approximate reconstruction
- It follows that $\hat{u}(x, y)$ is a random variable
- What are the mean and variance of $\hat{u}(x, y)$?

5.8.2 CBP Approximation

- Convolution Backprojection(CBP):

$$u(x, y) = \int_0^\pi \int_{-\infty}^\infty g(l, \theta) c(x\cos\theta + y\sin\theta - l) dl d\theta$$

- Approximations

- M angles; $\Delta\theta = \pi/M$
- N+1 detectors; $\Delta l = T$
- $\tilde{c}(l) \approx c(l)$

- Discrete CBP:

$$\hat{u}(x, y) = \left(\frac{\pi}{M}\right) \sum_{j=1}^M T \sum_{i=-N/2}^{N/2} g(iT, j\pi/M) \tilde{c}(x\cos\theta_j + y\sin\theta_j - iT)$$

- Approximations:

- \bar{N}_{ij} is mean for i-th detector and j-th angle
- N_{ij} is independent for different measurements
- $\bar{N}_{ij} = \bar{N}$, an "object uniformity" assumption
- $\tilde{c}(l)$ is created using rectangular window $W(\rho)$ with cutoff ρ_0

5.9 Conclusions

Since g_{ij} are assumed to be independent random variables, the variance of the sum is the sum of the variances, given by

$$\begin{aligned} \sigma^2(x, y) &= \text{var}[\hat{u}(x, y)] \\ &= \frac{\pi^2 T^2}{M^2} \sum_{j=1}^M \sum_{i=-N/2}^{N/2} \text{var}[g_{ij}] [c(x\cos\theta_j + y\sin\theta_j - iT)]^2 \\ &= \frac{\pi^2 T^2}{M^2} \sum_{j=1}^M \sum_{i=-N/2}^{N/2} \frac{1}{\bar{N}_{ij}} [c(x\cos\theta_j + y\sin\theta_j - iT)]^2 \end{aligned}$$

To proceed, we make a rather drastic approximation: $\bar{N}_{ij} = \bar{N}$. That the mean number of detected photons is a constant is clearly false for nearly all objects; however, by using this approximation, we can develop some important relationships that are otherwise obscured in the summations. Using the approximation,

$$\sigma^2(x, y) = \sigma_\mu^2 = \frac{\pi^2 T^2}{M^2 \bar{N}} \sum_{j=1}^M \sum_{i=-N/2}^{N/2} [c(x \cos \theta_j + y \sin \theta_j - iT)]^2$$

For large N and M, we may make the approximation that discrete is close to continuous

$$\begin{aligned} \frac{\pi}{M} \sum_{j=1}^M T \sum_{i=1}^N [c(x \cos \theta_j + y \sin \theta_i - iT)]^2 &\approx \int_0^{pi} \int_{-\infty}^{\infty} [c(x \cos \theta + y \sin \theta - l)]^2 dl d\theta \\ &= \pi \int_{-\infty}^{\infty} [c(l)]^2 dl \\ &= \pi \int_{-\infty}^{\infty} [C(\rho)]^2 d\rho \\ &= \pi \int_{-\infty}^{\infty} [W(\rho)|\rho|]^2 d\rho = \pi \int_{-\rho_0}^{\rho_0} \rho^2 d\rho = \frac{2\pi\rho_0^3}{3} \end{aligned}$$

Thus, for a rectangular windowed ramp filter and the approximation $\bar{N}_{ij} = \bar{N}$, the reconstructed image variance is independent of (x,y), and is given by

$$\sigma_\mu^2 \approx \frac{2\pi^2 \rho_0^3}{3} \frac{1}{M} \frac{1}{\bar{N}/T}$$

5.10 Signal-to-noise Ratio

- Definition(usual)

$$SNR = \frac{C\bar{\mu}}{\sigma \hat{\mu}}$$

- After substitution:

$$SRN = \frac{C\bar{\mu}}{\pi} \sqrt{\frac{3MN}{2T\rho_0^3}}$$

5.11 SNR in a Good Design

- What should be?
- Let detector width= d
- ρ_0 should be anti-aliasing filter:

$$\rho_0 = \frac{k}{d}$$

where $k \approx 1$

- In 3G CT scanner $d = T$

- Then

$$SNR \approx 0.4kC\bar{\mu}d\sqrt{\bar{N}M}$$

5.12 SNR in Fan-Beam Case

$$SNR = 0.4kC\bar{\mu}L\sqrt{\frac{\bar{N}_f M}{D^3}}$$

where, \bar{N}_f is mean photon count per fan, and D is number of detectors, and L is length of detector array.

If you pay attention, you will find out that in 3G fan-beam systems, increasing D decreases SNR. The reason for this is because this analysis ignores resolution.

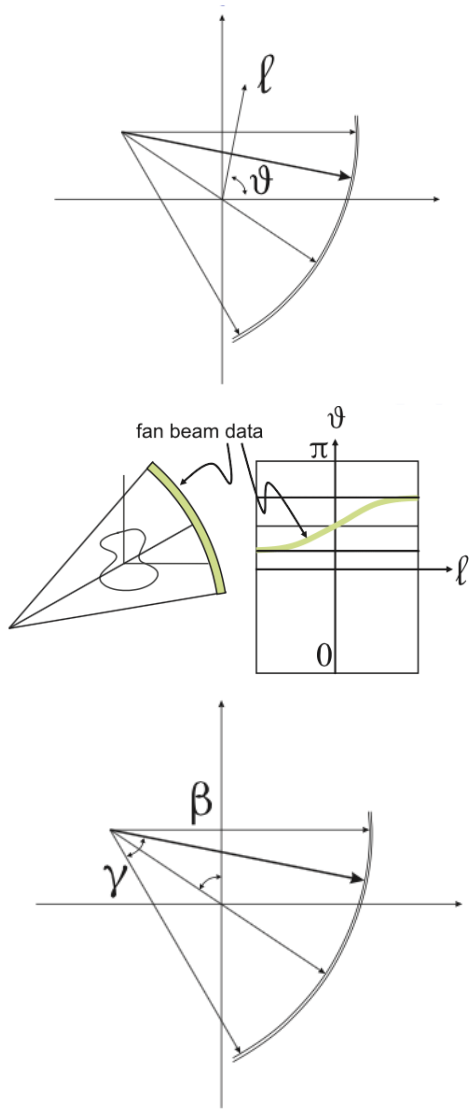
5.13 Rule of Thumb

- Variables:
 - D is number of detectors
 - M is number of angles
 - J^2 is number of pixels in image
- Very approximate "rule":

$$D \approx M \approx J$$

- Typical numbers:
 - Low: $D \approx 700, M \approx 1000, J \approx 512$
 - High: $D \approx 900, M \approx 1600, J \approx 1024$

5.14 Fan Beam Geometry



Formula

$$f(x, y) = \int_0^{2\pi} \frac{1}{(D')^2} \int_{-\gamma_m}^{\gamma_m} p(\gamma, \beta) c'(\gamma' - \gamma) d\gamma d\beta$$

D' depends on (x, y)

c' is a different filter than \tilde{c}

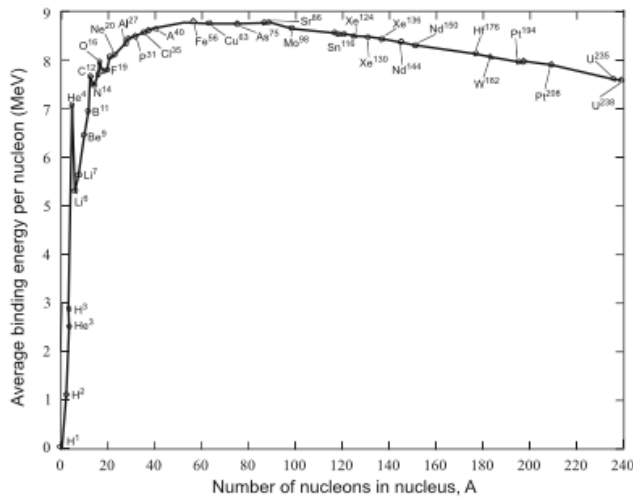
6 Physics of Nuclear Medicine

6.1 Nomenclature

- Atomic number: Z, number of protons in nucleus
- Mass number: A, number of nucleons in nucleus
- Nuclide: unique combination of protons and neutrons in nucleus
- Radionuclide: a nuclide that is radioactive
- Isotope: atoms with same Z, different A
- Isobar: atoms with same A, different Z

6.2 Mass Defect and Binding Energy

- Mass defect = Mass of constituents of atom - actual mass of atom
- unified mass unit, u, = 1/12 mass of C-12 atom
- Binding energy = mass defect $\times c^2$
- One u is equivalent to 931 MeV
- Generally, more massive atom, more binding energy



Now consider the following example:

$$A = A_0 e^{-\lambda t}, \text{ average behavior}$$

Now consider a small interval Δt (A_0 is not changing), we have

$$\Delta t A = \Delta t A_0 e^{-\lambda \Delta t}$$

$$\text{Use Taylor series } e^x \cong (1 + x + \frac{x^2}{2!} + \dots)$$

$$N = N_0 e^{-\lambda \Delta t} \approx N_0 (1 - \lambda \Delta t) = N_0 - N_0 \lambda \Delta t$$

Note that $N_0 \lambda \Delta t$ is the number of disintegrations in Δt , which can be seen as the probability of having one disintegration from N_0 radioatoms in time interval Δt , which is equal to the expected value(mean value). Also note that this is a Poisson random variable.

Let parameter $a = N_0 \lambda t$, then $\text{Prob}[\Delta N = k] = \frac{a^k e^{-a}}{k!}$, substitute a in, we get the following expression:

$$\text{Prob}[\Delta N = k] = \frac{(N_0 \lambda t)^k e^{-N_0 \lambda t}}{k!}$$

Note: ΔN = disintegrations you get over Δt

e.g., consider $k = 1$, and a small Δt , we have

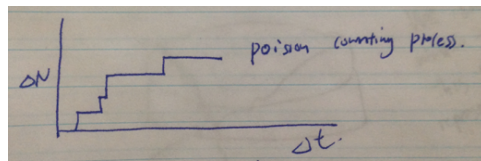
$$\text{Prob}[\Delta N = 1] = \frac{(N_0 \lambda \Delta t)^1 e^{-N_0 \lambda t}}{1} \approx N_0 \lambda t$$

- Δt has units of time
- $N_0 \lambda$ has units of frequency dps
- Poisson rate = radioactivity

e.g., $N_0 = 1$, Probability of decay in Δt :

$$\text{Prob}[\Delta N = 1] \approx \lambda \Delta t$$

Note: λ = Probability of a single radioatom decaying in Δt time.



6.3 Radiotracers

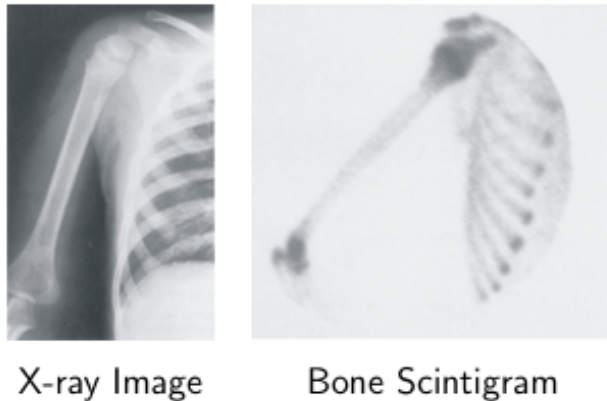
- Gamma Ray Emitters:

- Iodine-123(13.3h, 159 keV)
 - Iodine-131(8.04d, 364 keV)
 - Iodine-125(60d, 35 keV) Not desirable
 - Thallium-201 (73h, 135 keV)
 - Technetium-99m (6h, 150 keV)
- Positron Emitters:
 - Fluorine-18 (110 min, 202 keV)
 - Oxygen-15 (2 min, 696 keV)

7 Planar Scintigraphy

Broad Purpose

- Gamma emitter in body; where is it?
- Planar camera; like radiography
- 2D projection of 3D concentration



X-ray Image

Bone Scintigram

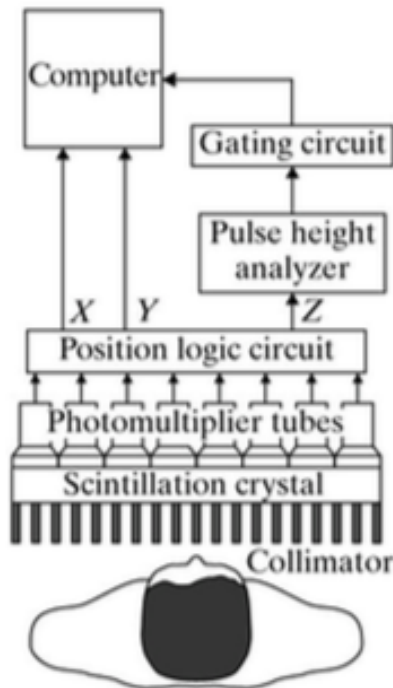
7.1 Gallium-67 scan

A gallium scan is a type of nuclear medicine study that uses a radioactive tracer to obtain images of a specific type of tissue, or disease state of tissue. Gallium-67 is imaged with a gamma camera, with a SPECT camera, or with SPECT/CT hybrid machines. Gallium is taken up by tumors, inflammation,

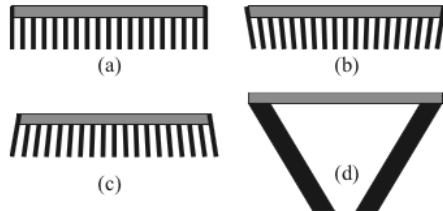
and both acute and chronic infection, allowing these pathological processes to be imaged by nuclear scan techniques. Gallium is particularly useful in imaging osteomyelitis that involves the spine, and in imaging older and chronic infections that may be the cause of a fever of unknown origin

- Gallium-67 citrate (metastatic tumors, focal site of infection)
- half-life is 78 hr
- 93 keV (40 percent), 184 keV (24 percent), 296 keV (22 percent), and 388 keV (7 percent)
- 150-220 MBq (4-6 mCi) intravenously
- 48 hr after injection, about 75 percent remains in body
- equally distributed among the liver, bone and bone marrow, and soft tissues.
- Scintigrams 24 to 72 hrs after injection

7.2 Gamma/Anger Camera Components



7.2.1 Collimators

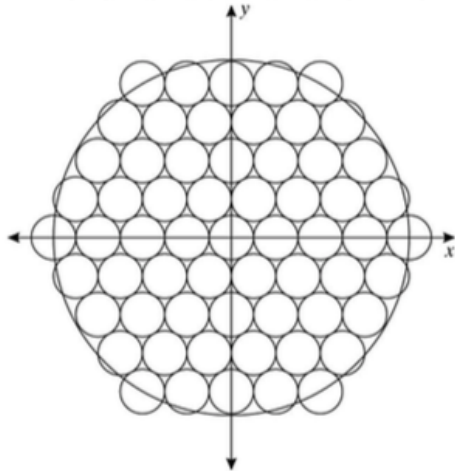


- (a) Parallel hole
- (b) Converging hole (magnifies)
- (c) Diverging hole (minifies)
- (d) Pin-hole (2–5 mm)

7.2.2 Detector

- Single large-area NaI(Tl) crystal
- Diameters:
 - 30-50 cm in diameter
 - Mobile units: 30 cm
 - Fixed scanners: 50 cm
- Thickness:
 - High-E emitters: 1.25 cm thick
 - Low-E emitters: 6-8 mm thick

7.2.3 Photomultiplier Tube Array

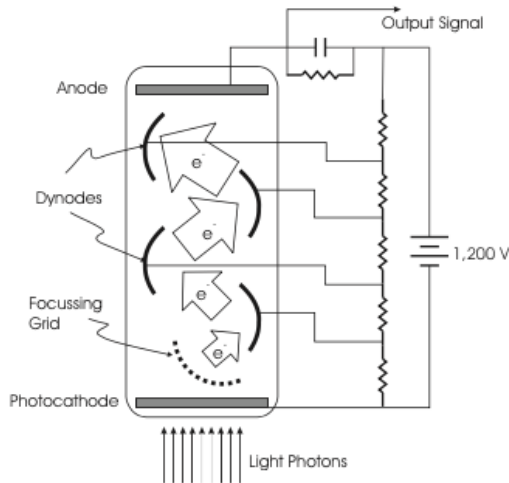


7.2.4 Photomultiplier Tube

Photomultipliers are constructed from a glass envelope with a high vacuum inside, which houses a photocathode, several dynodes, and an anode. Incident photons strike the photocathode material, which is present as a thin deposit on the entry window of the device, with electrons being produced as a consequence of the photoelectric effect. These electrons are directed by the focusing electrode toward the electron multiplier, where electrons are multiplied by the process of secondary emission.

The electron multiplier consists of a number of electrodes called dynodes. Each dynode is held at a more positive voltage, by 100 volts, than the previous one. A primary electron leaves the photocathode with the energy of the incoming photon, or about 3 eV for "blue" photons, minus the work function of the photocathode. As a group of primary electrons, created by the arrival of a group of initial photons, moves toward the first dynode they are accelerated by the electric field. They each arrive with ≈ 100 eV kinetic energy imparted by the potential difference. Upon striking the first dynode, more low energy electrons are emitted, and these electrons in turn are accelerated toward the second dynode. The geometry of the dynode chain is such that a cascade occurs with an ever-increasing number of electrons being produced at each stage. For example, if at each stage an average of 4 new electrons are produced for each incoming electron, and if there are

12 dynode stages, then at the last stage one expects for each primary electron about $5^{12} \approx 10^8$ electrons. This large number of electrons reaching the last stage, called the anode, results in a sharp current pulse that is easily detectable, signaling the arrival of the photon at the photocathode about a nanosecond earlier.



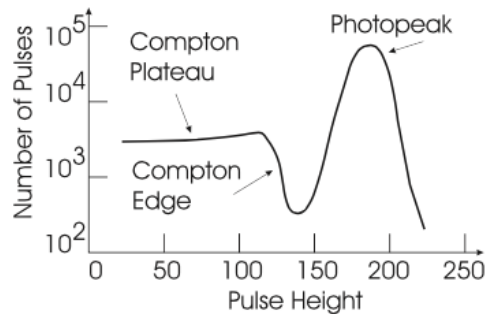
7.2.5 Pulse Height

- Response to **single** gamma ray photon
- PMT responses, a_k , $k = 1, \dots, K$
- Total response of camera is Z-pulse

$$Z = \sum_{k=1}^K a_k$$

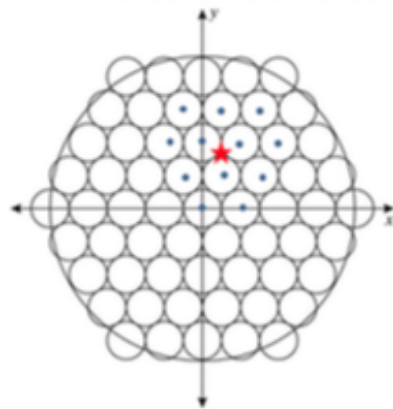
- Height of Z pulse is important
 - Can remove Compton photons
 - Can reject multiple hits

7.3 Pulse Height Analysis



Note: Discriminator circuit rejects non-photopeak events.

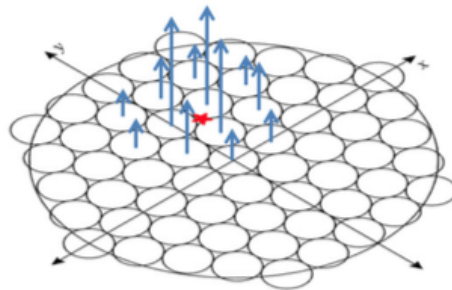
7.3.1 Gamma Camera Photon Detection



Process:

1. Gamma ray photon hits scintillator
2. Photon "stopped" by photoelectric effect
3. Light flash detected by multiple PMTs

7.3.2 Gamma Camera Event Positioning



- PMT height (Z-height) is related to event distance
- Center of mass is approximate position
- Compton scattering happens and leaves a compton e^- inside the crystal.
- $\theta = 180^\circ$, namely backscattering, deposits the most energy in the crystal

7.3.3 Event Positioning Logic

- Tube centers at (x_k, y_k) , $k=1, \dots, K$
- Center of mass of pulse responses is

$$X = \frac{1}{Z} \sum_{k=1}^K x_k a_k$$

$$Y = \frac{1}{Z} \sum_{k=1}^K y_k a_k$$

- This is pulse location

7.4 Acquisition Modes

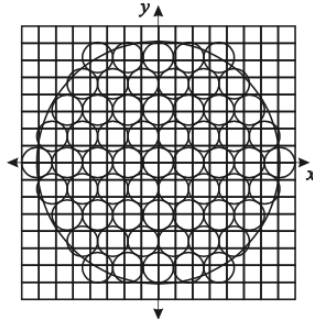
- How to use the camera to make images?
 - List mode
 - Static frame mode

- Dynamic frame mode
- Multiple-gated acquisition
- Whole body mode
- List mode

$$\begin{aligned}
 & (X_1, Y_1, Z_1, t_1) \\
 & (X_2, Y_2, Z_2, t_2) \\
 & (X_3, Y_3, Z_3, t_3) \\
 & \vdots \\
 & (X_n, Y_n, Z_n, t_n) \\
 & \vdots
 \end{aligned}$$

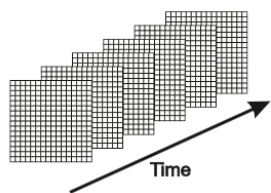
Complete information, but memory hog

- Static Frame Mode



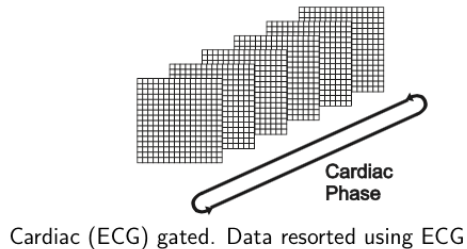
Matrix sizes: 64×64 , 128×128 , 256×256

- Dynamic Frame Mode

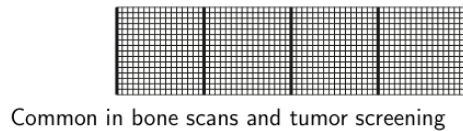


Useful for imaging transient physiological processes

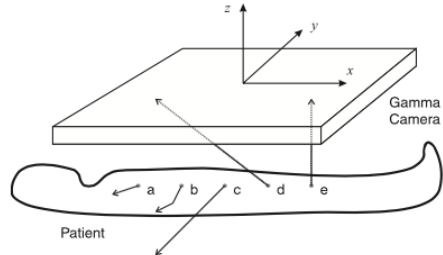
- Multiple Gated Acquisition



- Whole Body Mode



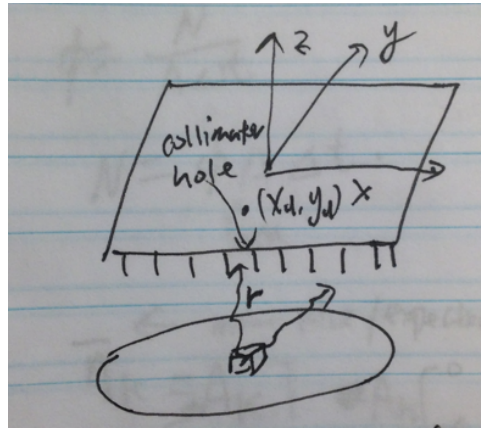
7.5 Imaging Geometry and Assumption



- Lines defined by (parallel) collimator holes
- Ignore Compton scattering
- Radioactivity concentration : $f(x,y,z)$
- Monoenergetic photons, energy E

Now consider N number of radionuclides in a small volume V . The radioactivity is equal to $A = \lambda N$, and radioactivity concentration is $\frac{A}{V} = \frac{\lambda N}{V} = f(x, y, z)$, which is the basic quantity that is observed.
Differential radioactivity:

$$dA(x, y, z) = f(x, y, z) dx dy dz$$



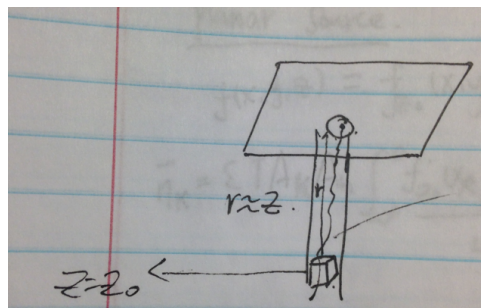
Differential photon fluence rate:

$$d\phi(x_d, y_d) = \frac{dA}{4\pi r^2} \times \exp\left\{-\int_0^r \mu(s, E) ds\right\}$$

Note that the E above is the energy of gamma ray (one energy).

7.5.1 Photon Fluence in Collimator Hole

Photon Fluence in Collimator Hole at (x_d, y_d)



- Depth-dependent effects from:
 - inverse square law, and
 - Object-dependent attenuation

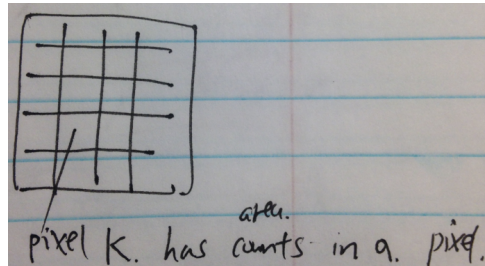
Assume $f(x, y, z)$ is constant for fixed z in tube.

$$\begin{aligned}\phi(x_d, y_d) &= \int \int_{tube} \int_z \frac{f(x_d, y_d, z) dx dy dz}{4\pi r^2} \exp\left\{-\int_0^r \mu(s, E) ds\right\} \\ &= A_h \int_{-\infty}^0 \frac{f(x_d, y_d, z)}{4\pi z^2} \exp\left\{-\int_z^0 \mu(x, y, z'; E) dz'\right\} dz\end{aligned}$$

Note: $\int \int_{tube} dx dy = A_h$, which is the area of collimator hole. μ is the attenuation coefficient of body. Also, assume that μ is constant over the plane for fixed z .

- Consequences:
 - Near activity is brighter
 - Front and back are different

7.6 Planar Sources



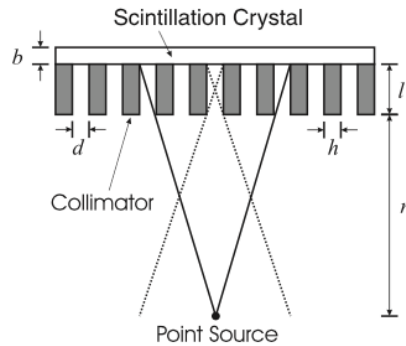
Given the size of a pixel being A_k , $\phi = \frac{N}{A_k \Delta t}$ and $N = \phi A_k \Delta t$, and detected mean pixel count for pixel k is:

$$\bar{n}_k = \varepsilon T A_k A_h \frac{f_{z_0}(x_k, y_k)}{4\pi z_0^2} \exp\left\{-\int_{z_0}^0 \mu(x_k, y_k, z'; E) dz'\right\}$$

- ε is detector efficiency
- A_k is area, size of pixel
- A_h is area of collimator hole
- T is observation time

- Two terms attenuate desired result
 - inverse square law: constant for (x,y)
 - μ is not constant for $(x_k, y_k)!!$, which means it depends on (x_k, y_k) position.

7.7 Collimator Resolution



- Collimator Resolution=FWHM=

$$R_C(|z|) = \frac{d}{l}(l + b + |z|)$$

- Gaussian approximation

$$h_c(x, y; |z|) = \exp\left\{-4(x^2 + y^2) \frac{\ln 2}{R_C^2(|z|)}\right\}$$

- Planar source is blurred

$$\phi(x, y) = \frac{A_h f_{z_0}(x, y)}{4\pi z_0^2} \times \exp\left\{-\int_{z_0}^0 \mu(x, y, z'; E) dz'\right\} * h_c(x, y; |z_0|)$$

7.8 Intrinsic Resolution

- Where did the x-ray photon hit?
 - Compton in crystal spreads out light
 - Crystal thickness
 - Noise in light, PMTs, and electronics

- Gaussian approximation

$$h_I(x, y; |z|) = \exp\{-4(x^2 + y^2) \frac{\ln 2}{R_I^2}\}$$

- Planar source is further blurred

$$\phi(x, y) = \frac{A_h f_{z_0}(x, y)}{4\pi z_0^2} \times \exp\left\{-\int_{z_0}^0 \mu(x, y, z'; E) dz'\right\} * h_c(x, y; |z_0|) * h_I(x, y)$$

7.9 Collimator Sensitivity

- Collimator Efficiency = Sensitivity =

$$\epsilon = \left(\frac{Kd^2}{l(d+h)}\right)^2$$

where $K \approx 0.25$

- ϵ is the fraction of photons (on average) that pass through the collimator for each emitted photon directed at the camera

7.10 Resolution vs. Sensitivity

Table: Resolution and Sensitivity for Several Collimators

collimator	d (mm)	l (mm)	h (mm)	resolution @ 10 cm (mm)	relative sensitivity
LEUHR	1.5	38	0.20	5.4	12.1
LEHR	1.9	38	0.20	6.9	20.5
LEAP	1.9	32	0.20	7.8	28.9
LEHS	2.3	32	0.20	9.5	43.7

LEUHR = low energy ultra-high resolution

LEHR = low energy high resolution

LEAP = low energy all purpose

LEHS = low energy high sensitivity

7.11 Detector Efficiency

- Depends on crystal thickness
 - thicker \Rightarrow more efficient

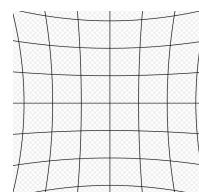
- 100 percent at 100 keV; 10-20 percent at 511 keV
- Tradeoff:
 - If $E_\gamma low \Rightarrow$ use thinner crystal
 - If $E_\gamma high \Rightarrow$ use thicker crystal
 - Higher E_γ , less absorption in body

Consider \bar{N} photons are detected

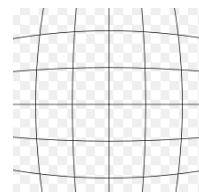
$$\sqrt{\frac{\bar{N}}{J^2}} = \frac{\sqrt{\bar{N}}}{J} = \text{intrinsic SNR per pixel}$$

7.12 Geometry and Nonuniformity

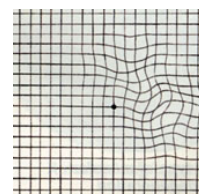
- Geometric distortion
 - Pincushion distortion, which is the exact opposite of barrel distortion straight lines are curved outwards from the center.



- Barrel distortion



- wavy line distortion



- Image nonuniformity

- Variation as much as 10 percent
- non-uniform detector efficiencies
- geometric distortions \Rightarrow "hot spot"
- edge packing

7.13 Image SNR

- Suppose \bar{N} photons are detected
- Then intrinsic SNR of frame mode is:

$$SNR(\text{intrinsic}) = \frac{\sqrt{\bar{N}}}{J}$$

where J^2 is the number of pixels in image

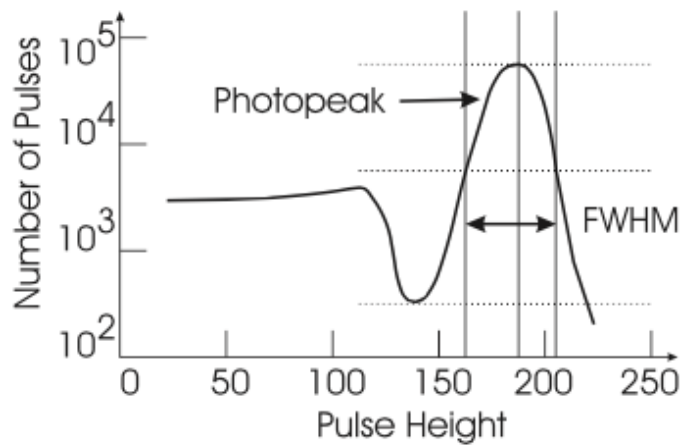
- For similar areas of target and background:

$$C = \frac{I_t - I_B}{I_B} = \frac{N_t - N_B}{N_B}$$

$$SNR = \frac{N_t - N_B}{\sqrt{N_B}} \frac{N_t - N_B}{N_B} \frac{N_B}{\sqrt{N_B}} = C \sqrt{\bar{N}_B}$$

7.14 Energy Resolution

- Energy resolution = FWHM of photopeak



7.15 Pulse Pileup

- Pulse pileup = two simultaneous γ -rays
- Event rejected
 - because of energy discrimination
 - results in wasted photons
- cannot improve image using larger dose
- instead, keep dose low and image longer

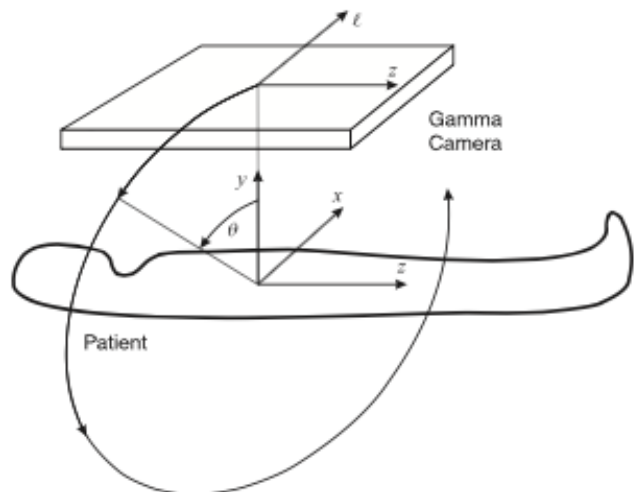
8 Emission Tomography

8.1 SPECT

8.1.1 SPECT Hardware

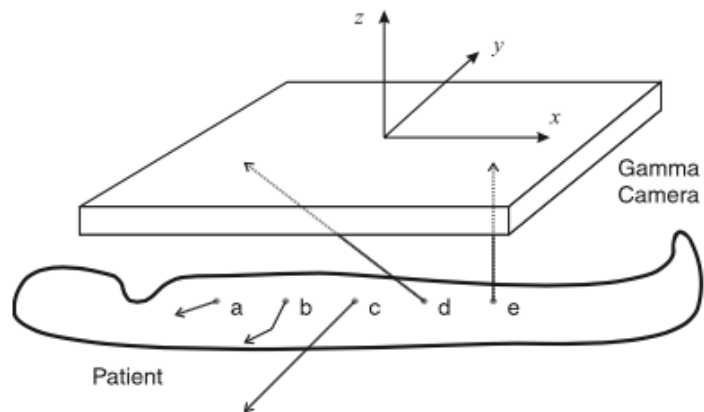
- Rotating gamma camera
- Each "row" is separate slice
- Multiple heads (2 or 3) are common
- High-performance cameras used
 - $\leq 1\%$ nonuniformity required
 - need good mechanical alignment

8.1.2 SPECT Coordinate System



"Home position:" $x \rightarrow z$, $y \rightarrow \ell$, $z \rightarrow y$

"Home position"



8.1.3 Multiple Head Tradeoffs

Table: Comparison of acquisition times and relative sensitivities for single- and multi-head systems with identical camera heads and collimation.

	360°		180°	
	Acq Time	Rel Sens	Acq Time	Rel Sens
Single	30	1	30	1
Double (heads@180°)	15	2	30	1
Double (heads@90°)	15	2	15	2
Triple	10	3	20	1.5

8.2 Basic Imaging Equation

- Parallel hole collimators
- Camera fixed distance R from origin (origin in patient)
- From planar scintigraphy, we have

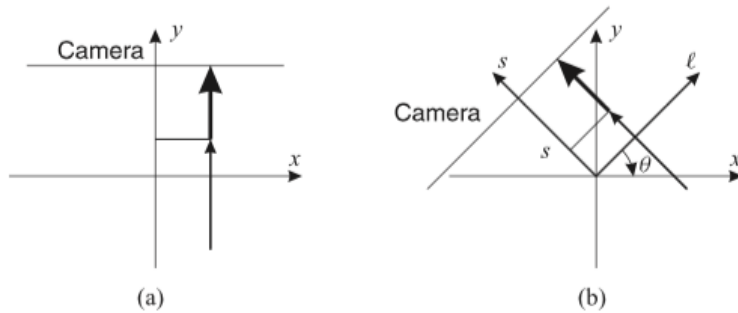
$$\phi(x_d, y_d) = A_h \int_{-\infty}^0 \frac{f(x_d, y_d, z)}{4\pi z^2} \exp\left\{-\int_z^0 \mu(x, y, z'; E) dz'\right\} dz$$

- Imaging equation in "home" position:

$$\phi(z, l) = A_h \int_{-\infty}^R \frac{f(x, y, z)}{4\pi(y - R)^2} \exp\left\{-\int_y^R \mu(x, y', z; E) dy'\right\} dy$$

Note that ϕ is in units of $\frac{\text{number of photons}}{\text{area} \times \text{time}}$

- For a fixed z, we have



where, Line L is described by

$$L(l, \theta) = \{(x, y) | x\cos\theta + y\sin\theta = l\}$$

8.3 Tomographic Imaging Equation

$$\bar{n}_k(l, \theta) = \int_{-\infty}^R \frac{\epsilon T A_k A_h f(x(s), y(s))}{4\pi(s-R)^2} \exp\left\{-\int_s^R \mu(x(s'), y(s'); E) ds'\right\} ds$$

- Two unknowns: $f(x, y)$ and $\mu(x, y)$
- Generally intractable ⇒
 - Ignore attenuation(often done)
 - assume constant
 - measure and apply attenuation correction

8.4 Approximate SPECT Imaging Equation

- Bold approximations: ignore attenuation, inverse square law, and scale factors:

$$\bar{n}_k(l, \theta) = \epsilon T A_k A_h \int_{-\infty}^{\infty} f(x(s), y(s)) ds$$

- Define measurements as

$$g(l, \theta) = \frac{\bar{n}_k(l, \theta)}{\epsilon T A_k A_h}$$

- Using line impulse:

$$g(l, \theta) = \int_{-\infty}^{\infty} \int_{-\infty}^{\infty} f(x, y) \delta(x\cos\theta + y\sin\theta - l) dx dy$$

8.5 SPECT Reconstruction

- Use convolution backprojection

$$f(x, y) = \int_0^{pi} \int_{-\infty}^{\infty} g(l, \theta) \tilde{c}(x\cos\theta + y\sin\theta - l) dl d\theta$$

- Approximate ramp filter:

$$\tilde{c}(l) = \mathcal{F}_{1D}^{-1}\{|\rho|W(\rho)\}$$

8.6 Approximate SPECT Attenuation Correction

- Suppose $\mu(x, y; E)$ is known
- Compute \bar{n}_k for artificial flood field $f_a(x, y) = 1$
- Reconstruct image $a(x, y)$ from computed \bar{n}_k
- Form attenuation corrected image from reconstructed image $f(x, y)$:

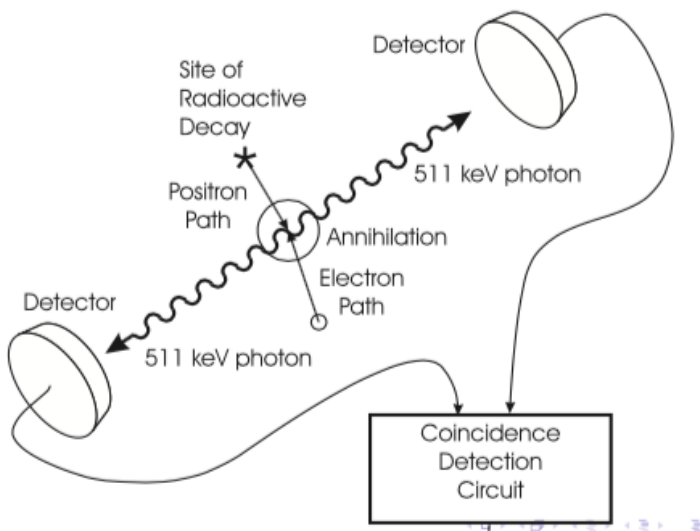
$$f_c(x, y) = \frac{f(x, y)}{a(x, y)}$$

8.7 Myocardial Perfusion SPECT Dose

Study	Injected Activity	Effective Dose Estimate
1-day rest/stress ^{99m}Tc based	10 mCi rest	9.3 mSv ^{99m}Tc tetrofosmin
	30 mCi stress	11.4 mSv ^{99m}Tc sestamibi
1-day stress/rest ^{99m}Tc based	10 mCi stress	9.3 mSv ^{99m}Tc tetrofosmin
	30 mCi rest	11.4 mSv ^{99m}Tc sestamibi
2-day stress/rest or rest/stress ^{99m}Tc based	25 mCi stress	11.6 mSv ^{99m}Tc tetrofosmin
	25 mCi rest	14.8 mSv ^{99m}Tc sestamibi
Stress-only ^{99m}Tc based	25 mCi stress	5.8 mSv ^{99m}Tc tetrofosmin 6.8 mSv ^{99m}Tc sestamibi
1-day ^{201}Tl rest/ ^{99m}Tc based stress	3.5 mCi ^{201}Tl	21.2 mSv ^{201}Tl / ^{99m}Tc tetrofosmin
	25 mCi ^{99m}Tc m	22.1 mSv ^{201}Tl / ^{99m}Tc sestamibi
1-day stress/redistribution ^{201}Tl	3.5 mCi ^{201}Tl stress	15.3 mSv
1-day stress/reinjection/redistribution ^{201}Tl	3.0 mCi ^{201}Tl stress	19.7 mSv
	1.0 mCi ^{201}Tl reinjection	
Attenuation correction ^{153}Gd X-ray CT		< 0.3 mSv < 1 mSv

8.8 PET Principles

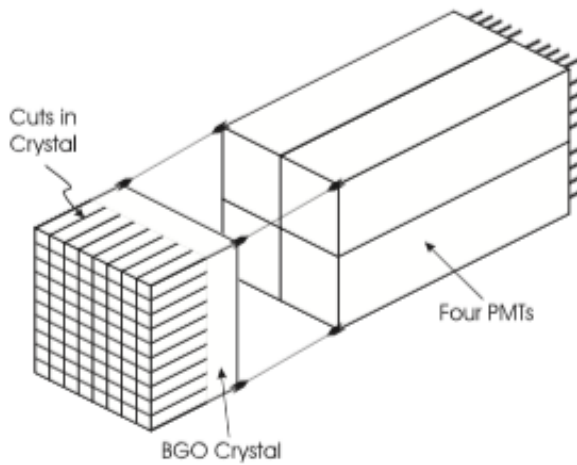
- Positron emitters
- Positron annihilation:
 - short distance from emission
 - produces two 511 keV gamma rays
 - gamma rays 180 degrees opposite directions
- Principle: detect coincident gamma rays



8.8.1 Annihilation Conincidence Detection (ACD)

- Event occurs if detections are conincident
- Time window is typically 2-20 ns
- 12 ns is common setting
- No detector collimation required
- Dual-head SPECT systems can be used

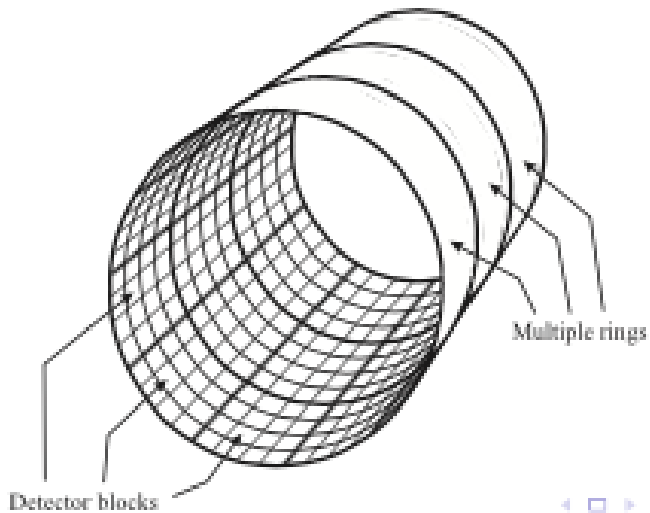
8.8.2 PET Detector Block



- Crystals plus PMTs
- BGO = Bismuth Germanate
- BGO has 3x stopping power than NaI(Tl)

8.8.3 Typical PET Detector Arrangement

- 2mm × 2mm elements
- 8 by 8 elements per blocks; 2 by 2 PMTs per block
- 48 blocks per major ring; 3 major rings
- ⇒ 24 detector rings; 384 detectors per ring
- *Rightarrow* 8216 crystals total

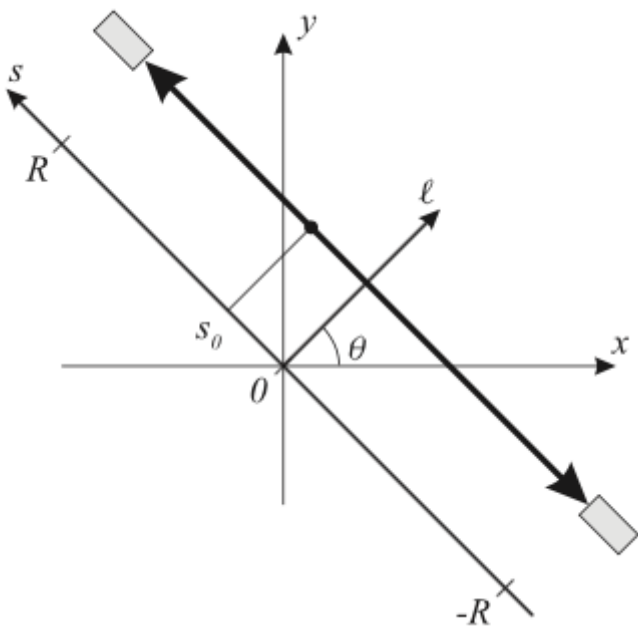


A set of small, semi-transparent navigation icons typically used in presentation software like Beamer. They include symbols for back, forward, search, and other slide controls.

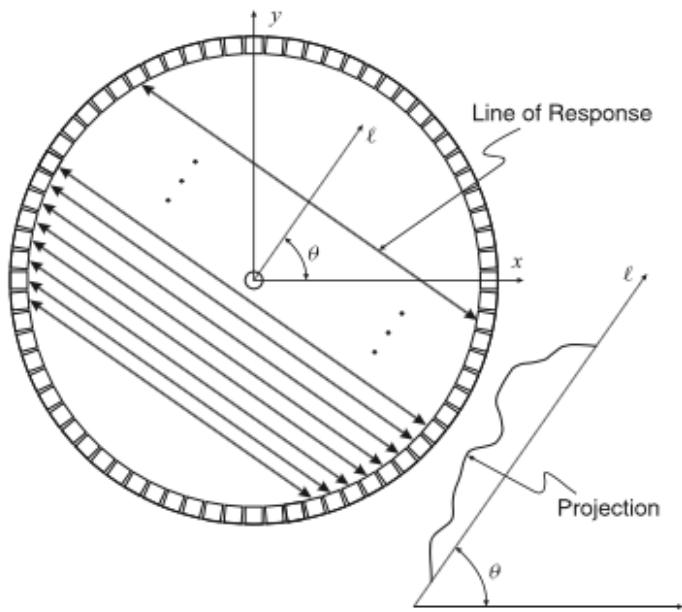
8.8.4 2-D or 3-D PET Geometry

- Septa or no septa between rings?
- Septa: \Rightarrow multiple 2-D PET rings, which is like reconstruction in 2-D CT
- No septa: \Rightarrow 3-D PET, which needs 3-D reconstruction algorithms
- We focus on 2-D PET

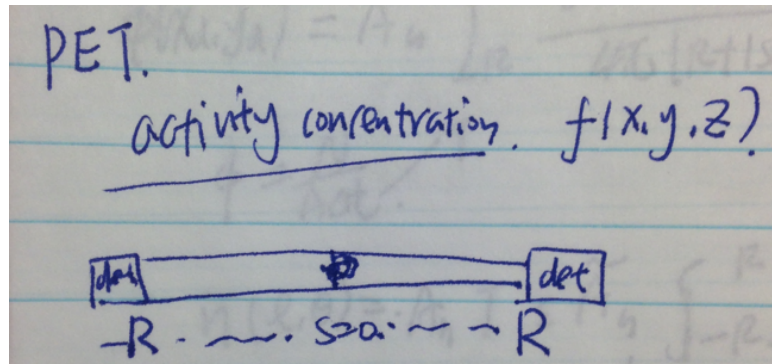
2-D PET Geometry



Lines of Response (LORs)



8.9 PET Imaging Equation



A differential activity

$$dA(x, y, z) = f(x, y, z) dx dy dz$$

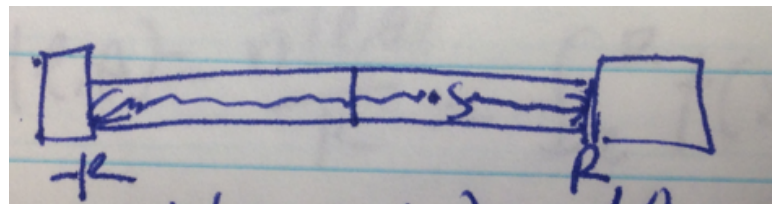
Ignore attenuation

$$d\phi(x_d, y_d) = \frac{dA}{4\pi R^2}$$

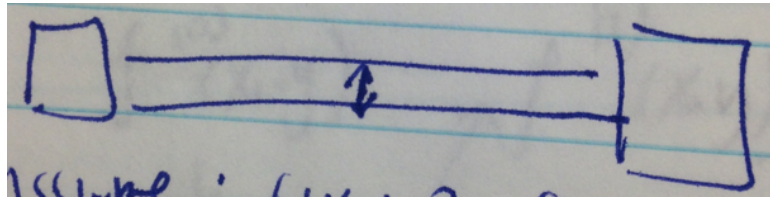
Attenuation

$$d\phi(x_d, y_d) = \frac{dA}{4\pi R^2} \exp\left\{-\int_{-R}^R \mu(s'; E) ds'\right\}$$

Now move the source



$$d\phi(x_d, y_d) = \frac{dA}{4\pi(R + |s|)^2} \exp\left\{-\int_{-R}^R \mu(s'; E) ds'\right\}$$



Assume: $f(x,y,z)$ = concentrations along vertical direction

A_h is area of the detector tube \approx area detector face

Note: $\tilde{A}_h \leq A_h$ (because at the top of the tube, it gets less and less counts)

$$\phi(x_d, y_d) = \tilde{A}_h \int_{-R}^R \frac{f(x(s), y(s))}{4\pi(R + |s|)^2} \exp\left\{-\int_{-R}^R \mu(s'; E) ds'\right\} ds$$

The attenuation term doesn't depend on s, the location of annihilation

$$\bar{n}(l, \theta) = A_h T \epsilon \tilde{A}_h \int_{-R}^R \frac{f(x(s), y(s))}{4\pi R^2} \exp\left\{-\int_{-R}^R \mu(x(s'), y(s'); E) ds'\right\} ds$$

Unknowns $\mu(x, y)$ and $f(x, y)$ separate Now let $k = A_h T \epsilon \tilde{A}_h$ and ignore inverse square term.

$$\bar{n}(l, \theta) = k \int_{-R}^R f(x(s), y(s)) ds \exp\left\{-\int_{-R}^R \mu(x(s'), y(s'); E) ds'\right\}$$

Define $g_c(l, \theta)$, attenuation corrected sinogram

$$g_c(l, \theta) = \frac{\bar{n}(l, \theta)}{k} = \int_{-R}^R f(x(s), y(s)) ds \exp\left\{-\int_{-R}^R \mu(x(s'), y(s'); E) ds'\right\}$$

$\mu(x, y)$ found from CT

8.10 PET Reconstruction

- Final approximate imaging equation

$$g_c(l, \theta) = \int_{-R}^R f(x(s), y(s)) ds$$

- Convolution backprojection yields

$$\hat{f}(x, y) = \int_0^{\pi} \int_{-\infty}^{\infty} g_c(l, \theta) \tilde{c}(x \cos \theta + y \sin \theta - l) dl d\theta$$

8.11 Iterative Reconstruction Concept

- Sequence of estimated cross sections:

$$f^{(0)}(x, y), f^{(1)}(x, y), \dots$$

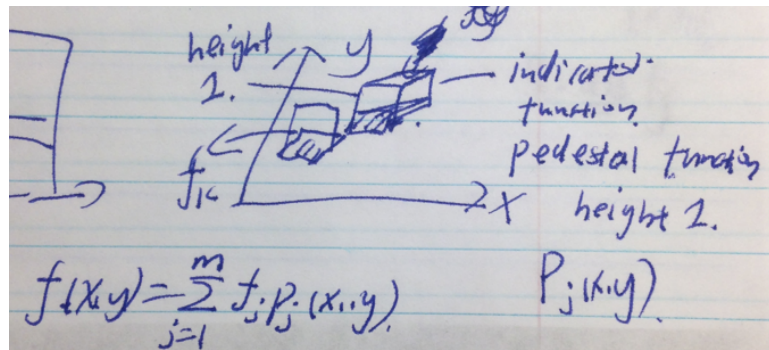
- Computed measurements

$$g^{(0)}(l, \theta), g^{(1)}(l, \theta), \dots$$

- Compare computed measurements to actual measurements $g(l, \theta)$ in order to update estimated cross section

8.11.1 Digital Representation of Cross Section

- Image Values: $f_j, j = 1, \dots, m$
- Pixel indicator function: $p_j(x, y), j = 1, \dots, m$



- Continuous image representation:

$$f(x, y) = \sum_{j=1}^m f_j p_j(x, y)$$

- In emission tomography, $f(x, y)$ is activity concentration

8.11.2 Computed Measurements in SPECT and PET

- In SPECT:

$$g(l, \theta) = \frac{\bar{n}_k(l, \theta)}{TA_k A_h \epsilon}$$

- In PET:

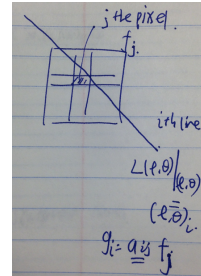
$$g(l, \theta) = \frac{\bar{n}(l, \theta)}{k}$$

where $k = A_h T \epsilon \tilde{A}_h$

- Substitute $f(x, y)$ into imaging equations to yield

$$g_i = \sum_{j=1}^m a_{ij} f_j$$

where i-ith line, j-jthe pixel



- Vector/Matrix Form

Vector representations

$$\mathbf{g} = \begin{bmatrix} g_1 \\ \vdots \\ g_n \end{bmatrix}; \quad \mathbf{f} = \begin{bmatrix} f_1 \\ \vdots \\ f_m \end{bmatrix}; \quad \mathbf{a}_i = \begin{bmatrix} a_{i1} \\ \vdots \\ a_{im} \end{bmatrix}$$

Line integral measurement is

$$\mathbf{g}_i = \mathbf{a}_i^T \mathbf{f}$$

All measurements

$$\mathbf{g} = A\mathbf{f}; \quad A = [a_{ij}]$$

Note: vector f = entire image pixel values. a_i represents the contribution from the i th line and m th pixel. g is a vector

$$\hat{g} = A\hat{f} + \eta$$

If no η , $\hat{f} = A^{-1}\hat{g}$, and

$$\hat{f} = (A^T A)^{-1} A^T \hat{g}$$

8.12 Algebraic Reconstruction Technique(ART)

- Iterative solution: for $k=0,1,\dots$

$$\hat{f}^k = \hat{f}^{k-1} - \frac{a_i^T \hat{f}^{k-1} - g_i}{a_i^T a_i}$$

- g_i is true measurement
- $a_i^T \hat{f}^{k-1}$ is forward operator
- compare forward projection to measurements by subtraction

8.13 Maximum Likelihood Expectation Maximization(ML-EM)

- Directly express photon counts at each detector ,and observe n counts. n is a Poisson variable:

$$\bar{n}_i(f) = a_i^T f + \bar{r}_i$$

where \bar{r}_i represents random and scattered counts

- Form likelihood assuming pixels are independent

$$L(f) = \sum_{i=1}^n [n_i \ln \bar{n}_i(f) - \bar{n}_i(f)]$$

8.14 Resolution in Emission Tomography

- Approximation:

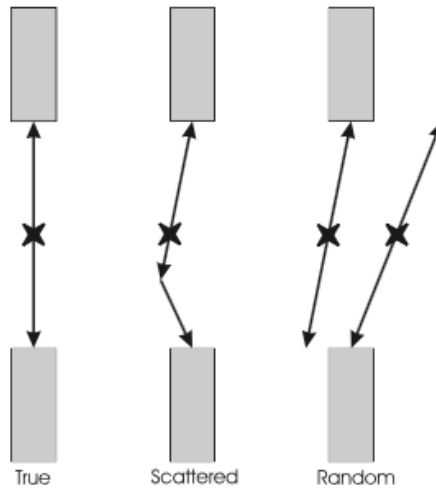
$$\hat{f}(x, y) = f(x, y) * h(r)$$

- In SPECT, $h(r)$ includes:

- Collimator and intrinsic resolutions

- ramp filter window effect
- In PET, $h(r)$ includes:
 - the positron range function
 - detector width effects
 - ramp filter window effect

PET Events



8.14.1 Conincidence Timing

- Three classes of events
 - true coincidence
 - scattered coincidence
 - random coincidence
- Sensitivity in PET, measures capability of system to detect "trues" and rejects "randoms"

9 Ultrasound Physics

9.1 3-D Wave Equation

- Acoustic pressure: $p(x, y, z, t)$

- 3-D wave equation

$$\nabla^2 p(x, y, z, t) = \frac{1}{c^2} p_{tt}(x, y, z, t)$$

where $\nabla^2 p = p_{xx} + p_{yy} + p_{zz}$
and c is the speed of sound

- since general solution is very complicated, we go after plane waves and spherical waves

9.2 Plane Waves

- Plane wave in z direction:

$$p(z, t) = p(x, y, z, t)$$

- Plane wave equation:

$$p_{zz}(z, t) = \frac{1}{c^2} p_{tt}(z, t)$$

- General solution:

$$p(z, t) = \phi_f(t - c^{-1}z) + \phi_b(t + c^{-1}z)$$

9.2.1 Harmonic Waves

- Harmonic plane wave

$$p(z, t) = \cos[k(z - ct)]$$

- Definitions:

- wavenumber: k
- frequency: $f = kc/2\pi$
- period; $T = 1/f$
- wavelength: $\lambda = c/f$

9.2.2 Spherical Waves

- 3-D spherical wave:

$$p(r, t) = p(x, y, z, t)$$

where $r = \sqrt{x^2 + y^2 + z^2}$

- Spherical wave equation:

$$\frac{1}{r} \frac{\partial_2}{\partial r^2}(rp) = \frac{1}{c^2} \frac{\partial_2 p}{\partial t^2}$$

- General solution(outward expanding):

$$p(r, t) = \frac{1}{r} \phi_0(t - c^{-1}r)$$

9.2.3 Characteristic Impedance

- Characteristic Impedance

$$Z = \rho c$$

where ρ is density

- Why impedance?

$$p = Zv$$

where v is particle velocity $v \neq c$

- p is like voltage
- v is like current

9.2.4 Acoustic Energy

- kinetic energy density:

$$w_k = \frac{1}{2} \rho_0 v^2$$

- Potential energy density:

$$w_p = \frac{1}{2} \kappa p^2$$

where κ is compressibility

- Acoustic energy density:

$$w = w_k + w_p$$

9.2.5 Acoustic Power

- Acoustic Intensity:

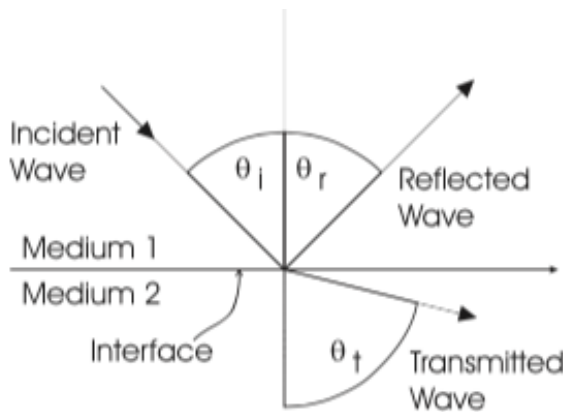
$$I = p v = \frac{p^2}{Z}$$

(like electrical power $p=vi$)

- Propagation of acoustic power (plane wave):

$$\frac{\partial I}{\partial z} + \frac{\partial w}{\partial z} = 0$$

9.2.6 Reflection and Refraction



Snell's Laws:

$$\begin{aligned}\theta_r &= \theta_i \\ \frac{\sin \theta_i}{\sin \theta_t} &= \frac{c_1}{c_2} \\ \theta_{critical} &= \sin^{-1}\left(\frac{c_1}{c_2}\right)\end{aligned}$$

for $c_2 \geq c_1$

e.g., Given the following setup, what is the reflected intensity?

e.g.	Face	tiver.
Transducer	c_1	c_2
	z_1	z_2

Soln: We know that $R = \frac{Z_2 - Z_1}{Z_2 + Z_1}$, $R_I = \frac{I_r}{I_i}$, $I = \frac{p^2}{z}$

Also, $I_r = \frac{p_r^2}{Z_1}$, $I_i = \frac{p_i^2}{Z_1}$.

Plug them them in, we get $R_I = \frac{p_r^2}{p_i^2} = R^2$

Plug in the numbers, $R_I = 0.103$, about 10 percent, which is reflected back.

9.2.7 Reflected and Refracted Waves

- Pressure reflectivity:

$$R = \frac{p_r}{p_i} = \frac{Z_2 \cos \theta_i - Z_1 \cos \theta_t}{Z_2 \cos \theta_i + Z_1 \cos \theta_t}$$

- Pressure transmittivity

$$T = \frac{p_t}{p_i} = \frac{2Z_2 \cos \theta_i}{Z_2 \cos \theta_i + Z_1 \cos \theta_t}$$

- At normal incidence:

$$R = \frac{Z_2 - Z_1}{Z_2 + Z_1}$$

9.2.8 Attenuation and Absorption

- Phenomenological model:

$$p(z, t) = A_0 e^{-\mu_a z} f(t - c^{-1} z)$$

- μ_a is amplitude attenuation factor [cm^{-1}]
- Absorption coefficient: $\alpha = 20(\log_{10} e)\mu_a [dB/cm]$
- In range $1MHz \leq f \leq 10MHz$

$$a \approx af$$

and

$$a \approx 1dB/cm - MHz$$

e.g., known A_0 at $z = 0$, we have $A_0 e^{-\mu_0 z}$ at z

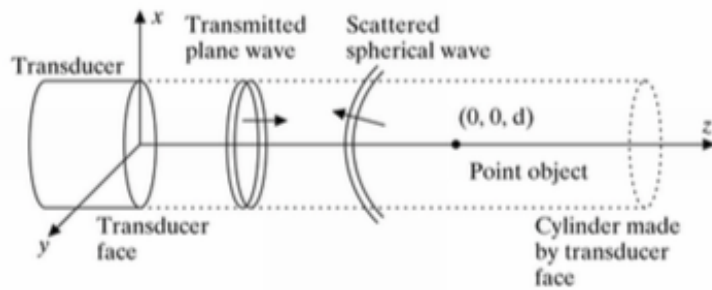
$$\begin{aligned} 20 \log_{10} \frac{A_0 e^{-\mu_0 z}}{A_0} &= 20 \log e^{-\mu_0 z} \\ &= 20(-\mu_0 z) \log_{10} e \\ &= -(20 \mu_0 \log_{10} e) z \end{aligned}$$

9.2.9 Scattering

- Particle at (0,0,d), reflection coefficient R
- Generates spherical wave

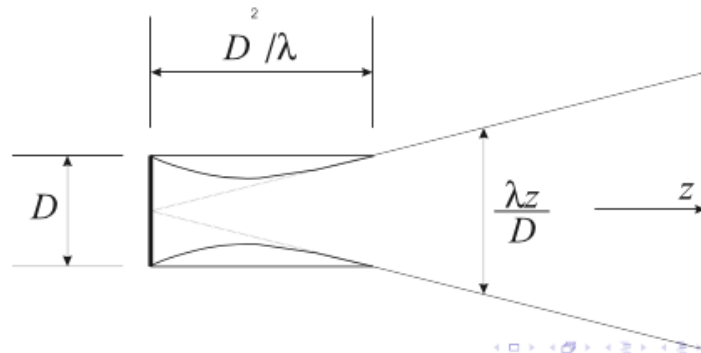
$$p_s(r, t) = \frac{Re^{-\mu_a r} A_0 e^{-\mu_a d}}{r} f(t - c^{-1}d - c^{-1}r)$$

- $c^{-1}d$ term is the time delay for the wave to get to d .
- r is distance from (0,0,d)



9.2.10 Field Patterns

- Geometric approximation
- Diffraction formulation
- Simple model:



Beam width:

$$W(z) = \begin{cases} D & \text{if } z \leq D^2/\lambda \\ \lambda z/D & \text{if } z > D^2/\lambda \end{cases}$$

9.2.11 Far Field=Fraunhofer Pattern

- Transducer face indicator function:

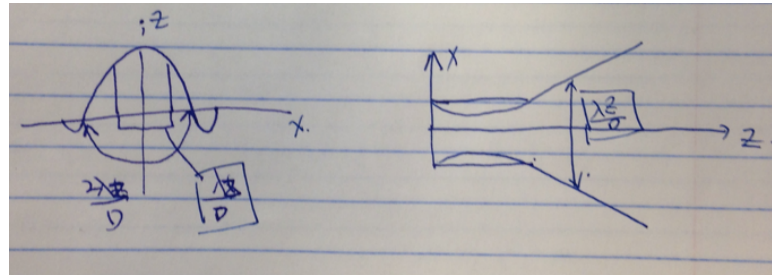
$$s(x, y) = \begin{cases} 1 & \text{if } (x, y) \text{ in face} \\ 0 & \text{if otherwise} \end{cases}$$

- Far field pattern:

$$q(x, y, z) \approx \frac{1}{z} e^{jk(x^2+y^2)/2z} S\left(\frac{x}{\lambda z}, \frac{y}{\lambda z}\right)$$

e.g., a 1-D example: $s(x) = \text{rect}(\frac{x}{D})$ and $S(u) = D \text{sinc}(uD)$

$S\left(\frac{x}{\lambda z}\right) = D \text{sinc}\left(\frac{xD}{\lambda z}\right)$, where $u = \frac{x}{\lambda z}$
 For a sinc function, the first zero occurs at
 $\frac{xD}{\lambda z} = 1 \Rightarrow x = \frac{\lambda z}{D} = W(z)$ at far field!!

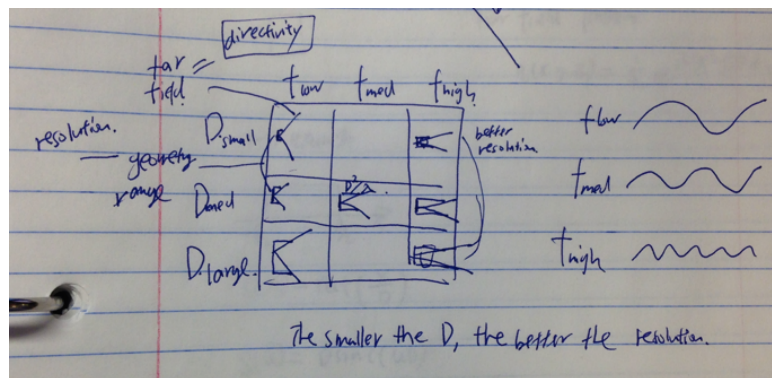
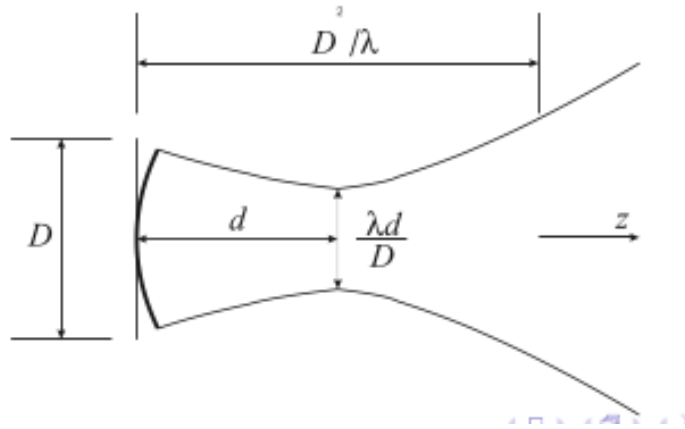


- $S(u, v)$ is Fourier transform of $s(x, y)$
- Pulse-echo sensitivity: $q^2(x, y, z)$

9.2.12 Focusing

- Focal length field pattern:

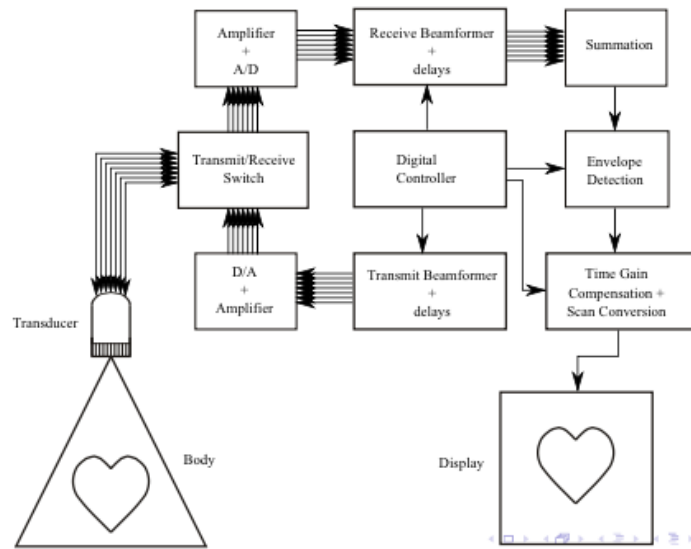
$$q(x, y, z) \approx \frac{1}{d} e^{jk(x^2+y^2)/2d} S\left(\frac{x}{\lambda d}, \frac{y}{\lambda d}\right)$$



10 Ultrasound Imaging

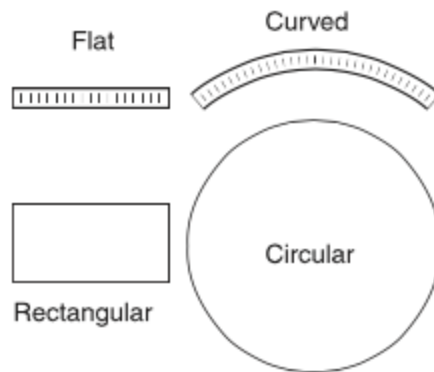
10.1 Ultrasound System Components

Block Diagram

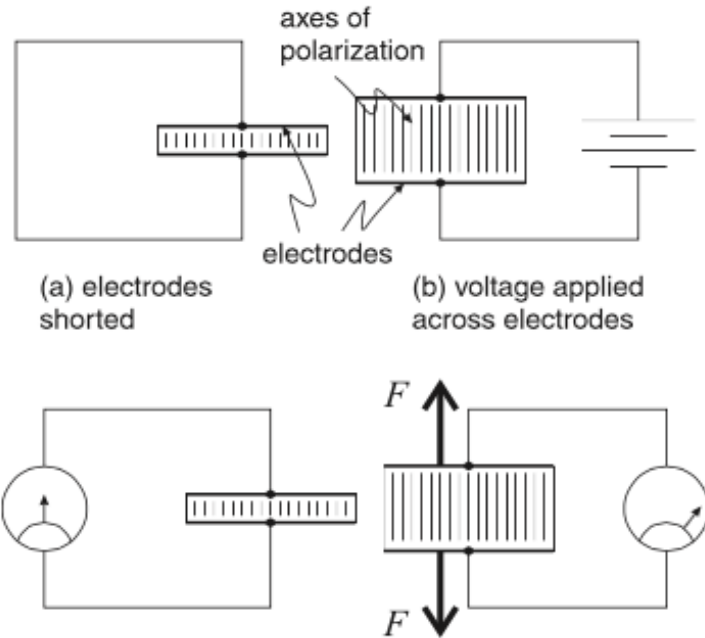


10.2 Transducers

- Lead Zirconate Titanate(PZT)
 - piezoelectric crystal
 - good transmit and receive efficiencies
 - different shapes:

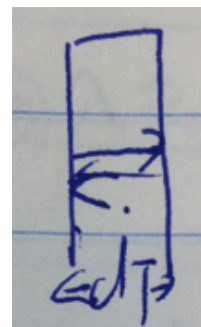


10.2.1 Piezoelectric Effect



10.2.2 Resonance

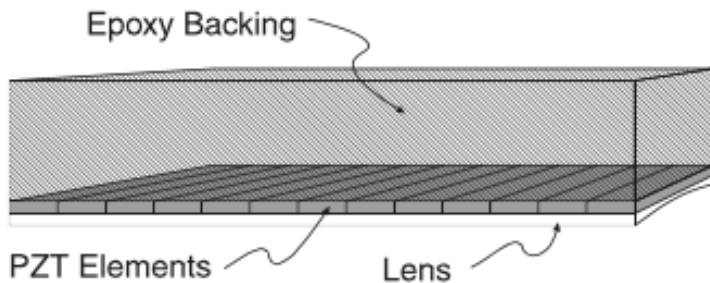
- Shock excite yields resonant pulse
- Resonant frequency:



$$f_T = \frac{c_T}{2d_t}$$

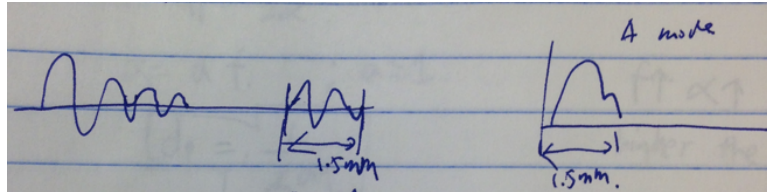
- Damps out after 3-5 cycles

10.2.3 Electronic Scanner



- Linear arrays:
 - 64-256 elements, fire in groups
 - each element \approx 2 mm by 10 mm
- Phased arrays:
 - 30-128 elements; electronically steered
 - each element \approx 0.2 mm by 8 mm

10.3 Shock Excitation



$$c \cong 1500 \text{ m/s} = 1.5 \text{ mm/us}$$

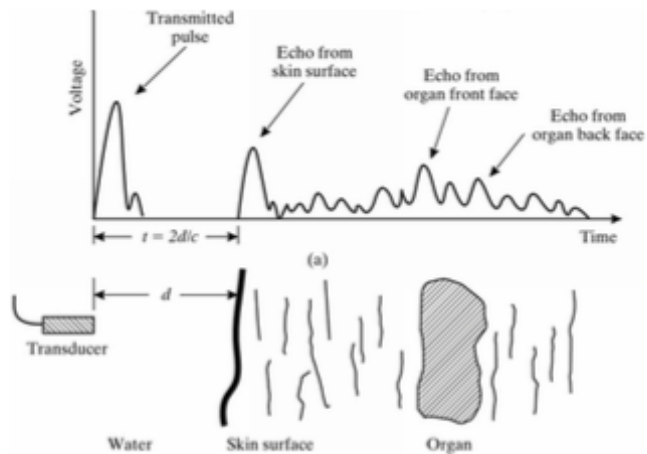
$$c = \lambda f \Rightarrow \lambda = \frac{c}{f} = cT$$

$$@ 5 \text{ MHz } T = \frac{1}{f} = \frac{1}{5 \text{ MHz}} = 0.2 \text{ us}$$

$$\lambda = cT = \frac{1.5 \text{ mm}}{\text{us}} \times 0.2 \text{ us} = 0.3 \text{ mm}$$

If the pulse has 5 cycles, then its duration = 1.5 mm and range resolution = 1.5 mm.

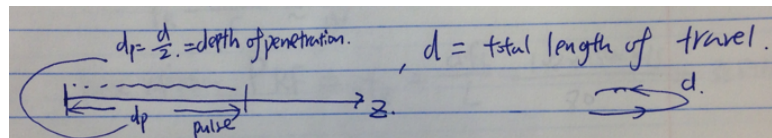
10.3.1 A-mode Display



The Range Equation

$$z = \frac{ct}{2}$$

10.3.2 Depth of Penetration



Suppose it travels d distance, the loss is

$$L = d\alpha \text{ in } [dB]$$

For example, if the system's sensitivity is $L \approx 80dB$, after $d \geq \frac{L}{\alpha}$ the echo is invisible.

$$d_p = \frac{L}{2\alpha}, \text{ recall that } \alpha = af; a \approx 1 \Rightarrow d_p = \frac{L}{2af}$$

The higher the frequency, the higher the absorption, the lower the depth of penetration.

e.g., $L = 80dB$, $f = 2MHz$, what is the depth of penetration?

Soln:

$$d_p = \frac{L}{2af} = \frac{80dB}{2 \times \frac{1dB}{cm \times MHz} 2MHz} = 20cm$$

10.3.3 Pulse Repetition Time

- The time that needs to wait till the very last pulse gets reflected back to fire a new pulse.

$$T_R = \frac{2d_p}{c} \approx \frac{L}{afc}$$

- Pulse repetition frequency/rate:

$$f_R = \frac{afc}{L} = \frac{1}{T_R}$$

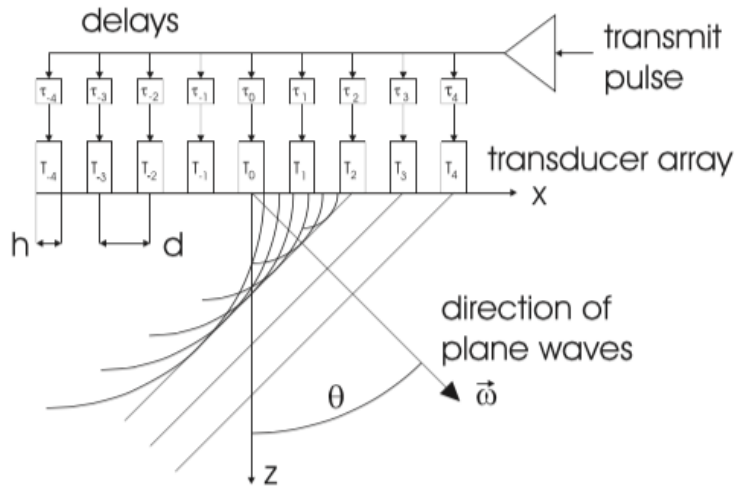
e.g., $f_R = 3850\text{Hz}$, number of scan line =N:one needs to go through all the scan lines to get a new image

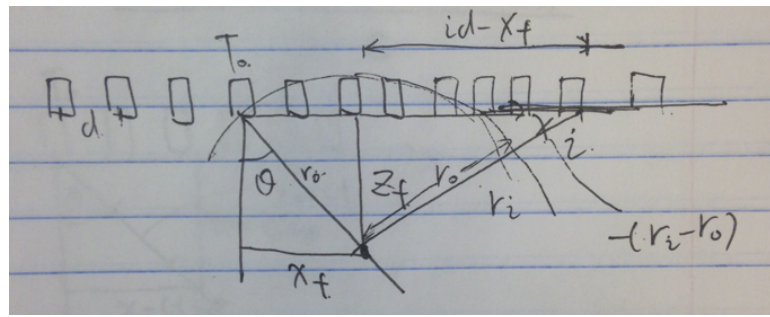
Frame rate(number of pictures you see per second), $f_F = \frac{f_R}{N}$, suppose N=256.

$$\frac{3850\text{Hz}}{256} \approx 15\text{Hz} = f_F$$

which is not fast enough \Rightarrow aliasing (frame rate on a motion module is approximately 24 Hz)

10.4 Phased Arrays: Transmit Steering

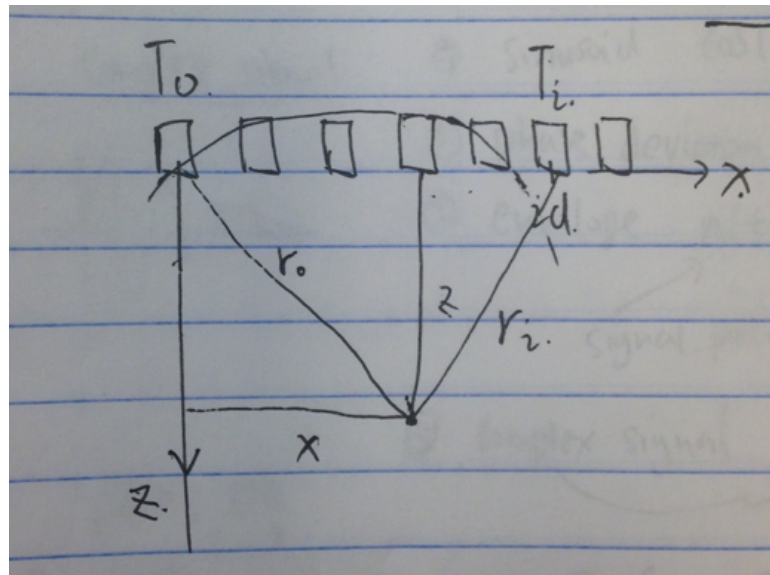




$$r_0 = \sqrt{x_t^2 + z_t^2} \text{ and } r_i = \sqrt{z_t^2 + (id - x_f)^2}$$

Delay is

$$t_i = \frac{r_0 - r_i}{c} = \frac{\sqrt{x_t^2 + z_t^2} - \sqrt{z_t^2 + (id - x_f)^2}}{c}$$

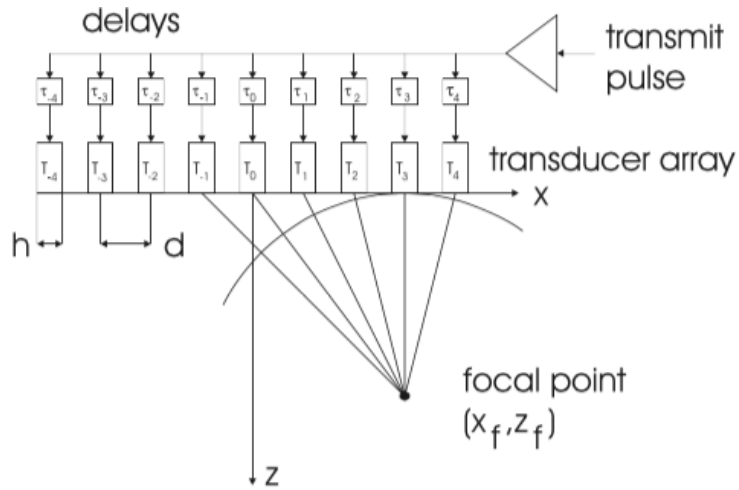


- echo from T_0 : $t_0 = \frac{r_0 + r_0}{c}$

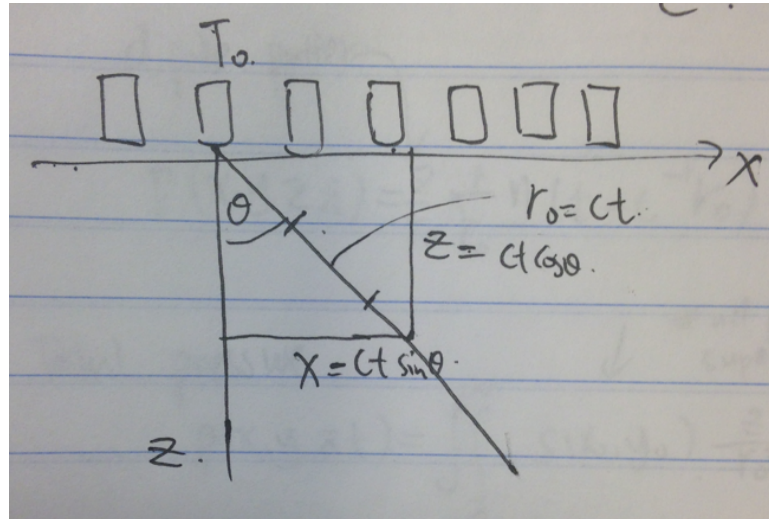
- what about T_i : $t_i = \frac{r_0 + r_i}{c}$

- Time difference: $\tau_i = t_0 - t_i = \frac{2r_0}{c} - \frac{(r_0 + r_i)}{c} \Rightarrow \tau_i = \frac{r_0 + r_i}{c} = \frac{\sqrt{x_t^2 + z_t^2} - \sqrt{z_t^2 + (id - x_f)^2}}{c}$

10.5 Phased Arrays: Transmit Focussing



10.5.1 Dynamic Focusing



$$\tau_i(t) = \frac{\sqrt{x(t)^2 + z(t)^2} - \sqrt{z(t)^2 + (id - x(t))^2}}{c}$$

10.6 Imaging Equation

- Sinusoid $\cos(2\pi f_0 t)$
- Phase deviation $\cos(2\pi f_0 t - \phi)$

- Envelope $n(t) = n_e(t)\cos(2\pi f_0 t - \phi)$
- Complex signal $\underline{n}(t) = n_e(t)e^{j\phi}e^{-j2\pi f_0 t}$
- A complex envelope $n_e(t)e^{j\phi}$
- A complex signal $e^{-j2\pi f_0 t}$
- $n(t) = \operatorname{Re}\{\underline{n}(t)\}$, RF signal
- $n_e(t) = |\underline{n}(t)|$, a mode signal

